12-20-2022 1:00 PM

S100A7 as a biomarker for predicting transformation in a potentially malignant lesion: lichen planus.

Jeff J. Lovell, *The University of Western Ontario*

Supervisor: Darling, Mark, *The University of Western Ontario*

A thesis submitted in partial fulfillment of the requirements for the Master of Science degree in Pathology and Laboratory Medicine

Abstract

Oral Lichen Planus (OLP) is a potentially malignant disorder that has a malignant transformation rate of approximately 1%. Current management includes incisional biopsy and grading of dysplasia, if present. This may not be a reliable predictive tool for malignant transformation. Tissue biomarkers such as S100A7 may provide a more accurate method of risk determination. The proposed mechanism is an association between S100A7 and the MAPK signalling pathway. Paraffin embedded sections of OLP that progressed and did not progress on serial biopsy were selected. The tissues were stained via S100A7 immunohistochemistry. S100A7 was quantified using an Immunoreactivity score, QuPath and Straticyte™. Phosphorylated MAPK proteins and WNT proteins were also evaluated. Based on Pearson correlation coefficients, the Immunoreactivity score correlated well with both Straticyte™ and Qupath scores. The 3 predictive scores can distinguish Lichen Planus from Normal tissue based on quantification of S100A7, however, S100A7 cannot predict which Lichen Planus lesion might progress to malignancy. Furthermore, the pathway involved in progression of this inflammatory lesion also remains uncertain. Biomarker S100A7 does not aid in the accurate prediction of transformation in Lichen Planus and hence should not be used to guide clinical management.

Keywords: Potentially malignant disorder, Lichen planus, Dysplasia.

Summary for Lay Audience

Oral Lichen Planus is a relatively common disorder of the oral cavity with a small risk of turning into cancer. It is difficult to predict which individuals living with this disorder will develop cancer. S100A7 is a cellular protein that has been found to be present in increased amount in certain cancers including those of the head and neck. We attempted to show that S100A7 would be elevated in the Oral Lichen Planus lesions that eventually turned into precancerous and cancerous tissue. We used an antibody that attaches to S100A7 protein and measured the amount of S100A7 using three different methods. We compared the amount of S100A7 in Oral lichen planus that was known to progress to cancer, precancerous tissue, and stay the same on repeat biopsy. For comparison, we also contrasted the above tissues with S100A7 in normal tissue, inflamed tissue and healing tissue.

To determine how S100A7 may be involved with progression to precancer/cancer, we examined for a possible relationship with the Mitogen activated Protein Kinase (MAPK) system along with Beta-Catenin and Cyclin D1. These are two different cellular protein signaling mechanisms that have been shown to be involved with key steps in the development of cancer.

Our results show that S100A7 was elevated in Oral Lichen Planus and other inflamed tissues when compared to normal tissue; however, it could not be used to accurately predict precancerous and cancerous transformation. The cellular pathways involved in the transformation process need to be better elucidated. This will likely aid in selection of biomarker(s) to predict this rare event. Epithelial to Mesenchymal transition through E-Cadherin and Beta-Catenin may be worth looking further into. In summary, S100A7 should not be used to guide clinical management of Lichen Planus. Studies to confirm or refute our results as well as

investigating other potential biomarker are required if biomarkers are to be used to guide management in these lesions.

Dedication

I would like to dedicate this work to my wife Shanna and children, Ben and Josie, who have supported me throughout my scholastic endeavors.

Acknowledgments

I would like to thank Dr. Mark Darling for all of his time, guidance, and expertise on this topic. I would also like to thank Linda Jackson-Boeters for her guidance in the laboratory. Linda sacrificed many hours to help in the lab. I would like to thank Dr. Michael Robinson for his statistical expertise and input. I would also like to thank Drs. Joe Armstrong, Christina McCord, and Doug Hamilton for their role as committee members. Lastly, I would like to thank Dr. Andra Sterea for her contributions to this project.

Table of Contents

List of Tables

List of Figures

List of Abbreviations

(Abbreviations Listed in Alphabetical Order)

Abbreviation	Definition
AUROC	Area Under Receiver Operating Characteristic Curve
BAX	Bcl-2 Associated X Protein
BCL-2	B Cell Lymphoma 2
BMI1	B-cell-specific-Moloney Murine Leukemia Virus Integration Site 1
Cav-1	Caveolin-1
CB	Cathepsin B
CDK	Cyclin-Dependent Kinase
COX	Cyclooxygenase
CTX-1	C-Terminal Telopeptide 1
ECM	Extracellular Matrix
EGFR	Epidermal Growth Factor Receptor
EMT	Epithelial to Mesenchymal Transition
ERK	Extracellular Signal-Regulated Kinase
GBM	Gradient Boosting Machine
GRB2	Growth Factor Receptor-Binding Protein 2
GvHD	Graft Vs. Host Disease
HPV	Human Papilloma Virus
IL	Interleukin
JNK	C-Jun N-terminal kinase
MAP	Microtubule Associated Protein

MAPK	Mitogen Activated Protein Kinase
MAPKAPK	Mitogen Activated Protein Kinase Activated Protein Kinases
MCL-1	Myeloid Leukemia Cell Differentiation Protein
MDM2	Mouse Double Minute 2 Homolog
MEK	Mitogen Activated Protein Kinase Kinase
MiRNA	Micro Ribonucleic Acid
MKK 3	Mitogen Activated Protein Kinase Kinase 3
MKK 6	Mitogen Activated Protein Kinase Kinase 6
MMP-9/8	Matrix Metalloproteinases- 9/8
OLL	Oral Lichenoid Lesions
OLP	Oral Lichen Planus
OOB	Out Of Bag
OPMD	Oral Potentially Malignant Disorders
OSCC	Oral Squamous Cell Carcinoma
PMD	Potentially Malignant Disorder
RAF	Rapidly Accelerated Fibrosarcoma
RAS	Rat Sarcoma Virus
RFA	Random Forest Analysis
RNA	Ribonucleic Acid
RTK	Receptor Tyrosine Kinase
SAPK	Stress Activated Protein Kinases
SOS	Sons Of Sevenless
SUMO-1	Small Ubiquitin-related Modifier 1

TAK1	Transforming Growth Factor Beta-Activated Kinase 1
TCR	T Cell Antigen Receptor
TGF-β	Transforming Growth Factor Beta
TIMP	Tissue Inhibitors of Matrix Metalloproteinases
TNF-α	Tumor Necrosis Factor Alpha
VEGF	Vascular Endothelial Growth Factors
WHO	World Health Organization
WNT	Wingless-related Integration Site

Chapter 1

1.0 Introduction

Oral Lichen Planus (OLP) is a Potentially Malignant Disorder (PMD) of the oral cavity[1,2]. It is one of the most common mucosal conditions of the mouth[3]. The modified WHO definition clinical criteria include: 1) the presence of bilateral, more or less symmetrical lesions, and 2) presence of a lace-like network of slightly raised gray-white lines (reticular pattern)[1]. Erosive, atrophic, bullous and plaque-type lesions are accepted only as a subtype in the presence of reticular lesions elsewhere in the oral mucosa[4]. In all other lesions that resemble OLP but do not complete the aforementioned criteria, the term "clinically compatible with" should be used[5]. The histopathologic criteria include: 1) the presence of a well -defined band like zone of cellular infiltration that is connected to the superficial part of the connective tissue, consisting mainly of lymphocytes, and 2) signs of liquefactive degeneration in the basal cell layer, and the absence of epithelial dysplasia[2]. When the histopathologic features are less obvious, the term "histopathologically compatible with" is used as per the 2003 World Health Organization guidelines[5]. OLP is a chronic inflammatory disease characterized by a T-cell mediated response against basal cells of the epithelium[4]. Treatment is symptomatic and has no curative intent. It affects females more than males and is most common in middle aged and elderly individuals[6,7]. Currently, diagnosis of OLP relies on clinical presentation and histopathological analysis[2]. Although disputed, OLP has a reported malignant transformation rate of approximately 1.3% whereas Oral Lichenoid lesions (OLL) have a transformation rate of up to 5%[8]. Smoking, alcoholism, hepatitis C infection, female sex, tongue lesions, and erosive lesions have a higher rate of transformation[8]. DNA aneuploidy may also be associated with progression of OLP to

Oral Squamous Cell Carcinoma (OSCC)[9]. Progression of PMD's such as OLP and OLL to oral cancer can have significant impact on quantity and quality of life[10].

1.1 Oral Cancer

Cancer is the second leading cause of mortality in developed countries[11]. Cancer within the oral cavity accounts for 3% of diagnosed malignancies worldwide[12]. Oral cancer is the 12th most common cancer in women and 6th most common cancer in men with the most common primary malignancy found within the oral cavity is Oral Squamous Cell Carcinoma[13].

1.1.1 Oral Squamous Cell Carcinoma

Oral Squamous Cell Carcinoma (OSCC) accounts for 92-95% of all oral cancers and likely many other malignancies, its etiology is multifactorial[14,15]. There are numerous predisposing factors to OSCC including tobacco smoke, alcohol, phenol, viral, bacterial, fungal, radiation, immunosuppression, expression of oncogenes, deactivation of tumor suppressor genes, malnutrition, and chronic inflammation[15]. OSCC has a five- year survival rate of 53-56%[15]. However, aside from its high mortality rate, treatment of OSCC can have significant morbidity including changes in oral function (speech and swallowing) and esthetic deformity[16]. This can lead to psychological and social consequences that can negatively impact quality of life[17]. Future reduction in the mortality and morbidity associated with OSCC will require preventative measures and early detection of Potentially Malignant Disorders (PMDs) within the oral cavity.

1.2 Oral Potentially Malignant Disorders (PMD)

The transformation of oral lesions to malignancy was first described by Sir James Paget in 1870[15]. The World Health Organization (WHO) has since defined a known subset of oral lesions/conditions that predispose one to developing malignancy as Potentially Malignant Disorders (PMD)[1]. A PMD is "the risk of malignancy being present in a lesion or a condition

either during the time of initial diagnosis or at a future date"[15]. According to Mortazavi *et al*, oral PMDs have a prevalence of 1-5% and the average age at diagnosis is 50-69 years old[15,18]. Furthermore, 5% of PMDs are noted to be in patients under the age of 30[18]. The most common locations for PMDs include the buccal mucosa, gingiva, tongue, and floor of mouth[15].

The World Health Organization has further classified PMD's into premalignant lesions and premalignant conditions[15]. A premalignant lesion is a benign condition with morphologically abnormal tissue that has a higher than average risk of transforming into malignancy[19]. In contrast, a premalignant condition is a disease or habit that does not necessarily alter the clinical appearance of tissue but is associated with increased risk of developing a precancerous or cancerous lesion[19]. Premalignant lesions include but are not limited to leukoplakia, erythroplakia, proliferative verrucous leukoplakia, oral submucous fibrosis, actinic cheilosis, and keratoacanthoma[19,20]. Premalignant conditions include oral lichen planus, discoid lupus, epidermolysis bullosa, verruciform xanthoma, GvHD, cheilitis glandularis, xeroderma pigmentosum, malnutrition and more[19].

Current diagnosis and management of oral premalignant lesions and some premalignant conditions includes incisional biopsy, grading of dysplasia, and close clinical follow up or excision depending on the presence and severity of dysplasia[21]. Current literature reports that incisional biopsy and grading of dysplasia are not reliable diagnostic or predictive tools for malignant transformation[22]. As a result of this finding, novel and more accurate methods for predictive risk of malignant transformation in these lesions should be examined.

1.2.1 Oral lichen planus

Lichen Planus is a mucocutaneous inflammatory disorder which can affect the skin and/ or mucous membranes with a variety of clinical appearances as mentioned above[2]. It was first

discovered by British physician Erasmus Wilson in 1869[23]. Lichen planus affects 1-2% of the general population[24]. The etiology of lichen planus remains unknown but microbes, psychological stress, local and systemic cell-mediated hypersensitivity, and immune dysregulation are thought to contribute[25]. The first case of Oral Lichen Planus (OLP) transforming to malignancy was described in 1910[25]. Since this time, the evolving diagnostic criteria, clinical and histopathologic similarities to other PMDs, clinical subtypes, and confounding factors (smoking, HPV, alcohol etc.) have led to uncertainty in its malignant transformation rate (0-10% in the literature)[25]. A study by Mehdipour *et al* reported a one-hundred-fold increase in annual risk of malignant transformation in OLP[24]. The transformation rate does appear to be higher in the atrophic and erosive subtypes as compared to the others and time to transformation is on average 5.5 years[26]. The same author states that the malignancy need not develop in the OLP lesion itself but may develop anywhere within the oral cavity[24]. The uncertainty regarding the risk of malignant transformation of OLP/ OLL and the poor predictability of incisional biopsy and grading of dysplasia has made clinical management of OLP, OLLs and dysplastic oral lesions challenging. A study by Fitzpatrick *et al* alludes to the importance of future molecular study of the malignant potential of OLP and OLL prior to the development of dysplasia to aid in clinical management of these lesions[27]. Tissue, serum, and salivary biomarkers could provide a method to accurately predict the risk of malignant transformation in OLP and other PMDs[28–30].

1.3 Biomarkers in Oral Potentially Malignant Disorders

An ideal diagnostic biomarker should have high disease sensitivity and specificity, mandatory presence in all affected patients, and provide a cutoff value with minimal overlap between normal and disease states[31]. Various biomarkers have been studied as prognostic

indicators for OSCC, but also in an attempt to predict malignant transformation in OLP and other PMDs[32,33]. Biomarkers used for transformation of OLP can be apoptosis related, cell cycle regulators, tissue remodeling factors, inflammation related factors, galectins, and intracellular adhesion proteins[14,29]. Some other biomarkers studied include Micro RNAs, Caveolin-1, Claudins -(1,4,7), E-cadherin, Cathepsin B, MMP-9/8, HPV 16/18, TIMP, TGF-β, and CTX-1. Interestingly, these biomarkers can even be collected non-invasively from saliva, such as miR-21[24,34–36].

The extrinsic and intrinsic apoptotic pathways are well mapped out and the end point of both pathways is the activation of caspases leading to cellular destruction[14]. Apoptosis of the basal keratinocytes through activation of CD8 T cells is important in the pathogenesis of lichen planus and could also be important in the transformation to OSCC[37]. Multiple studies have shown a decrease in the number of apoptotic inflammatory cells in Lichen Planus that transforms into OSCC[14]. A study by Kaur *et al* described less inflammatory apoptotic cells in the saliva of oral PMD (lichen planus, leukoplakia, oral submucous fibrosis) as compared to normal controls[14]. The same author also found a further decrease in these cells in OSCC.

P53, p63, caspase 3, BCL-2/BAX, MCL-1 MDM2, SUMO-1, and survivin are proapoptotic molecules that have been investigated.

P53 is a protein that regulates processes such as cell cycle arrest, senescence and apoptosis[38]. A study by Valente *et al* showed an enhanced expression of p53 in OSCC and OLP that transformed into OSCC as compared to OLP that did not transform[39]. They concluded that p53 mutation and overexpression may be a mechanism and marker for malignant transformation of OLP[39]. Other studies have confirmed these findings and have purported that oral PMDs with

p53 expression, especially in the suprabasal layer should be monitored for malignant transformation[40,41].

SUMO-1 and MDM-2 are molecules that are involved in cell proliferation and apoptosis. SUMO-1 activates MDM-2 which in turn degrades p53 leading to less cell apoptosis[42,43]. A study investigated the expression of these proteins in OLP and found an increase in MDM-2 and p53 in OLP samples as compared to normal mucosa[44]. As a result, MDM-2 may provide future utility as a marker of malignant transformation in OLP[14].

BCL-2 is an inhibitor of apoptosis while BAX is pro-apoptotic and a component of the intrinsic pathway[45]. A study by Pigatti *et al* found upregulation of BCL-2 in the inflammatory infiltrate in OLP and upregulation of BAX in the epithelial layer[46]. These results have been replicated and as a result BCL-2 and BAX are not recommended for use as prognostic markers[28].

MCL-1 is an anti-apoptotic member of the BCL-2 family[47]. Its mechanism is through inhibition of apoptosis inducing BAK[47]. MCL-1 has been shown to be upregulated in OLP and OSCC as compared to normal oral mucosa[48]. The expression of MCL-1 has also been shown to decrease in cancer cell lines after treatment with mithramycin A and sorafenib[49]. As a result, MCL-1 has potential as a marker of malignant transformation in OLP.

Survivin is an inhibitor of apoptosis functioning through the blockade of caspases 3, 7, and 9[50]. Survivin is downregulated by p53 which has also been shown to be upregulated but mutated in OLP and OSCC[51,52]. Thus, it is possible that Survivin is not inhibited by the mutated protein and leads to cell survival.

Cell cycle regulators have also been studied as potential markers for OLP

transformation[53]. Cyclin-Dependent Kinases, their inhibitors (p16, p21, p27), B-cell-specific-Moloney murine leukemia virus integration site 1 (BMI1) and Ki67 have been presented in the literature[54]. Cyclin dependent Kinases such as CDK4 and CDK6 promote progression of cells through the cell replication cycle[55]. P16 is a tumor suppressor protein that inhibits CDK activity[56]. Loss of p16 is commonly found in neoplasms and carcinogenesis[14]. P16 has been shown to be increased in OLP; however, this is thought to be secondary to inflammatory cytokine release such as TNF-α[57]. Due to this reason, Salehinejad states that p16 should not be used as a marker of malignant transformation in OLP. Goel *et al* found elevated p16 and CDK4 in OLP as compared to normal tissue but less than in OSCC and recommended that p16 and CDK4 might be a reasonable predictor of OLP progression[58].

BMI1 is a stem cell factor that is involved in the cell cycle[59]. An increase in the expression of BMI1 has been shown in many tumors and cell dysplasia[28]. Ma *et al* found elevated BMI1 expression in OLP that transformed, leukoplakia, and OSCC as compared to OLP that did not transform and normal tissue[60]. BMI1 appears to be increased in a stepwise manner from OLP to dysplasia and OSCC indicating that it is expressed early in carcinogenesis and has potential to be a valuable marker[60].

Ki67 is a ubiquitous marker of cell proliferation[61]. Zargaran *et al* investigated Ki67 expression in oral epithelial hyperplasia, OLP, dysplasia, and frank OSCC[62]. They found a stepwise increase in Ki67 and that OLP had similar Ki67 levels to mild dysplasia[62].

A current proposed hypothesis for malignant transformation of OLP is centered around chronic inflammation beneath the basement membrane activating different pathways that can lead to tumor development through proliferation and migration of the basal-layer cells[14]. More

specifically, the inflammatory process creates a hypoxic environment with significant oxidative stresses present within. As a result, proteases are upregulated in the ECM and epithelium facilitating cell invasion and migration.

Tissue Remodeling Factors/proteases (MMPs and TIMPs) have been investigated. Matrix Metalloproteinases (MMPs) are secreted by macrophages, neutrophils and fibroblasts following stimulation by TGF-beta and IL-8[63]. MMPs increase angiogenesis through VEGF, affect cell-cell and cell-ECM adhesion, and they may also inhibit NK cell function[64,65]. Gianellia *et al* was the first to study MMPs in relation to OLP and hypothesized that dysregulation of MMPs and TIMPs cause disruption to the basement membrane. MMP-9 is an inducible enzyme that has been shown to be a diagnostic marker in tissue, saliva and serum of OSCC[63]. The same author completed a systematic review on the expression of MMP-9 in oral PMDs (including Lichen Planus) and found MMP-9 to be upregulated in these lesions but not to the same extent as in OSCC. They recommended further study regarding the utility of salivary and serum biomarker. A study by Chen *et al* investigated MMP-2 and MMP-9 in normal oral mucosa, OLP, and OSCC[66]. They found a stepwise increase in MMP-9 expression from normal mucosa to OSCC and purported that MMP-9 might be a predictor of OLP transformation[66]. The same study showed elevated MMP-9 in tissue, saliva, and serum of patients with premalignant lesions such as OLP[66]. Furthermore, multiple studies have shown that MMP 2 and 3 are within the epithelium of OLP and MMP 9 is within the adjacent inflammatory infiltrate[67]. Agha-Hosseini *et al* have shown a relative stepwise increase in MMP-3 expression in reticular LP erosive LP, early OSCC, to advanced OSCC[14]. Cathepsin B (CB) is a ubiquitous cysteine protease belonging to the papain family that is activated at low pH. It functions to increase the effectiveness of MMPs and has been linked to brain, lung, prostate, breast, colorectal and oral cancer[23]. Satelur *et al* found an

increase in stromal CB using immunohistochemistry in OLP tissue samples[23]. They proposed that this is a plausible mechanism for invasion of the overlying epithelium and hence, malignant transformation[23].

Inflammation related markers such as cytokines, cyclooxygenase 2 enzyme expression and galectins have been investigated. Cytokines are released by inflammatory cells and may be involved in angiogenesis, cell proliferation and malignant transformation[14]. IL-6, IL-7, IL-23 contribute to tumor progression. TNF-α, TGF-β and IL-6 have a direct effect on cell growth and rate of survival[30]. Rhodus *et al* examined the quantity of TNF-α, IL-1, IL-6, and IL-8 in the saliva of people with OLP, OLP with dysplasia (various grades), OSCC, and normal controls[15]. They found that salivary TNF-α was increased in OLP patients with moderate to severe dysplasia akin to levels in OSCC[68]. Tampa, M. *et al.* corroborated these results and they proposed that TNF-α and IL-6 could be used as prognostic markers in OLP transformation and detection of OSCC[14].

Cyclooxygenase is an enzyme with two isoforms, COX-1 and COX-2[69]. COX-1 is ubiquitous and plays a part in physiologic homeostasis[69]. In contrast, COX-2 is induced by inflammatory molecules, growth factors and hormones[14]. COX-2 has been implicated in cancers such as gastric and lung cancers[70]. It is postulated that this enzyme inhibits apoptosis, stimulates angiogenesis and induces immunosuppression[70]. Nonetheless, there are conflicting results in the literature regarding COX-2 expression in OLP. Changkong *et al* found increased COX-2 expression in OLP and this was also correlated with disease severity[71]. Other studies have suggested COX-2 as a marker of malignant transformation in oral precancerous lesions[28]. However, Neppelberg and Johannessen concluded that COX-2 is not a reliable marker for transformation of OLP to OSCC[72].

Galectins are endogenous carbohydrate binding proteins that alter immune cellular processes through stimulation of inflammation, activation of T cells and modulation of T regulatory cell activity[14]. They are involved with angiogenesis, cell growth, migration, adhesion, and apoptosis. Muniz *et al* found higher expression of Galectin 9 in OSCC as compared to Oral PMDs and normal tissue[73]. Ding *et al* found overexpression of Galectin 1 in OSCC and leukoplakia lesion that progressed to OSCC[74]. Galectin 1 has also been shown to be overexpressed in laryngeal cancer, melanoma and prostate cancer[75].

The role of intercellular adhesion protein, E- Cadherin has been investigated. E- cadherin is involved with cellular adhesion and differentiation[76]. In relation to cancer, the loss of E-Cadherin has been associated with poor cellular differentiation, invasion and metastasis[76]. In relation to oral PMD, Lichen Planus, results are unclear. Neppelberg and Johannessen found no correlation between the loss of E-Cadherin and transformation of OLP[72]. Sridevi *et al* found a decrease in the expression of E-Cadherin in poorly differentiated OSCC; however, they found no evidence to support that the loss of E-cadherin can be a useful predictor of transformation in OLP[77]. Claudins and E-cadherin are markers of Epithelial to Mesenchymal Transition (EMT). EMT is a physiologic process that occurs during growth; however, it is a pathologic process in relation to tumorigenesis. Hamalaienin *et al* found downregulation of Claudin 1 and 4 as well as E-cadherin in OLP[78]. They proposed that this may compromise cell-cell adhesion, tight junctions and permeability as well as contribute to pathogenesis and transformation. Further study is required in order to assess utility in predicting transformation of OLP.

Aghbari *et al* examined salivary and serum miRNA 27b and miRNA 137[31]. MicroRNA is noncoding RNA that regulates gene expression and plays a role in cell division, proliferation, differentiation and cell death. miRNA 137 is a tumor suppressor gene that has been shown to be

downregulated in OSCC[79]. Dysregulation in miRNA expression has also been associated with autoimmune conditions. This investigator found a decrease in the expression of miRNA 137 in the saliva and serum of OLP patients and an even greater decrease in expression in OSCC as compared to normal controls[31]. In addition, they also found a more significant reduction in miRNA 137 in the erosive subtype of OLP which coincides with its increased rate of malignant transformation[31]. They concluded that miRNA 137 could have utility in predicting and monitoring for malignant transformation and disease activity of OLP[31].

Caveolin-1,2, and 3 are highly expressed human membrane proteins that form caveolae, which play a role in intracellular signaling[80]. Studies suggest that Caveolin-1 expression is related to malignant transformation, differentiation, angiogenesis, tumor stage, and metastasis[81]. Research has also shown a stepwise increase in expression of Caveolin-1 (Cav-1) from normal oral mucosa to precancerous lesions and OSCC[82]. Aslani *et al* investigated Caveolin-1 expression in OLP, hyperkeratosis, epithelial dysplasia, and OSCC in an attempt to see if Cav-1 could be used as a predictive/prognostic marker for transformation of OLP[83]. Aslani found decreased expression of Cav-1 in OLP versus hyperkeratosis, ED, and OSCC possibly coinciding with its lower rate of malignant transformation[83]. They recommended further investigation of molecules that interact with Cav-1 and are involved in malignant transformation of oral epithelium. These molecules include Epidermal Growth Factor Receptor (EGFR) and E-cadherin-catenin complex.

1.4 MAPK proteins and S100A7 as biomarkers for predicting transformation in potentially malignant lesions

1.4.1 Mitogen Activated Protein Kinase (MAPK) Signalling Cascade

The mitogen activated protein kinases (MAPK) are central signaling elements that regulate cellular processes including proliferation, differentiation and stress responses[84]. MAPK is known to play an important role in apoptosis, angiogenesis, and tumor metastasis[85]. There are 4 distinct MAPK pathways: ERK1/2, p38, JNK 123, and ERK 5[84]. Each signaling cascade typically consists of 3-5 tiers of kinases including MAP4K, MAP3K, MAP2K, MAPK, and MAPK- activated protein kinases (MAPKAPK)[84]. These kinases activate downstream proteins. The diagram below is a diagrammatic representation of the 4 cascades (Fig. 1.1).

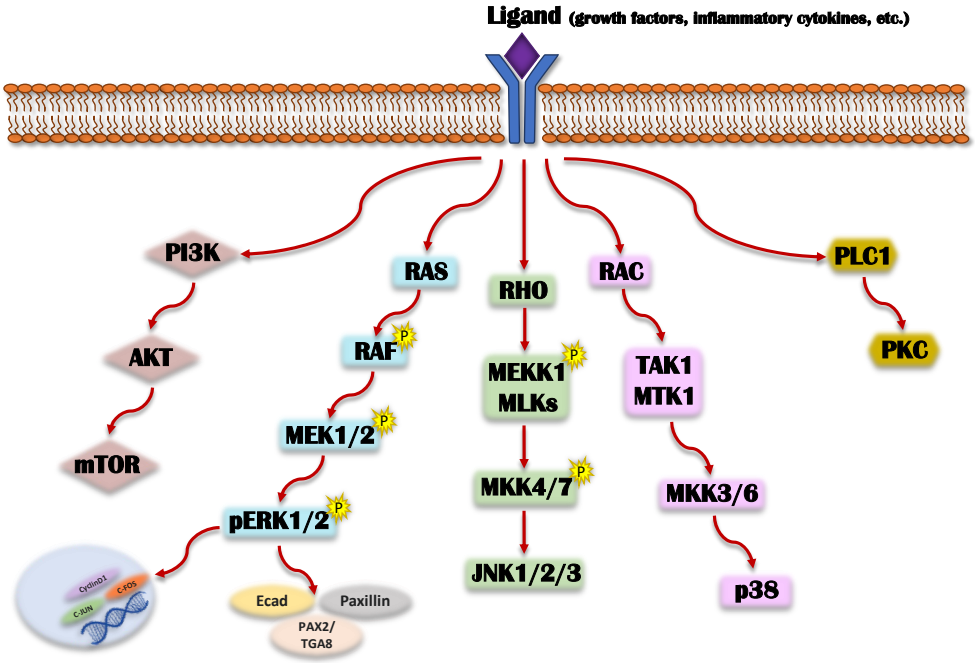

Figure 1.1 Schematic summary of the multiple MAPK pathways
Ligands or Cellular Stress activate the downstream signaling cascades of the JNK, p38, and ERK1/2 pathways.

JNK and p38 MAPK pathways have been shown to be related to stress and apoptosis while the ERK/MAPK functions more in proliferation, differentiation, and cell signal transduction[84].

ERK1/2 Signaling pathway

The ERK cascade was the first to be identified. It is involved in basic cellular processes including cell proliferation and differentiation[86]. Due to the important roles of these proteins, they are highly regulated through bispecific phosphatases, scaffold proteins, signal transduction and intensity, and the dynamic subcellular localization of cascade components[84]. This cascade involves a MAPK tertiary enzymatic cascade[84]. This consists of Ras as the upstream activating protein, Raf as a MAP3K component, MEK as a MAP2K component, and ERK as the MAPK component forming the Ras-Raf-MEK-ERK pathway. It is activated mainly through Receptor Tyrosine Kinase (RTK) activity. It has been found to be a major signaling route for EGFR. The final step in the MAPK/ERK signaling cascade is the phosphorylation of Extracellular signal-regulated kinase 1/2 which transmits extracellular signals to intracellular targets[84]. This ultimately leads to regulation of transcription in the cytoplasm and nucleus through Ecad, Paxillin, c-fos, c-Jun, and Cyclin D.

ERK Family and Cellular location

ERK is a serine/threonine Kinase that transmits mitogenic signals. It is located in the cytoplasm and enters the nucleus upon activation where it regulates gene expression[84]. Investigators have shown the presence of ERK 1, 2, 3, 5, and 5. ERK1/2 are the subtypes associated with MAPK. Growth factors, cytokines, viruses, G-protein-coupled receptor ligands,

and oncogenes activate the ERK pathway[86]. The G proteins involved in the MAPK/ERK pathway are discussed above and include Ras-Raf-MEK.

Ras

Ras is a G-protein product of the ras oncogene. It is activated by Epidermal Growth Factor, Tumor Necrosis Factor, Protein kinase C, and Src family members[84]. When one of these extracellular signals binds to their receptor, interaction between growth factor receptor-binding protein 2 (Grb2) and Son of Sevenless (SOS) leads to conversion of inactive Ras- GDP to active Ras-GTP[84].

Raf

Raf is a protein kinase encoded by the Raf gene. The Raf kinase family consists of three subtypes: Raf-1, A-Raf, and B-Raf. These subtypes differ in their tissue distribution, activity, and mode of regulation[87]. Raf-1 has an important role in the Ras/Raf/MEK/ERK cell proliferation signaling pathway[84]. Activated Ras binds to the Raf-1 on the inner surface of the membrane and then activates Raf-1 through tyrosine kinase[88]. Activated Raf-1 then activates MEK.

MEK

MAPK/ERK (MEK) is a Ser/ Thr Kinase which is activated through interaction with activated Raf[87]. MEK has two subtypes: MEK1 and MEK2 which in turn activate ERK through phosphorylation of tyrosine and threonine regulatory sites[84].

ERK

MEK has the ability to activate ERK and also anchors ERK in the cytoplasm when the pathway is inactive. When the pathway is activated, ERK is phosphorylated, dimerizes, and translocates to the nucleus. While in the cytoplasm, ERK can phosphorylate Microtubule-

associated protein (MAP)1, MAP2, and MAP4. In the nucleus, ERK phosphorylates nuclear transcription factors such as proto-oncogenes c-fos, c-jun, c-myc. ERK1/2 is also able to negatively feedback to cytoplasmic SOS, Raf-1, and MEK[84].

ERK and Cancer development

Disorders associated with ERK dysregulation have been shown to induce diseases such as inflammation, developmental disorders, neurological disorders, and cancer[84]. Elevated ERK expression has been detected in ovarian, colon, breast, and lung cancer[84]. Activation mutations of this pathway are the most abundant oncogenic factor across all cancer types[84]. Continuous ERK/MAPK signaling can promote the transformation of normal cells into tumor cells. Conversely, inhibition of ERK/MAPK signaling can inhibit tumor growth in vivo[84]. It is able to do this through promoting proliferation and having an anti-apoptotic effect. For example, VEGF release secondary to hypoxic stress can inhibit apoptosis through activation of ERK/MAPK pathway[84]. The same author notes this pathway's role in promoting invasion and metastasis, degradation of tumor extracellular matrix through MMPs, tumor cell migration, and tumor angiogenesis. Albanell *et al*, used a specific EGF receptor tyrosine kinase inhibitor (Iressa) and a chimeric anti-EGF receptor antibody (Cetuximab) to inhibit ERK1/2 activation and autocrine cell proliferation in head and neck cancers[89]. The same author suggested that ERK1/2 could be used as a potential surrogate marker in clinical therapeutic studies.

P38 signaling Pathway

There are four P38 kinases in mammals including alpha, beta, gamma, and delta[90]. P38 alpha subtype is most studied and is present in most cell types. Together with the JNK family, P38 MAPK are known as the Stress- Activated Protein Kinases (SAPK). Both are activated by MKK3 and MKK6 in the presence of inflammatory cytokines and environmental stress. Growth

factors do not have a large activating role[90]. Activation occurs through dual phosphorylation of Thr-Gly-Tyr motif[90]. A general overview of the P38 signaling cascade is displayed below (Figure 1.2). More recently, it was discovered that P38 could be activated outside of the MK3-Mk2-P38MAPK pathway. Auto phosphorylation can occur via TAK1[90]. A second independent mechanism of activation occurs through T cell antigen receptor (TCR). P38MAPK interacts with multiple scaffold and binding proteins that can help to regulate signaling.

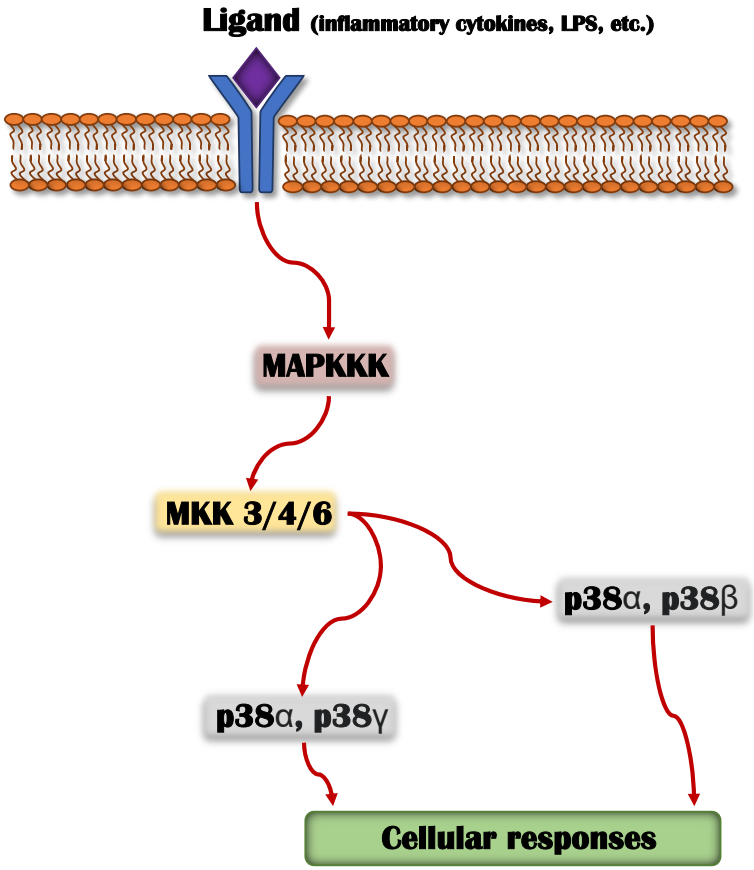

Figure 1.2 P38 MAPK signaling pathway
P38 MAPK activation and signaling pathway.

P38MAPK is located in the cytoplasm and nucleus of quiescent cells. Once activated, downstream targets exist in both the cytoplasm and nucleus[90]. Some of these targets include:

transcription factors, protein kinases, cytoskeletal proteins, translational machinery, and enzymes such as glycogen synthase or cytosolic phospholipase A2[90].

P38MAPK function

P38 has been proposed to play a role in cellular differentiation. Some of the processes involved include osteoclastogenesis, adipogenesis, intestinal epithelial cell differentiation, neuronal plasticity[90]. Myocyte and keratinocyte differentiation have also been proposed. The keratinocyte differentiation process begins in the basal layer of the epithelium and continues through the metabolically active spinous and granular layers. The mechanism of Keratinocyte differentiation is thought to be through protein: Involucrin[90]. Studies have found that increased expression of multiple P38 (alpha and delta) isoforms may be associated with upregulation of Involucrin mRNA.

P38MAPK has been implicated in angiogenesis, cell motility and cell invasion. One mechanism is through Matrix Metalloproteinases (MMPs). It has been shown that inhibition of P38 alpha blocks MMP-9 expression in human squamous cell carcinoma[90].

P38MAPK and inflammation

P38 alpha has a role in regulating the biosynthesis of inflammatory cytokines such as IL-1, IL-6, and TNF alpha[90]. COX-2 has also been shown to be regulated by P38 alpha[90]. Inflammatory cytokines play an important role in inflammatory diseases and rheumatic disease. Some of these conditions include Inflammatory Bowel Disease, Rheumatoid Arthritis, Psoriasis, Ankylosing Spondylitis, and asthma.

P38MAPK and Cancer Development

P38 may have a tumor suppressor role and oncogenic role. P38 may be involved in self-sufficiency in growth signals, unlimited replication potential, protection against apoptotic death, de novo angiogenesis, tissue invasion and metastasis and a regulator of checkpoint controls[90]. The oncogenic role may also be through mechanisms such as: promoting VEGF and angiogenesis and MMP-9 regulation. Through upregulation of MMPs, P38MAPK has been shown to correlate with invasive phenotypes of cancer cells.

Its tumor suppressive function is mainly through negative regulation of cell cycle progression and the induction of apoptosis[91]. In a cell type dependent manner, P38 either causes progression or inhibition through regulation of cyclin levels.

C-Jun N-terminal kinase (JNK) signaling pathway

C-Jun N-terminal kinases (JNKs), previously known as Stress-activated protein kinase (SAPK) also belongs to the MAPK family[91]. JNK is involved in a wide variety of cellular processes including cell proliferation, differentiation, migration, inflammation, and apoptosis. The JNK family consists of three members encoded by three genetic loci: JNK 1 and 2 are present in most tissues, whereas JNK 3 is localized to the brain, heart, and testes. There are at least 10 different isoforms of JNK due to splicing[91]. Like P38MAPK, JNK responds less so to RTK and more to stress signals. JNK is activated by cytokines such as TNF alpha and IL-1, UV radiation, cellular stress (inflammation, ischemia, hypoxia), reagents that cause DNA damage, G-protein- coupled receptors (e.g. RAS), serum growth factors. The signaling cascade that results in activation of JNK through phosphorylation is demonstrated in Figure 1.4. Once JNK is activated/phosphorylated in the cytoplasm, it translocates to the nucleus where it interacts with

downstream targets include c-Jun, ATF-2, p53, ELK1, Smad4, STAT3, and NFAT4 displayed diagrammatically below:

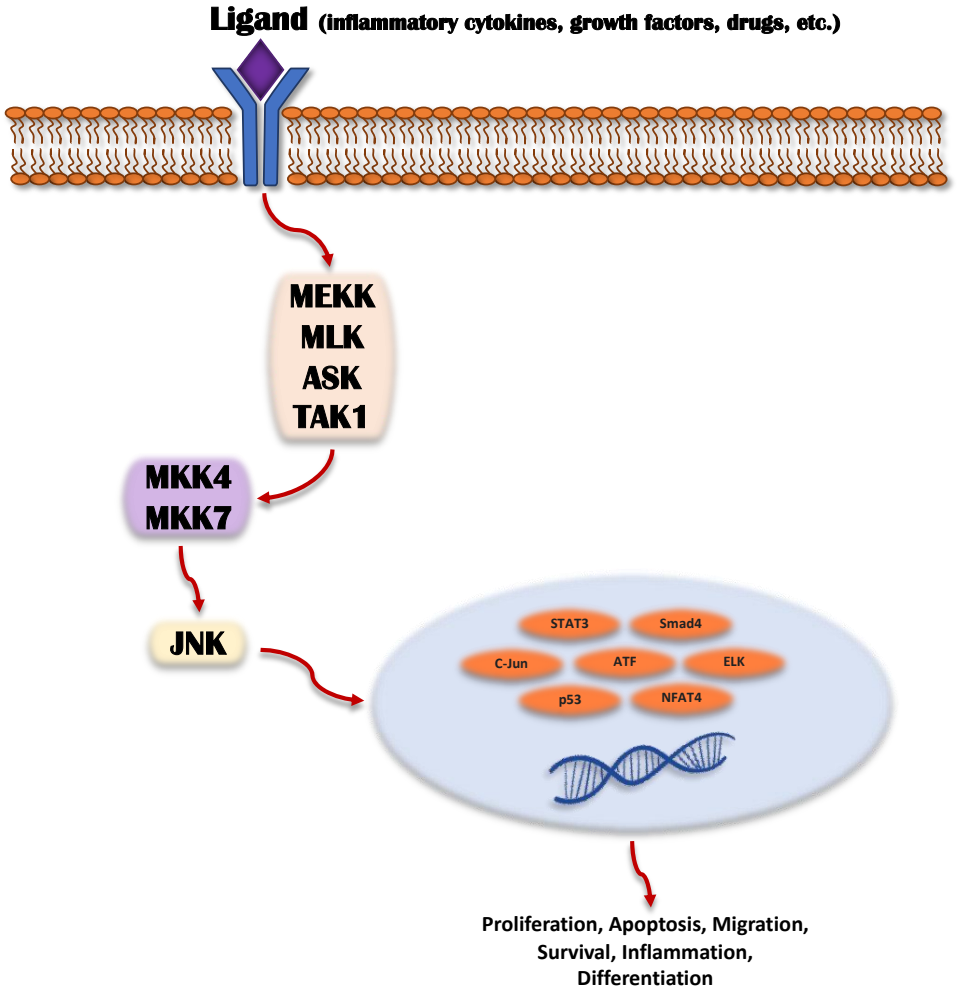

Figure 1.3 Activation and downstream targets of the JNK signaling pathway
JNK signaling pathway is displayed including downstream targets: SMAD 4, p53, NFAT, and STAT3, C-Jun, ELK, and ATF. These molecules regulate inflammation, proliferation, apoptosis, migration, survival, and differentiation.

JNK and Cancer Development

Like P38MAPK, JNK likely has an oncogenic and tumor suppressive role. It is proposed that short term stimulation of JNK may lead to apoptosis, however, long term stimulation may lead to cell survival[88]. The tumor suppressor role may be related to their pro-apoptotic activity.

The oncogenic role of JNK is likely related to phosphorylation of the AP1 target: c-Jun[91]. AP1 targets have effect on cell cycle control, survival and apoptosis, MMPs, and nuclear hormone receptors.

The role of JNK is not completely understood but it is believed to have tumor promoting and suppressing functions in different types of malignant cells, including oral cancer[92]. The chosen role is tissue specific and cell-type dependent. It is also dependent on tumor stage and availability of upstream and downstream molecules[92].

Less is known about the ERK 5 pathway, however Kurtzeborn *et al* state that this pathway is also activated by inflammatory cytokines, ischemia, hypoxia, and to a lesser extent RTK[93]. Again, the cellular processes associated with this signaling cascade are proliferation, migration, survival, and angiogenesis.

1.4.2 S100 Protein Family

S100 proteins are the largest subgroup of a superfamily of calcium binding proteins called EF hand (helix-loop-helix structure). S100 proteins are expressed in a cell specific and tissue specific manner and have intracellular and extracellular functions[94]. Among these include: regulation of calcium homeostasis, cell proliferation, apoptosis, cell invasion and motility, cytoskeleton interactions, protein phosphorylation, regulation of transcriptional factors, autoimmunity, chemotaxis, inflammation, and pluripotency[68]. S100 proteins have been associated with cardiovascular disease, inflammation, autoimmune pathology, brain disease, and cancer. Twenty-two of the S100 genes are located at chromosome locus 1q21. S100 proteins on the 1q21 locus such as S100A4, S100A7, S100A8/A9, S100P, and S100B have been implicated in tumor progression, angiogenesis, and metastasis. Rearrangements and deletions in this region in particular have been found to be implicated in cancers. It appears that this family of S100

proteins is a current target for oncologic therapy as well. Selective inhibitors of S100 proteins are in clinical trials[95].

S100A7 Protein

S100A7 (Psoriasin) is a 11.4KDa protein encoded by the 1q21.3 chromosome locus (epidermal differentiation complex). S100A7 was first described as a secreted and nuclear/cytoplasmic protein in psoriatic keratinocytes[95]. Studies by Padilla *et al* and Martinsson *et al* found S100A7 upregulation with changes in environmental conditions such as hypoxia, soluble factors (IL-6, TNF alpha), increased cell density/confluence, and loss of cell attachment to the basement membrane (anoikis)[96]. Retinoic acid, extracellular calcium, UV radiation, and changes in cell adhesion have been shown to increase S100A7 expression in vitro[96]. Many of the above factors are also known to lead to keratinocyte differentiation through KRT-1. It is therefore proposed that S100A7 is involved with keratinocyte differentiation more than proliferation.

S100A7 expression in Normal Epithelium

Zhou found no expression in the dividing basal layer of normal tongue tissue[97]. The same author found low level scattered expression of S100A7 in the suprabasal layers of normal tongue epithelium. Other studies have produced similar results and have found low levels of expression of S100A7 in normal keratinocytes and fetal skin[98]. Conversely, S100A7 has been shown to be upregulated and present in the cytoplasm and nucleus of keratinocytes in benign hyperplastic epithelium, wounded epithelium, inflammatory epidermal conditions (psoriasis, atopic dermatitis, mycosis fungoides, Darier's disease, and lichen sclerosis et atrophicus), dysplasia and multiple cancers[97].

S100A7 and Wound Healing

S100A7 is thought to be associated with processes which are fundamental in wound healing such as keratinocyte growth, proliferation, differentiation, adhesion, and migration. S100A7 has been shown to be upregulated in the suprabasal layers of acutely wounded epidermis as compared to chronic wounds and unwounded tissue[98]. The same study found that S100A7 was upregulated in accordance with cellular mitotic rate. In vitro experiments have shown downregulation of S100A7 at wound edges leading to increased rate of cell migration across a wound. It is thought that S100A7, when present, may block an alternative pathway that leads to cell growth and migration. Multiple studies have confirmed that increases in the rate of keratinocyte adhesion, migration and growth have been observed in Psoriasin deficient cells. A study by Lee and Eckert proposed that S100A7 is upregulated in wounded tissue, secreted into wound exudate and serves an antibacterial function as well[99].

S100A7 and Malignancy

S100A7 has been shown to be upregulated in the epithelium of lung, ovarian, cervical, pancreatic, stomach, larynx, esophageal, skin, ER-positive breast, and oral dysplastic lesions and malignancy[100]. Like in wounded tissue, there also appears to be differential expression within the layers of the epithelium[101]. The stratum basal of epithelium seems to have minimal expression of S100A7 whereas the differentiating layers of the epithelium have increased expression. Martinsson *et al* found S100A7 upregulation in the higher and more differentiated epithelium in epidermoid carcinomas[96]. In contrast, they found reduced to absent expression in the undifferentiated periphery of the invading epithelium. Other studies have reported increased S100A7 in well differentiated versus poorly differentiated cancers[102]. These findings further support the hypothesis that S100A7 is involved with cell differentiation more than proliferation.

More recently, a "biphasic" expression of S100A7 has been associated with certain types of malignancy such as ER-positive breast cancer and OSCC[97]. Yadwinder S. Deol *et al* found a tumor suppressive effect (reduction of proliferation, chemotaxis, and wound healing) of S100A7 in ER-positive breast cancer through down modulation of the beta catenin/ T- Cell Factor 4 pathway (proto-oncogenes: Cyclin-D1 and C-myc)[103].

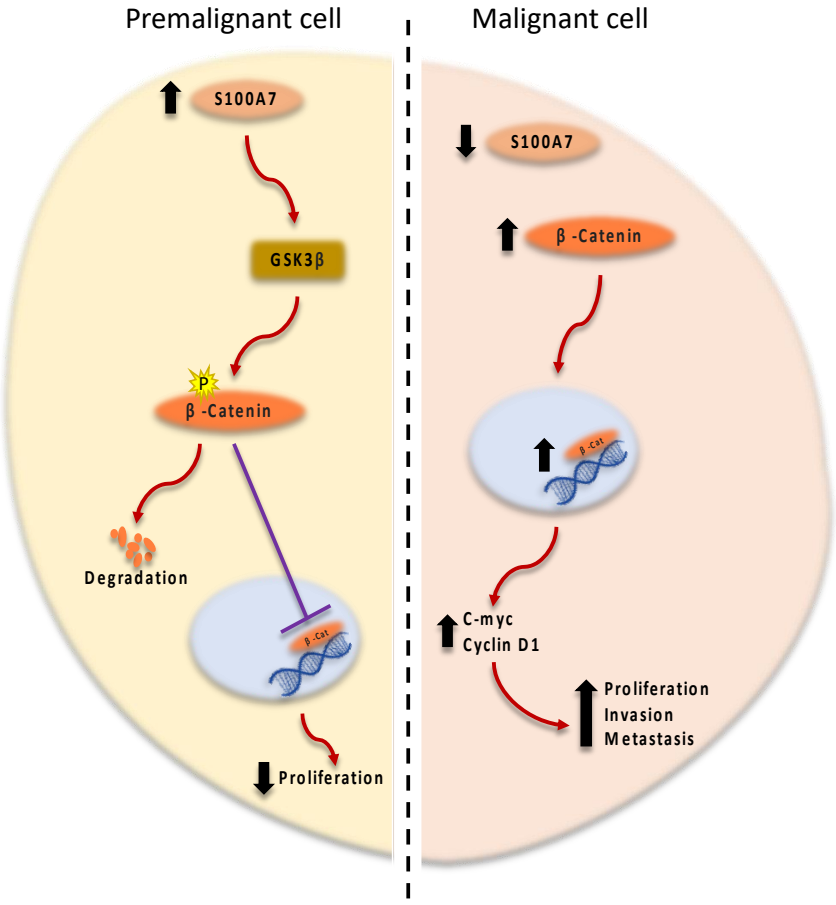

Figure 1.4 S100A7- mediated signaling that inhibits proliferation and motility
S100A7 is upregulated in premalignant lesions and suppresses tumor progression by inhibiting the downstream actions of Beta-Catenin. Conversely, downregulation of S100A7 promotes tumor progression through upregulation of Beta-Catenin and TCF4 which then up-regulates targets Cyclin D1 and C-Myc. This may be responsible for increased proliferation/tumor growth.

Zhou *et al* corroborated these findings in OSCC[97]. They found a reciprocal relationship between S100A7 and B-Catenin signaling. During the early stages of tumorigenesis, S100A7 is

upregulated and reciprocally inhibits the pro-oncogenic B-Catenin signaling. The mechanism of B-Catenin inhibition is strongly suggested to be post-transcriptional regulation (proteasome mediated protein degradation). Later in tumorigenesis, S100A7 is down regulated by the B-Catenin signaling pathway and leads to tumor growth, progression, and invasion. The mechanism of negative feedback on S100A7 is unknown. The same author showed reduced E-cadherin cell-cell adhesion with decreased expression of S100A7. Therefore, it has been proposed that B-Catenin signaling function is a "master switch" for proliferation vs. differentiation and that S100A7 overexpression may be a protective (Pro-differentiation and anti-proliferation/migration) mechanism against early tumorigenic changes[97,104].

Overexpression of S100A7 has been shown in psoriatic skin lesions with minimal B-catenin/C-Myc signaling activation. This is thought secondary to abnormal keratinocyte differentiation[105].

In summary, it appears as though S100A7 is upregulated in both benign and malignant keratinocyte hyperplasia and there is a preferential expression in differentiated epithelium. It also appears to have a very cell/tumor specific pro or anti carcinogenic role possibly mediated by the B Catenin signaling pathway.

S100A7 role outside of the epithelium

S100A7 has also been localized outside of the epithelium. Alowani *et al* found S100A7 in the dermis adjacent to lesions with a high level of S100A7 within the epidermis[101]. Other studies have examined the extracellular/stromal effects when S100A7 is secreted into the extracellular environment and acts on various receptors such as RAGE[106]. Some of these effects being: immune cell and tumor cell migration and proliferation of endothelial cells through interaction with the RAGE receptor[106,107].

S100A7 and the MAPK Signaling Pathway

A study completed by Dey *et al*, examined the relationship between S100A7 and the MAPK Pathway[108]. Quantitative real-time PCR analysis showed that S100A7 expression was reduced by siRNA transfection, leading to the downregulation of the RAB2A gene through the p38 MAPK signaling pathway[106]. Knockdown of S100A7 gene decreased cell migration in wound healing assay and Boyden chamber assay. They also noted that Knockdown of S100A7 reduces activation of MMP 2 and 9 and increases E cadherin expression at the cell surface[106]. They concluded that a reduction in S100A7 expression may decrease invasion and improve cell-cell adhesion.

A study by Kaur *et al* examined multiple biomarkers and their expression in oral dysplastic lesions and concluded that among the biomarkers examined, S100A7 was overexpressed in dysplastic oral lesions, and that S100A7 overexpression alone or in combination with dysplasia grade might have the potential to serve as a useful marker for estimating the risk of oral dysplastic lesions progressing to malignancy[109].

Sivadasan *et al* also demonstrated elevated salivary S100A7 in leukoplakia and OSCC[68]. Their conclusion was that S100A7 shows significant potential for use as an early and non-invasive detection marker in dysplastic PMD: Leukoplakia and OSCC.

Mclean *et al*, examined the expression of S100A7 in transforming and non-transforming dysplastic oral lesions and found limited usefulness for this marker in predicting malignant transformation[110]. They recommended further study of S100A7 to corroborate or refute their findings.

To date, there does not seem to be any investigation involving the utility of S100A7 in predicting malignant transformation in OLP and hence the need for this study.

Epidermal Growth Factor Receptor (EGFR) is a plasma membrane glycoprotein that dimerizes upon ligand binding leading to tyrosine auto phosphorylation through protein kinase (RTK) activity[111]. This leads to mitogenic signal transduction cascades that regulate cell proliferation, differentiation, survival, and transformation[89]. Downstream signaling of the EGFR receptor includes the Ras-Raf-MAPK pathway. Activation of Ras leads to phosphorylation of ERK 1/2, which have been shown in vitro to regulate cell proliferation, survival, and transformation[89]. Albanell used immunohistochemistry on 101 primary head and neck squamous cell carcinoma paraffin-embedded specimens to identify phosphorylated/activated ERK 1/2[89]. They found that ERK 1 and 2 are commonly activated and result in an increased tumor proliferative index in head and neck primary tumors and may have a role in malignant progression. Albanell *et al*, also found a positive correlation between the expression of EGFR and TGF-alpha and the activation of ERK 1/2 in vivo[89]. Conversely, some tumors displayed high levels of EGFR family activation with low ERK 1/2 phosphorylation. They hypothesize that this may be due to activation of another signal transduction pathway through the EGFR receptors such as JAK/STAT or phosphatidylinositol- 3-kinase. Albanell *et al*, were also able to show that inhibiting EGFR activation decreased ERK 1/2 expression[89].

1.5 The Straticyte Test

As mentioned above, the current standard of care prognostic tool to predict malignant transformation in PMDs is problematic: poor predictive value of histopathological grades of dysplasia and great inter and intraobserver variability among pathologists[112]. The poor predictive value of histopathologic grading may be anxiety producing for the clinician and patient when deciding how to manage PMDs (mild ED, Lichen planus, lichenoid mucositis). Being able to better prognosticate may improve physician confidence in managing PMDs and

communicating a prognosis to the patient. S100A7 has been described as a biomarker for head and neck cancer and oral dysplasia[113]. The two have been linked qualitatively and now quantitatively using the straticyte test[112]. Straticyte uses quantitative biomarker measurement and statistical modeling. Straticyte can calculate the 5-year probability that dysplastic lesions will progress to cancer and provides greater objectivity, sensitivity, and predictive power than histopathologic grading. Straticyte categorizes lesions with high, intermediate, and low risk of malignant transformation. Sensitivity and specificity are generally inversely related, so straticyte maximizes specificity when categorizing lesions as high or non-high risk. Conversely, Straticyte maximizes sensitivity when categorizing lesions as low or intermediate risk. Therefore, high risk cases are more likely to progress, and low risk cases are more likely to not progress. Hwang *et al* stated that straticyte will have its most significant impact on clinical management for cases with mild epithelial dysplasia as moderate and severe tend to be excised if feasible[112]. They report that a potentially malignant lesion with mild epithelial dysplasia and a low risk Straticyte can be confidently monitored by the clinician whereas mild dysplasia with an intermediate or high risk Straticyte may be excised or monitored more closely.

Hwang *et al* observed Straticyte's superior performance to histopathologic grading in a single cohort; however, the authors recommended another independent cohort to provide validation[112]. Mclean *et al* recently examined the ability of Straticyte to predict malignant transformation using marker S100A7 in dysplastic oral lesions[110]. This study found Straticyte to be neither superior nor inferior to manual scoring methods in predicting malignant transformation. Hwang *et al* recommended further examination to see if Straticyte is prognostic for progression to cancer in pathologic conditions such as oral lichen planus, where dysplasia is absent[112].

Chapter 2

2.1 Hypothesis

We hypothesize that S100A7 is increased in the epithelium of Lichen Planus lesions and potentially malignant lesions which transform into squamous cell carcinoma. The proposed mechanism is through association with proteins P38, ERK1/2, and JNK1/2 of the MAPK signaling pathway.

2.2 Rationale

Oral Lichen Planus is classified as a Potentially Malignant Disorder (PMD), and as such, is capable of malignant transformation into oral squamous cell carcinoma. Oral squamous cell carinoma continues to be diagnosed quite late in the disease process contributing to its poor prognosis. Current prognostic indicators of PMDs have proven to be subjective and less than ideal in predicting malignant transformation in premalignant lesions. Biomarkers such as S100A7 are currently being investigated in attempt to add objectivity and accurate prediction of transformation in PMDs. To date, many biomarkers have been studied to predict severity of disease and transformation in a specific PMD, OLP. Some markers appear to show promising results, but none are ready for clinical application. S100A7 has been shown to have an effect on downstream signalling pathway: MAPK. This pathway participates in cancer progression through Epithelial to Mesenchymal Transition, inhibition of apoptosis, and invasion through activation of MMPs. The literature regarding the utility of S100A7 in predicting transformation in other PMDs, such as leukoplakia/dysplasia is conflicting. To my knowledge this is the first study to examine biomarker S100A7 in OLP.

Straticyte is a tool that utilizes quantitative biomarker measurement and statistical modeling. Straticyte can calculate the 5-year probability that dysplastic lesions will progress to cancer and provides greater objectivity, sensitivity, and predictive power than histopathologic grading. Quantification of S100A7 using Straticyte in OLP could provide a more objective and accurate method of risk determination compared to the current standard. This could aid in clinical management of OLP and PMD's through risk stratification and prevention/early intervention of OSCC.

2.3 Aims

1) To show that there is greater expression of S100A7 in Lichen Planus and other PMDs than in normal epithelial control tissues.

2) To show that there is a greater expression of S100A7 in Lichen Planus and other PMDs that progress to dysplastic lesions and frank OSCC than in lesions that do not progress.

3) To evaluate the expression of P38, ERK1/2, and JNK in Lichen planus lesions that progress vs. lesions that do not progress.

4) To test the utility of an image-based algorithm (Straticyte) utilizing S100A7 in Lichen Planus and other PMDs in accurately predicting progression.

Chapter 3

3.0 Materials & Methods

3.1 Lichen Planus

3.1.1 Case Selection

All patient biopsy reports showing an initial diagnosis of Lichen Planus or clinical and histopathological features consistent with Oral Lichen Planus and the subsequent intraoral biopsies were selected from the University of Western Ontario Oral Pathology database. Biopsy reports were collected from the time period between year 2003 to 2018. Cases were excluded from the Lichen Planus group if the initial diagnosis contained dysplasia or carcinoma (in situ or invasive).

3.1.2 Specimen Location

No region of the oral cavity was excluded from this study. The location of the sampled tissue as well as other areas of involvement within and outside of the oral cavity were recorded. If the lesion transformed on subsequent biopsies, the location of the malignancy, type of malignancy, or location and grade of dysplasia was recorded. For the Non-progressing cases, the location and subtype of the original sampled tissue was recorded along with the location and subtype of the subsequent tissue sample. The time in between the original biopsy and follow-up biopsy was also recorded.

3.1.3 Demographics

From the pathology reports, demographic data such as sex and age at time of biopsy was obtained. The time lapse from the initial biopsy to the biopsy showing malignancy/dysplasia was recorded. For the non-progressing cases, the time lapse between tissue sampling was also recorded. Known risk factors for the development of premalignant and malignant oral squamous

cell carcinoma independent of the presence of Lichen Planus are tobacco and alcohol use. In an attempt to control for these confounders, this information was taken from the report if provided.

3.2 Lichenoid Mucositis and Dysplasia

3.2.1 Case Selection

The same patient data base was examined as above. Patients whom had serial biopsies from 2003 to 2018, with the initial diagnosis of "lichenoid mucositis" or "lichenoid inflammation" were included in this subgroup. Based on the clinical information given, these specimens did not satisfy the WHO criteria for OLP.

3.2.2 Specimen Location

Similar to the Lichen Planus group above, this study is inclusive of any specimen within the oral cavity with a histopathologic and clinical diagnosis of Lichenoid mucositis/inflammation. Like the Lichen Planus group, the initial Lichenoid mucositis specimen location within the oral cavity and the ensuing dysplasia grade and location was recorded. If the Subsequent biopsy showed malignancy, the type and location of the malignancy was recorded.

3.2.3 Demographics

As above, the demographic data inclusive of age at original biopsy, sex, time from initial biopsy to progression and confounding risk factors were recorded.

3.3 Lichen Planus and Lichenoid Mucositis H and E evaluation

The hematoxylin and Eosin stained specimens coinciding with each of the progressing and non-progressing cases was pulled from the Oral Pathology archives at Western University in London Ontario. The histologic component of the diagnosis of Lichen Planus was confirmed by an Oral and Maxillofacial Histopathologist and a graduate student based on the cardinal features

such as: a subepithelial lymphocytic infiltrate, lymphocyte exocytosis, basal cell liquefactive necrosis. The lichenoid mucositis and dysplastic hematoxylin and Eosin stained sections were also reviewed to ensure correct histopathologic diagnosis.

3.4 S100A7 Staining and Analysis

3.4 1 Specimen Preparation

Hematoxylin and Eosin stained tissue slides corresponding to the above biopsy reports were recovered from the Oral Pathology archives. These slides were logged and stored by case number for future tissue examination and confirmation of histopathological diagnosis. Tissue blocks corresponding with the chosen patient biopsy reports were recovered from Oral Pathology archives. Fifteen five micrometer tissue sections from each tissue block were retrieved using a microtome (Microm HM 325;GMI Inc., Ramsey, MN). The sections were floated on a water bath and picked up onto positively charged glass slides. The slides were dried in a thirty-seven-degree Celsius oven overnight. The glass slides were then arranged by case number and stored at room temperature in slide boxes.

3.4.2 S100A7 IHC Protocol

For each case, one slide for staining with the primary antibody (Mouse Monoclonal Psoriasin/S100A7 Antibody (47C1068**),** NB100-56559, Cedarlane Laboratories, Burlington, ON) and one slide with no primary antibody was selected. High risk and low risk control slides were used for comparison. The above tissue sections were rehydrated using a sequential timed protocol with 100% xylene (2x5 minutes and 1x minute), 100% ethanol (1x2 minutes and 1x1 minute), 95% ethanol (1x2 minutes and 1x1 minute), 70% ethanol (2 minutes), followed by tap water for 2 minutes. Antigen retrieval was performed in Tris-EDTA buffer with a pH of 9 in a

decloaking chamber set to 112.5 degrees Celsius for 1.5 minutes. The pressure was then reduced to 90 degrees Celsius for 10 seconds.

The slides were then cooled under running tap water and washed three times for three minutes with Tris Buffered Saline (TBS-T) under gentle agitation. The tissues were then blocked for 15 minutes using MACH 4 Background punisher (BP974L, Inter Medico, Markham, ON) (125 microliters per slide). The blocking agent was drained and Psoriasin/S100A7 mouse monoclonal IgG was diluted to 1:2000 in 1.5% horse serum. Negative controls received the 1.5% horse serum alone. The slides were then left to incubate for one hour at room temperature in a humidified chamber.

After primary antibody incubation, the slides were washed three times for three minutes with TBS-T under gentle agitation. The slides were then incubated in 3% Hydrogen Peroxide in TBS for 10 minutes to block endogenous peroxidase activity. The slides were then washed once with TBS-T for three minutes.

The slides were then incubated for fifteen minutes with 125 microliters of MACH 4 Mouse Probe (MACH 4 Universal HRP-Polymer kit, M4U534, Inter Medico, Markham, Ontario). Three x three minute rinses with TBS-T were completed. MACH 4 HRP Polymer (MACH 4 Universal HRP-Polymer kit M4U534, Inter Medico, Markham, Ontario) in the amount of 125 microliters was added to each slide followed by incubation for 15 minutes. Three x five minute rinses in TBS-T was then completed.

Slides were developed in freshly made Diaminobenzadine/DAB (VECT SK4100 MJS Biolynx, Brockville, ON) solution for 5 minutes. DAB solution consisted of 5mL distilled water, 84 microliters of buffer, 100 microliters of DAB and 80 microliters of hydrogen peroxide.

Slides were then placed in distilled water followed by a counterstain with Harris haematoxylin (3801561, Leica Microbiosystems, Richmond Hill, ON) for 1 minute. Slides were then washed in water and differentiated in 1% acid alcohol (HCl in 70% Ethanol) and washed again in water. The slides were blued in 2% Ammonium Hydroxide/70% ethanol, followed by another wash in water.

The tissue was then dehydrated using 70% Ethanol (1 minute), 95% Ethanol (2x2 minutes), 100% Ethanol (2x3 minutes), and xylene (2x5 minutes). The slides were cover slipped using Cytoseal (8310-4, Thermo Scientific London, ON).

3.4.3 Staining Controls

A tissue specimen with previously determined S100A7 expression and a high risk straticyte score was chosen for comparison. A positive was included for future comparison to study tissues and to ensure the staining protocol worked. A Negative of the same specimen was also included to ensure that we were not obtaining non-specific staining/background stain.

A separate tissue specimen with previously determined low levels of S100A7 expression and low straticyte score was chosen for comparison. Again, both a positive and negative was included.

3.4.4 Specimen Analysis

S100A7 IHC Specimen analysis- Semi quantitative and qualitative

Manual scoring of the S100A7 stained tissues was completed based on the percentage of cells stained. Two reviewers (oral histopathologist and graduate student) agreed on and assigned a score from 0 to 5 as per the table 3.1.

Table 3.1: Manual Score/ Immunoreactivity Score – Percent of Cells Stained

Score	Cells stained
0	zero
1	1-20%
2	21-40%
3	41-60%
4	61-80%
5	81-100%

Manual scoring based on the intensity of staining was completed in the same fashion by the same reviewers. Each tissue specimen was assigned a score from 0 to 3 as per the table 3.2.

Table 3.2: Manual Score/ Immunoreactivity Score – Stain Intensity

Score	Staining Intensity
0	none
1	mild
2	moderate
3	intense

Tissue level (basalis, granulosum, spinosum, lucidum and corneum) of stain was also recorded and whether the stain was widespread or focal.

S100A7 IHC Specimen analysis- Qupath

Microscopic photographs of the S100A7 stained tissues were taken and uploaded into Qupath software program. The epithelium (from basal layer up to and not including corneum) was delineated and the total area was measured. A second measurement was taken of the stained epithelium up to and not including the corneum. The percentage of stained epithelium was calculated as per the equation below:

(Area of stain / Total epithelial area) x 100 = Percent of stained epithelium

The measurements were completed by two independent observers (graduate student and undergraduate student) who were trained/calibrated together to minimize inter observer variability.

S100A7 IHC Specimen analysis- Straticyte

The S100A7 stained Lichen Planus, Lichenoid Mucositis, and dysplastic tissues were digitally scanned at 20x magnification on a Hamamatsu Nanozoomer-XR slide scanner (Toronto Centre for Phenogenomics, Toronto, Canada). The digital images of the slides were imported into Visiopharm VIS (Hoersholm, Denmark). Using Visiopharm VIS, up to five 500 μm diameter region of interests (ROIs) were centered on areas with the highest S100A7 expression in the stratified mucosal epithelium and the S100A7 positivity (given as a percentage) and average cell size (total area of the ROIs / total number of identified nuclei) were calculated and used to generate the Straticyte risk class and probability of cancer progression. The risk class and probability of cancer progression algorithm was generated using a clinical reference database of 150 unique cases (Proteocyte AI Inc., Toronto, Ontario).

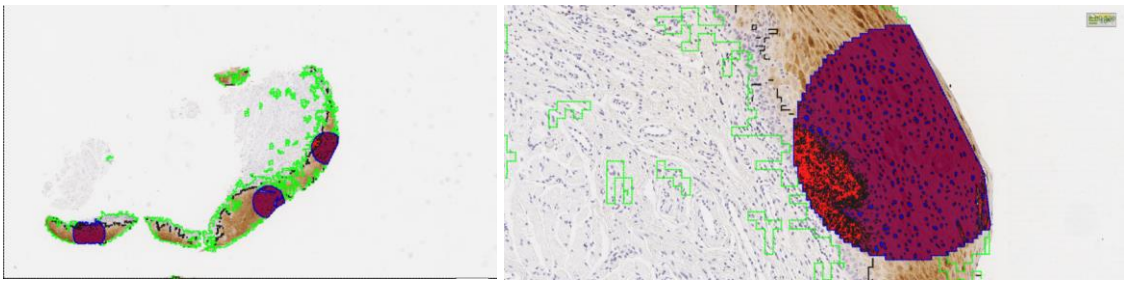

Figure 3.1 Visiopharm output of Lichen Planus – Malignancy specimen at low and high mag
Regions of interest (ROIs) are outlined in dashed blue. Within the ROIs: red = S100A7- negative cytoplasm; green = S100A7-negative nuclei; maroon = S100A7-positive cytoplasm and blue = S100A7-positive nuclei. Image provided by Dr. J. Hwang, Proteocyte AI, Toronto, ON, Canada.

Straticyte Risk Determination and Probability of 5-year Cancer Progression

The two principles below were used to determine a selection cut-off:

1. For all cases, a high cut-off was selected to differentiate the high-risk and non-high-risk groups, with specificity >85% and P value of log rank test between high- and non-high-risk groups <0.05.
2. For cases in the non-high-risk group, a low cut-off was selected to differentiate medium-risk and low-risk groups with sensitivity >90% and P value of log rank test between the medium- and low-risk groups <0.05.

For both cut-offs, once the criteria were met, the cut-off that gave the best-balanced accuracy (average of sensitivity and specificity) was chosen. The Nelson-Aalen-Breslow estimate, used to calculate the baseline cancer-free survival curve, was combined with the calculated risk scores from the 150 unique cases, to produce the expected 5-year cancer-free survival probability for a given case. Once this 5- year cancer progression algorithm is calculated, a new case can be assessed a 5-year probability of cancer progression and assigned a low-, medium-, or high-risk.

3.5 Normal Tissue and Hyperkeratosis Model

3.5.1 Specimen Selection

The corresponding histopathology code number for normal tissue samples was entered into the Western University Oral Pathology database. Seven tissue samples were selected ranging in date from 2017-2019. The biopsy report was reviewed by a graduate student. The histopathological diagnosis was one of “mucosal tag”, “tissue tag”, or “normal mucosa”.

In addition to the normal tissue above, 11 tissue samples with the diagnosis of hyperkeratosis in the absence of any other inflammatory or dysplastic change were selected for comparison.

3.5.2 Demographics

Demographic information was recorded from the histopathology biopsy reports if made available by the surgeon. Age at biopsy, sex, tobacco and alcohol use was recorded.

3.5.3 Slide Preparation

Ten tissue sections from each tissue normal tissue and hyperkeratosis block were retrieved using a microtome set at five micrometers. The sections were transferred onto labelled glass slides to dry. The glass slides were then arranged by case number and stored at room temperature. The slides were stained with Hematoxylin and Eosin and examined histologically to confirm that the epithelium did have normal architecture and maturation sequence and that the sub epithelial tissues were normal.

3.5.4 S100A7 Staining and Analysis

The S100A7 immunohistochemistry Protocol above was repeated for this experiment. Known positive and negative controls were run to ensure the integrity of the stain. The stained tissues were then analyzed as above with Immunoreactivity score, Qupath, and Straticyte.

3.6 Tissue Inflammation Model

3.6.1 Specimen selection

The University of Western Ontario Oral Pathology database was used to identify paraffin embedded tissue samples of Traumatic Ulcerative Granuloma with Stromal Eosinophilia (TUGSE) and Non-specific ulcers to use as our surrogate inflammation model. Biopsy reports and tissue blocks were collected from the year 2019. The Hematoxylin and Eosin stained tissue corresponding to the chosen tissue blocks were obtained and examined microscopically. The diagnosis assigned to each case was confirmed by an Oral and Maxillofacial Pathologist and graduate student. Cases were excluded if the initial diagnosis contained dysplasia or carcinoma

(in situ or invasive). Cases were also excluded if there was inadequate epithelial tissue for staining and examination.

3.6.2 S100A7 Staining and Analysis

Five 5 micrometer tissue sections were taken from each of the 10 blocks using a microtome. These were transferred to a glass slide and dried. One slide from each of the 10 cases was chosen for primary antibody (Anti-S100A7 monoclonal mouse IgG) IHC staining. One case was selected to have 2 slides (one with the primary antibody of interest and one without). High risk and low risk controls were preselected and stained with the samples above. The above IHC protocol was used for staining.

Analysis was completed as above using the total immunoreactivity score, Qupath analysis, and Straticyte risk assessment.

3.7 Tissue Injury Model

3.7.1 Origin of rat injury tissue

Rats were selected for gingival examination and injury (Hamilton, 2014). Gingiva was sampled from an eight-week-old healthy male rat for baseline examination. Subsequently, the rats for injury were selected and prepared. The anterior maxillary gingiva was injured and tissue was sampled at Days 0, 3, and 7. 45 Female Wistar rats, 8 weeks of age (average weight, 281 grams), were used for wound-healing studies. Animal procedures were conducted in accordance with protocols approved by the University Council on Animal Care at University of Western Ontario (AUP 2012-011). The rats were anesthetized by intraperitoneal injection of Ketamine (75 mg/kg) and Xylazine (10 mg/kg). Gingivectomy was performed on the maxillary palatal gingiva close to the upper molars. Yardley gingival cord packer (HF-120-G; Hu-Friedy; Chicago, IL) was used to disrupt the junctional epithelium and the connective tissue and tooth

interface to raise a full-thickness 1 mm wide gingival flap along the first, second and third molars. A no. 15 scalpel blade was used to excise the connective tissue and Corneal tweezers (81D40.21; Lee Valley; Ottawa, Ontario) was used to precisely remove the excised tissue. In a subset of animals (n = 9), maxillary palatal gingiva close to the right upper molars were left untouched to serve as a day 0 baseline. The animals received 0.5 mg/kg Buprenorphine by subcutaneous injection twice daily for 48 hours post-surgery as an analgesic. Animals were maintained on a standard lab chow powdered food diet and were allowed food and water *ad libitum* for the duration of the experiment. Animals were sacrificed at 1, 3, 7, and 14 days post-wounding (n = 9) at each time-point by carbon dioxide inhalation. Three groups of litters were subjected to tissue preparation.

Post euthanasia, rats were decapitated and the heads fixed in 10% neutral buffered formalin (Sigma Aldrich; St. Louis, MO) for 2 days. The 2 hemi-maxillae were dissected out and decalcified using Cal-Ex Decalcifier (Thermo Fisher Scientific; Waltham, MA) for 2 days. Hemi-maxillae were dehydrated through a graded series of ethanol and paraffin processed and embedded.

3.7.2 Specimen Selection

The tissue blocks containing the healthy uninjured tissue and injured tissue at days 0, 3, and 7 post injury were retrieved. Six 5 micrometer sections were taken from each block. The sections were transferred onto labelled glass slides to dry. The glass slides were then arranged by experiment number and stored at room temperature in slide boxes.

3.7.3 H and E Staining and Evaluation

One slide was taken from each tissue block and was prepared for Hematoxylin and Eosin staining. This was to confirm the correct orientation of the sampled tissue embedded in paraffin. The tissue sections were rehydrated using a sequential timed protocol with 100% xylene (2x5 minutes and 1x minute), 100% ethanol (1x2 minutes and 1x1 minute), 95% ethanol (1x2 minutes and 1x1 minute), 70% ethanol (2 minutes), followed by tap water for 2 minutes. H Xylene (13 minutes), absolute alcohol (3 minutes), 95% alcohol (3 minutes), 70% alcohol (1 minute), water (2 minutes) Harris Hematoxylin (3 minutes), tap water rinse, 2-3 dips in acid alcohol (1% hydrochloric acid in 70% alcohol), tap water rinse, 2-3 dips in ammonium alcohol (2% ammonium hydroxide in 70% alcohol), tap water rinse, Eosin stain (3 minutes), tap water rinse, 70% alcohol (10 dips), 95% alcohol (20 dips), absolute alcohol (20 dips), xylene (10 minutes). The slides were then mounted and cover slipped.

After confirming the orientation and quality of the sectioned tissue, one slide from days 0, 3, and 7 of the rat injury experiment was selected for S100A7 immunohistochemistry.

3.7.4 S100A7 Staining and Analysis

The tissue blocks containing the healthy uninjured 8-week-old rat tissue and injured tissue at days 0, 3, and 7 post injury were retrieved. Six 5 micrometer sections were taken from each block. The sections were transferred onto labelled glass slides to dry. The glass slides were then arranged by experiment number and stored at room temperature in slide boxes.

The dried tissue sections were then rehydrated using the standard protocol. The sections were submerged in EDTA (pH 9) for antigen retrieval. A decloaking chamber was then used (112.5 degrees Celsius for 90 seconds and 90 degrees Celsius for 10 seconds). The slides were then cooled under running tap water and washed for 3 x 3 mins TBS-T. The slides were blocked

for 30 minutes with 2.5% Horse Serum. Following blocking, Rabbit polyclonal antibody with reactivity to human and rat Psoriasin (Abcam: ab218207) was applied in 1/300 concentration. The tissues were incubated overnight at 4 degrees Celsius in a humidified chamber.

The tissues were washed for 3 x 3 minutes using TBS-T. The tissue peroxidases were then blocked with 3% Hydrogen Peroxide in TBS for 10 minutes. The tissues were washed 1 x 3 minutes. Impress Rabbit was then applied to each slide and left for 30 minutes. A 3 x 3-minute wash was then completed with TBS-T. DAB was applied for 5 minutes. The excess DAB was disposed of. The tissues were then rinsed in running tap water prior to Hematoxylin counterstaining. The tissues were dehydrated using standard protocol and cover slipped with Cytoseal.

S100A7 IHC Specimen analysis- Semi quantitative and qualitative

S100A7 expression was evaluated at days 0, 3, and 7 post injury. The injured tissue at the various time points was also compared to the 8-week-old rat uninjured tissue. Descriptive analysis was used based on the overall trend of staining within the epithelium at the different time points post injury. More specifically, the location of stain within the epithelium adjacent to the site of injury was of specific interest. The junctional, attached, and unattached tissue S100A7 expression was included in the evaluation if adjacent to the injury site.

3.8 P38 Staining and Analysis

3.8.1 Case Selection, specimen preparation and IHC Protocol

Five cases were selected for staining from each of the lichen planus progressing to malignancy, progressing to dysplasia, and non-progressing categories. For each case, one slide for staining with the primary antibody P38 at 1/200 (P38 MAPK (Tyr323) Rabbit polyclonal, BS5477R, Cedarlane Laboratories, Burlington, ON) and one slide with no primary antibody was selected. A known positive control tissue was ran alongside the samples during this experiment. The above tissue sections were rehydrated using a standard procedure (see S100A7 protocol above). The slides were then quenched with 3% Hydrogen Peroxide in methanol for 5 mins (prepared from 20 mL of 30% Hydrogen Peroxide and 180 mL of methanol). The slides were then rinsed in distilled water for 5 minutes then in Phosphate Buffered Saline (PBS) for 5 minutes with agitation. Antigen retrieval was done in citrate buffer (pH 6) in a decloaking chamber then slides are rinsed in running tap water and in PBS for 5 minutes. The slides were then blocked in 2.5% horse serum for 30 minutes at room temperature in a humidified chamber. The blocking serum was then drained onto a paper towel. The slides were then incubated with the primary antibody P38 at 1/200 dilution, which was determined by preliminary titrations performed before the experiment. The slides were incubated with the antibodies overnight at 4 degrees Celsius. The slides were then rinsed with PBS on a shaker for 3x5 minutes. The slides were then incubated with IMPRESS anti-rabbit horse-radish peroxidase micro-polymer solution (VECTMP740150 MJS Biolynx Inc, Brockville, ON) for 30 minutes at room temperature. The slides were then rinsed with PBS for 2 x 5 minutes on a shaker. Diaminobenzadine (DAB) solution was prepared (5 mL distilled water, 2 drops of buffer, 4 drops of DAB, 2 drops of hydrogen peroxide in that order with vortexing after each step). The slides were then incubated

with DAB for 6 minutes and drained into a waste contained using distilled water to stop the reaction. The slides were then stained in Harris Hematoxylin for 1 minute then rinsed in running tap water. The slides were dipped 1-2 times in acid alcohol (1 % hydrochloric acid in 70% alcohol) and rinsed in running tap water. The slides were then dipped 2-3 times in ammonium alcohol (2% Ammonium Hydroxide in 70% alcohol) and rinsed in running tap water. The dehydration process was then completed (70% alcohol for 1 minute, 95% alcohol for 2 minutes, Absolute alcohol for 3 minutes, xylene for 2x5 minutes). The slides were then mounted and cover slipped in Cytoseal permount in a fume hood.

3.8.2 P38 control

An Oral Squamous Cell Carcinoma was stained with the same protocol. A positive and negative was included.

3.8.3 P38 evaluation

The P38 stained tissues were descriptively analyzed by an Oral and Maxillofacial Histopathologist and a graduate student. The Layers of the epithelium including basal, spinosum, granulosum, and lucidum were assigned a binary positive or negative based on the presence of P38 positivity. The localization of the stain (nuclear, cytoplasmic, membrane/desmosomal) was also reported on. Lastly, a score from 0-3 based on the overall impression of the intensity of the stain was recorded for each specimen. To ensure accuracy, the connective tissue/extraepithelial tissue was examined for background stain.

3.9 ERK 1/2 Staining and Analysis

3.9.1 Case Selection, specimen preparation and IHC Protocol

Five cases were selected for staining from each of the lichen planus progressing to malignancy, progressing to dysplasia, and non-progressing categories. For each case, one slide

for staining with the primary antibody ERK1/2 at 1/400 (ERK1+ERK2 (T185+Y187+T202+Y204) Rabbit polyclonal, BS5469R, Cedarlane Laboratories, Burlington, ON) and one slide with no primary antibody was selected. A known positive control was used for comparison. The above tissue sections were rehydrated using the sequential timed protocol above (see S100A7 protocol). The slides were then quenched with 3% Hydrogen Peroxide in methanol for 5 mins (prepared from 20 mL of 30% Hydrogen Peroxide and 180 mL of methanol). The slides were then rinsed in distilled water for 5 minutes then in PBS for 5 minutes with agitation (on shaker). Antigen retrieval was not performed. The slides were then blocked in 2.5% horse serum for 30 minutes at room temperature. The blocking serum was then drained onto a paper towel. The slides were then incubated with the primary antibody (ERK 1/2) at 1/400 dilution, which was determined by preliminary titrations performed before the experiment. The incubation was completed in a humidified chamber over night at 4 degrees Celsius. The slides were then rinsed with PBS on a shaker for 5 minutes. The slides were then incubated with IMPRESS anti rabbit horse-radish peroxidase micro-polymer solution for 30 minutes at room temperature. The slides were then rinsed with PBS for 5 minutes on a shaker. Diaminobenzadine (DAB) solution was prepared (5 mL distilled water, 2 drops of buffer, 4 drops of DAB, 2 drops of hydrogen peroxide in that order with vortexing after each step). The slides were then incubated with DAB for 10 minutes and drained into a waste contained using distilled water to stop the reaction. The slides were then stained in Harris hematoxylin for 1 minute then rinsed in running tap water. The slides were dipped 1-2 times in acid alcohol (1 % hydrochloric acid in 70% alcohol) and rinsed in running tap water. The slides were then dipped 2-3 times in ammonium alcohol (2% Ammonium Hydroxide in 70% alcohol) and rinsed in running tap water. The dehydration process was then completed (70% alcohol for 1 minute, 95% alcohol for 2

minutes, Absolute alcohol for 3 minutes, xylene for 8 minutes). The slides were then mounted and cover slipped in Cytoseal permount in a fume hood.

3.9.2 ERK 1/2 Control

An Oral Squamous Cell Carcinoma was stained with the same protocol. A positive and negative was included.

3.9.3 ERK 1/2 Evaluation

The ERK1/2 stained tissues were descriptively analyzed by an Oral and Maxillofacial Histopathologist and a graduate student. The Layers of the epithelium including basal, spinosum, granulosum, and lucidum were assigned a binary positive or negative based on the presence of ERK1/2 positivity. The localization of the stain (nuclear, cytoplasmic, membrane/desmosomal) was also reported on. Lastly, a score from 0-3 based on the overall impression of the intensity of the stain was recorded for each specimen. To ensure accuracy, the connective tissue/extraepithelial tissue was examined for background stain.

3.10 JNK/SAPK IHC Staining and Analysis (Phospho-specific)

3.10.1 Case Selection, specimen preparation and IHC Protocol

Five cases were selected for staining from each of the lichen planus progressing to malignancy, progressing to dysplasia, and non-progressing categories. For one case, one slide for staining with the primary antibody Phospho-SAPK/JNK Rabbit mAb (Phospho-SAPK/JNK (Thr183/Tyr185) (81E11) Rabbit mAb, 46685, New England Biolabs, Whitby, ON) and one slide with no primary antibody was selected. A known positive control was used for comparison. The above tissue sections were rehydrated using the same sequential timed protocol above. Antigen retrieval was not performed. The slides were washed 3x 3mins TBS-T. They were then blocked in 2.5% horse serum for 30 minutes at room temperature. The blocking serum was then

drained onto a paper towel. The slides were then incubated with the rabbit anti-human mAb primary antibody Phospho-SAPK/JNK at 1/50 dilution, which was determined by preliminary titrations performed before the experiment. The incubation was completed in a humidified chamber over night at 4 degrees Celsius. The slides were then rinsed with TBS-T on a shaker for 3x 3 minutes. The slides were blocked with 3% hydrogen peroxide to block endogenous peroxidases and washed 1x3mins in TBS-T. The slides were then incubated for 30 minutes at room temperature with an anti-rabbit biotinylated antibody (MJS Biolyx VECTpk6101 Vectastain Elite ABC-peroxidase kit, Rabbit IgG) recognizing the primary. The slides were rinsed with TBS-T for 3 x 3 minutes on a shaker. Avidin Biotin antibodies (MJS Biolyx VECTpk6101 Vectastain Elite ABC-peroxidase kit, Rabbit IgG) was applied for 30 minutes duration. Slides were washed in TBS-T for 3 x 3 minutes, Diaminobenzadine (DAB) solution was prepared (5 mL distilled water, 2 drops of buffer, 4 drops of DAB, 2 drops of hydrogen peroxide in that order with vortexing after each step). The slides were then incubated with DAB for 10 minutes and drained into a waste contained using distilled water to stop the reaction. The slides were then stained in Harris hematoxylin for 1 minute then rinsed in running tap water. The slides were dipped 1-2 times in acid alcohol (1 % hydrochloric acid in 70% alcohol) and rinsed in running tap water. The slides were then dipped 2-3 times in ammonium alcohol (2% Ammonium Hydroxide in 70% alcohol) and rinsed in running tap water. The dehydration process was then completed (70% alcohol for 1 minute, 95% alcohol for 2 minutes, Absolute alcohol for 3 minutes, xylene for 2x5 minutes). The slides were then mounted and cover slipped in Cytoseal permount in a fume hood.

3.10.2 JNK/SAPK Control

An Oral Squamous Cell Carcinoma was stained with the same protocol. A positive and negative was included.

3.10.3 JNK/SAPK Evaluation

The JNK stained tissues were descriptively analyzed by an Oral and Maxillofacial Histopathologist and a graduate student. The Layers of the epithelium including basal, spinosum, granulosum, and lucidum were assigned a binary positive or negative based on the presence of JNK positivity. The localization of the stain (nuclear, cytoplasmic, membrane/desmosomal) was also reported on. Lastly, a score from 0-3 based on the overall impression of the intensity of the stain was recorded for each specimen. To ensure accuracy, the connective tissue/extraepithelial tissue was examined for background stain.

3.11 Beta-Catenin Staining and Evaluation

3.11.1 Specimen Preparation and Beta-catenin Staining

Automated staining utilizing a monoclonal mouse anti-human Beta-Catenin antibody (Code Number IR702, DAKO, Glostrup, Denmark) was performed, according to the manufacturer's instructions. Formalin-fixed paraffin-embedded (FFPE) tissue specimens were cut into 4 Micrometer sections. Pre-treatment with heat-induced epitope retrieval (HIER) was performed using the 3-in-1 specimen preparation procedure for Dako PT Link, and EnVision FLEX Target Retrieval Solution, High pH (50x) (Code Number K8004). Following staining, the sections were dehydrated, cleared and mounted.

The staining steps and incubation times were pre-programmed into the Autostainer Link software. The visualization system used was EnVision FLEX, High pH (Link) (Code Number K8000). Reagents were applied in a volume of 1 x 200 Microliters per slide. All incubation steps

were performed at room temperature. Counterstaining was performed using EnVision FLEX Hematoxylin (Link) (Code K8008). Positive and negative control tissues as well as negative control reagent (FLEX Negative Control, Mouse (Link); Code Number IR750) were run simultaneously using the same protocol as for the case specimens.

3.11.2 Beta-Catenin Control

Gastrointestinal tract tissues were used as positive controls.

3.11.3 Beta-Catenin Evaluation

The stained tissues were evaluated qualitatively. Special attention was directed to the location of the positivity within the strata of the epithelium and the cellular location (membrane, cytoplasmic, nuclear). The Beta- Catenin stained tissues were then qualitatively compared and contrasted to the Cyclin D1 and S100A7 stained tissues.

3.12 Cyclin D1 Staining and Evaluation

3.12.1 Specimen Preparation and Cyclin D1 Staining

Automated staining utilizing a monoclonal rabbit anti-human Cyclin D1 (Code Number IR083, DAKO, Glostrup, Denmark) was performed. FFPE tissue specimens were cut into 4 Micrometer thick sections. Heat-induced epitope retrieval (HIER) was performed using Dako PT Link. Tissues were pretreated using EnVision FLEX Target Retrieval Solution, High pH (50x) (Code Number K8004) for 20 minutes at 97°C followed by 5 minutes in EnVision FLEX Wash Buffer (20x) (Code Number K8007).

The visualization system used was EnVision FLEX, High pH (Link) (Code Number K8000). The staining steps and incubation times were pre-programmed into the Autostainer Link software. Reagents were applied in a volume of 1 x 200 Microliters per slide. All incubation

steps were performed at room temperature. Counterstaining was done using EnVision FLEX Hematoxylin (Link) (Code K8008). After staining, the sections were dehydrated, cleared and mounted.

Positive and negative control tissues as well as negative control reagent (FLEX Negative Control, Rabbit (Link) (Code Number IR600) were run simultaneously using the same protocol as the case specimens.

3.12.2 Cyclin D1 Control

Cyclin D1 control was from a sample of lymphoid tissue.

3.12.3 Cyclin D1 Evaluation

The stained tissues were evaluated qualitatively. Special attention was directed to the location of the positivity within the strata of the epithelium and nuclear positivity. The Cyclin D1 stained tissues were then qualitatively compared and contrasted to the Beta-Catenin and S100A7 stained tissues.

3.13 Statistical Analysis

Correlative value between three predictors: IRS, Qupath, and Straticyte

Due to a missing Straticyte value for one of the cases, Pearsons correlation was calculated to allow for imputation of this value. For each pair of numeric variables, Pearson's correlation was calculated. Pearson's correlation is a metric that takes value between -1 and 1. The higher the Person's correlation value, the more linearly correlated the two variables are. A threshold for significant correlation was set at 0.5. The Pearson Correlation Coefficient was calculated for:

Manual Score to the Straticyte score

Manual score to Qupath score

Qupath score to Straticyte score

A plot of correlation matrix was constructed. The three scores are highly correlated. A Multivariate Imputation by Chained Equation (MICE) was then used to impute the missing Straticyte value.

In attempt to determine whether the three predictors were able to accurately differentiate Lichen planus from normal tissue, hyperkeratosis, and TUGSE/TU, Random Forrest analyses were completed. The estimate of error rate was calculated as a percentage value and a confusion matrix was constructed. GBM was completed and AUC was calculated and displayed in graphic form. The GBM and Random Forrest Analysis were interpreted in light of the OOB error.

In attempt to determine whether the above 3 predictive scores could be used to determine if a Lichen Planus lesion will or will not progress, a Random Forest Analysis was again used. The OOB estimate of error rate was calculated as a percentage value. A Confusion Matrix was the constructed displaying the Classification error. The results were interpreted based on the level of error. Group Based Machine was completed and the AUC was calculated and displayed in graphic form.

Chapter 4

4.0 Results

4.1 OLP

4.1.1 Lichen Planus Case Selection

Five cases were selected that had an initial diagnosis of oral lichen planus and a subsequent biopsy showing oral squamous cell carcinoma. Three cases had an initial diagnosis of oral lichen planus and a subsequent biopsy showing dysplastic changes. Fifteen cases had an initial diagnosis of oral lichen planus and a subsequent biopsy showing no dysplastic or malignant transformation.

4.1.2 Lichen Planus Specimen Location

Of the Lichen planus biopsy specimen's that transformed to malignancy, one was located on the buccal mucosa and the remaining three cases were located on the gingiva (Table 4.1).

Table 4.1: Location of the original biopsy specimen, clinical subtype of Lichen Planus, and the location of the ensuing malignancy

Location of LP	Subtype of LP	Type of Malignancy	Location of Malignancy
Buccal Mucosa	Unspecified	OSCC	Tongue
Anterior Gingiva	Hypertrophic (Bilateral Wickham Striae present Strong autoimmune history + Sjogrens)	OSCC	Buccal Mucosa
Buccal Gingiva	Hypertrophic (Bilateral Wickham Striae present and diffuse gingival involvement) + Cutaneous Lichen Planus	OSCC	Buccal Mucosa

Anterior gingiva and Buccal Mucosa	Erosive (Bilateral Wickham Striae present and diffuse gingival involvement Waxing and waning x 5 years prior to Histopathologic diagnosis)	OSCC	Anterior gingiva
Ventrolateral tongue	Erosive (Bilateral Wickham Striae present and involvement of FOM and ventral tongue)	OSCC	Lateral tongue

Of the 3 Lichen Planus lesions that transformed to dysplasia, one was taken from the anterior gingiva, one from the floor of mouth and buccal mucosa, and the last was taken from the lower lip. Table 4.2 is included below which displays the location of the OLP biopsy specimen, the subtype of OLP, and the location and grade of the ensuing dysplasia:

Table 4.2: Location and subtype of Lichen Planus with location and grade of ensuing dysplasia

Location of Lichen Planus	Subtype of Lichen Planus	Grade of Dysplasia	Location of Dysplasia
Anterior Gingiva	Hypertrophic (Diffuse gingival involvement)	Mild	Anterior Gingiva
Floor of Mouth and Buccal Mucosa	Erosive (FOM and Buccal Mucosal involvement)	Mild	Floor of Mouth
Lower Lip	Hypertrophic (Bilateral lower lip striations)	Mild	Lower Lip

Of the fifteen cases that had an initial diagnosis of oral lichen planus and a subsequent biopsy showing no dysplastic or malignant transformation, 7 were taken from the buccal mucosa,

5 from the gingiva, 1 from the palate, and two from an unspecified location within the oral cavity.

Table 4.3: Location and subtype of original Lichen Planus and repeat biopsy showing no progression and time elapsed between biopsies

Location of Lichen Planus	Type of Lichen Planus	Location of subsequent biopsy	Diagnosis of subsequent lesion	Time lapse since original biopsy
Posterior Gingiva	Erosive/atrophic (Bilateral buccal mucosal involvement, FOM, and diffuse gingival)	Floor of Mouth	Hypertrophic LP	3 years
Palate	Hypertrophic (Bilateral mucosal and diffuse palatal involvement)	Palate	Lichen Planus	2 years
Buccal Mucosa	Erosive (Bilateral Wickham Striae. Gingival involvement)	Buccal Mucosa	Erosive Lichen Planus	1 year
Gingiva	Erosive (Bilateral Wickham Striae. Diffuse Bilateral gingival involvement)	Gingiva	Erosive Lichen Planus	2 years
Gingiva	Erosive (Diffuse gingival involvement)	Gingiva	Erosive Lichen Planus	3 years
Gingiva	Erosive (Bilateral maxillary mucosal involvement and gingiva)	Palate	Lichen Planus	3 years
Unknown site in oral cavity	Erosive (Wickham Striae present Bilateral buccal mucosal involvement)	Buccal Mucosa	Lichen Planus	3 years

Gingiva	Hypertrophic (Wickham Striae Present Bilateral gingival involvement)	Gingiva	Hypertrophic Lichen Planus	2 years
Buccal mucosa	Erosive (Bilateral buccal mucosal and tongue involvement)	Tongue	Erosive Lichen Planus	4 years
Buccal mucosa	Hypertrophic (Bilateral buccal mucosal involvement)	Buccal mucosa	Hypertrophic Lichen Planus	6 years
Buccal mucosa	Hypertrophic (Bilateral Buccal mucosal involvement)	Buccal mucosa	Hypertrophic Lichen Planus	1 year
Oral mucosa unspecified	Hypertrophic	Palate	Hypertrophic Lichen Planus	9 years
Buccal Mucosa	Erosive (Buccal mucosal and gingival involvement)	Gingiva	Erosive Lichen Planus	11 years
Buccal Mucosa	Erosive (+ Cutaneous LP. Buccal mucosal and gingival involvement. Diagnosis of OLP precedes this biopsy by “years”)	Gingiva	Erosive Lichen Planus	3 years
Buccal Mucosa	Hypertrophic (Bilateral buccal mucosal involvement)	Buccal Mucosa	Hypertrophic Lichen Planus	4 years

4.1.3 Lichen Planus demographics

The demographic data inclusive of the confounding risk factors for the initial biopsy of the Lichen Planus progressing and non-progressing cases are included in Tables 4.4, 4.5, and 4.6. Tobacco and alcohol use are known independent factors that contribute to the development of oral cancer. Unfortunately, due to privacy limitations, these confounders were poorly accounted

for. Of the 23 individuals with progressing and non-progressing Lichen Planus, tobacco use history was known in only 5. Of these 5, one individual was a lifelong non-smoker. One individual was a remote smoker having quit 30 years prior to histopathologic diagnosis of OLP. The remaining 3 individuals had an unknown duration and quantity of tobacco use. Of the 8 progressing cases, 2 had a history of tobacco use. One of the individuals had a remote history and the other was actively using. Of the non-progressing cases, 2 had a positive smoking history of unknown duration. One individual had known negative history for tobacco use. Alcohol use was also poorly accounted for.

Table 4.4: Lichen Planus Progressing to Malignancy – Demographics

Age at original Biopsy	Sex	Time from original Biopsy to Malignancy	Tobacco	Alcohol
58	M	11 years	Unknown	Unknown
55	F	10 years	Unknown	Unknown
41	M	9 years	Unknown	Unknown
60	F	4 years	Remote smoker. 30 pack year History. Quit 30 years prior to diagnosis of LP	Unknown
75	F	3 years	Unknown	Unknown

Table 4.5: Lichen Planus Progressing to Dysplasia – Demographics

Age at original biopsy	Sex	Time from original biopsy to dysplasia	Tobacco	Alcohol
78	F	9 years	Unknown	Unknown
36	F	2 years	(+) Unknown duration	Unknown
53	M	6 years	Unknown	Unknown

Table 4.6: Lichen Planus Non- Progressing – Demographics

Age at original biopsy	Sex	Time from original biopsy to follow-up	Tobacco	Alcohol
42	F	3 years	(+) unknown quantity	Unknown
50	F	2 years	(-)	(-)

63	M	1 year	Unknown	Unknown
55	F	2 years	Unknown	Unknown
54	F	3 years	Unknown	Unknown
61	M	3 years	Unknown	Unknown
68	F	3 years	Unknown	Unknown
61	F	2 years	Unknown	Unknown
67	F	4 years	Unknown	Unknown
48	M	6 years	(+)	Unknown
56	F	1 year	Unknown	Unknown
59	F	9 years	Unknown	Unknown
68	F	11 years	Unknown	Unknown
69	F	3 years	Unknown	Unknown
41	F	4 years	Unknown	Unknown

The distribution of subtype of progressing and non-progressing Lichen Planus Lesions is reflected in the tables below:

Table 4.7: LP Progressing Subtype Distribution

Subtype	Case Count
Hypertrophic	5
Atrophic	0
Erosive	3
Plaque-like	0
Bullous	0

Table 4.8: LP Non-Progressing Subtype Distribution

Subtype	Case Count
Hypertrophic	6
Atrophic	1
Erosive	8
Plaque-like	0
Bullous	0

The vast majority of the cases of OLP cases that did and did not progress were hypertrophic and erosive. There was one non-progressing case that was the atrophic histological subtype.

The distribution of the original lesion location of OLP for the progressing and non-progressing cases is depicted in the tables below:

Table 4.9: LP Progressing Oral Cavity Location

Lesion Location	Case Count
Gingiva	4
Palate	0
Buccal Mucosa	1
Tongue	1
Floor of Mouth	1
Lip	1
Unknown	0

Table 4.10: LP Non-Progressing Oral Cavity Location

Lesion Location	Case Count
Gingiva	4
Palate	1
Buccal Mucosa	7
Tongue	0
Floor of Mouth	0
Lip	0
Unknown	2

The site specificity of ensuing dysplasia is depicted in the table below:

Table 4.11: LP Progressing Cases Site Specificity

Site Specificity	Case Count
Specific	5
Not specific	3

The site- specific lesions were located on the gingiva, tongue, FOM, and lip. The non-site specific lesions were distributed as follows:

Table 4.12: Location of LP Progressing Cases that were not site specific

OLP Biopsy Location	Malignancy/Dysplasia Location
Gingiva	Buccal Mucosa
Gingiva	Buccal Mucosa
Unspecified	Tongue

The median age for the original histopathologic diagnosis of OLP in the progressing and non-progressing lesions is depicted in the table below:

Table 4.13: Median Age of Diagnosis of OLP in the Progressing and Non-Progressing Groups

	Median age at Diagnosis
Progressing	56.5
Non-progressing	59

Unfortunately, not having complete access to the clinical history precludes the ability to determine the duration of time from onset of clinical symptoms or appearance of lesions to diagnosis of dysplasia or malignancy. However, the time lapse from original biopsy to development of dysplasia and malignancy is depicted in the table below. The median time to progression was 7.5 years.

Table 4.14: Time from Original Biopsy of OLP to Diagnosis of dysplasia/malignancy in years

Type of Progression	Timing of Progression (years)
Malignancy	11
Malignancy	10
Malignancy	9
Malignancy	4
Malignancy	3
Dysplasia	9
Dysplasia	2
Dysplasia	6

The gender distribution for the progressing and non-progressing lesions is depicted in the table below:

Table 4.15: Gender distribution of the progressing and non-progressing LP cases

	Male	***Female***
Progressing	3	5
Non-progressing	3	12

4.2 Lichenoid Mucositis

4.2.1 Case Selection

Eight cases of progressing Lichenoid mucositis were included in this study to compare and contrast the results with Lichen Planus. Three cases were selected that had an initial diagnosis of Lichenoid mucositis/inflammation and a subsequent biopsy showing oral squamous cell carcinoma. Five cases had an initial diagnosis of Lichenoid mucositis/inflammation and a subsequent biopsy showing dysplastic changes.

4.2.2 Specimen Location

The distribution of biopsy location is present in the table below:

Table 4.16: Lichenoid Mucositis location with location of ensuing malignancy

Diagnosis	Location	Type of Malignancy	Location of Malignancy
Lichenoid Mucositis	Ventral Tongue	OSCC	Tongue
Lichenoid Mucositis	Lateral Tongue Patient did have more generalized erythroleukoplakia throughout mouth clinically	OSCC	Maxilla
Lichenoid Mucositis	Lateral Tongue Clinical history of leukoplakia tongue and buccal mucosa predating malignancy by 11 years	OSCC	Tongue

Information regarding the location of the Lichenoid mucositis lesions that progressed to dysplasia is included in the tables below:

Table 4.17: Lichenoid Mucositis location with location and grade of ensuing dysplasia

Diagnosis	Location	Grade of Dysplasia	Location of Dysplasia
Lichenoid Mucositis	Floor of mouth	Mild	Floor of Mouth
Lichenoid Mucositis	Gingiva	Mild-Moderate	Gingiva
Lichenoid Mucositis	Left Alveolar Mucosa	Mild	Left Gingiva
Lichenoid Mucositis	Lateral Tongue	Moderate	Floor of mouth
Lichenoid Mucositis	Lateral Tongue	Mild	Lateral Tongue

Table 4.18: Lichenoid Mucositis location distribution

Lesion Location	Case Count
Tongue	5
Floor of Mouth	1
Gingiva	1
Alveolar Mucosa	1

The site specificity from the original Lichenoid Mucositis to the ensuing dysplasia or malignancy is accounted for below:

Table 4.19: Progressing Lichenoid Mucositis site specificity

Site Specificity	Case Count
Specific	5
Not specific	3

The site-specific lesions were located on the tongue, floor of mouth, and gingiva. The site non-specific lesions were distributed as follows:

Table 4.20: Location of site specific progressing Lichenoid Mucositis

Location of Lichenoid Mucositis	Location of Malignancy/Dysplasia
Tongue	Maxilla
Alveolar Mucosa	Gingiva
Tongue	Floor of mouth

4.2.3 Lichenoid Mucositis Demographics

Table 4.21: Lichenoid Mucositis Progressing to Malignancy – Demographics

Age at original biopsy	Sex	Time from original biopsy to follow-up	Tobacco	Alcohol
45	M	5 years	(+) "heavy"	Unknown
38	M	8 years	Unknown	Unknown
43	M	2 years	(+)	Unknown

Table 4.22: Lichenoid Mucositis Progressing to Dysplasia – Demographics

Age at original biopsy	Sex	Time from original biopsy to follow-up	Tobacco	Alcohol
60	M	6 years	(+)	Unknown
57	M	12 years	(-)	(+) >5drinks/day x 7 yrs
75	F	10 years	Unknown	Unknown
81	F	4 years	(+)	Unknown
57	M	7 years	Unknown	Unknown

The group separated by listed gender included 6 males and 2 females. The median age at original biopsy for the progressing Lichenoid mucositis group was 57.

As above due to privacy issues some data including timing of clinical appearance of lesion/symptoms and confounders such as tobacco and alcohol use are incomplete. The median time to development of malignancy or dysplasia was 6.5 years. The tobacco use status was known in 5/8 individuals. 4/8 had a positive tobacco use history. One out of the eight individuals had a known negative history. The tobacco use status in the remaining 3/8 individuals was unknown. The alcohol use status was unknown in 7/8 individuals. One person was noted to drink 5 alcoholic units/day for a 7-year duration.

4.3 Hyperkeratosis

4.3.1 Specimen Selection and Location

Tissue diagnosis is displayed in table below:

Table 4.23: Hyperkeratosis tissue location

Tissue Diagnosis	Tissue Location
Hyperkeratosis	Lateral tongue
Hyperkeratosis	Retromolar trigone
Hyperkeratosis	Gingiva
Hyperkeratosis	Retromolar trigone
Hyperkeratosis	Gingiva
Hyperkeratosis	Lateral tongue
Hyperkeratosis	Retromolar trigone
Hyperkeratosis	Lateral tongue
Hyperkeratosis	Lateral tongue
Hyperkeratosis	Ventral tongue
Hyperkeratosis	Lateral tongue

Table 4.24: Hyperkeratosis tissue location distribution

Lesion location	Case Count
Tongue	6
Retromolar Trigone	3
Gingiva	2

4.3.2 Hyperkeratosis Demographics

Table 4.25: Hyperkeratosis Demographics

Age at Biopsy	Sex	Tobacco	Alcohol
61	F	Remote	None
59	M	None	None
51	F	Positive	None
41	M	Positive	None
48	M	None	None
65	F	None	None
60	M	Remote	None
46	F	None	None
24	M	None	None

53	F	None	None
66	M	Positive	None

Gender was divided 6/11 male and 5/11 female. The median age at diagnosis of hyperkeratosis in the absence of dysplasia/malignancy was 53 years old. Five of eleven individuals had a tobacco use history. Two of these labeled as remote. Six of eleven had known non-use.

4.4 Normal Tissue

4.4.1 Specimen Selection

The table below displays the histopathologic diagnosis and anatomic location of each tissue specimen:

Table 4.26: Normal Tissue diagnosis and location

Normal Tissue Diagnosis	Tissue location
Mucosal tag	Buccal mucosa
Mucosal tag	Buccal mucosa
Mucosal tag	Ventral tongue
Mucosal tag	Ventral Tongue

The distribution of normal tissue location is depicted in the table below:

Table 4.27: Normal Tissue location distribution

Lesion Location	Case Count
Buccal Mucosa	2
Ventral Tongue	2

4.4.2 Normal Tissue Demographics

The above 4 samples were diagnosed as mucosal tags based on clinical, gross pathologic, and histopathologic analyses. The age, sex, smoking and alcohol use status are displayed below:

Table 4.28: Normal Tissue demographics

Age at biopsy	Sex	Tobacco	Alcohol
20	F	Unknown	Unknown
60	M	Unknown	Unknown
65	F	Unknown	Unknown
40	F	Unknown	Unknown

4.5 Tissue Inflammation Model

4.5.1 Specimen Selection

Five tissue samples of Traumatic Ulcerative Granuloma with Stromal Eosinophilia (TUGSE) and 5 samples of Non-specific ulcers were selected to be used as our surrogate inflammation model. The diagnosis and anatomic location of the sampled tissue is displayed below:

Table 4.29: Inflammatory Tissue diagnosis and location

Tissue Diagnosis	Tissue Location
TUGSE	Lateral tongue
Non-specific ulcer	Buccal mucosa
TUGSE	Lateral tongue
TUGSE	Lateral tongue
TUGSE	Lateral tongue
Non-specific ulcer	Lip
Non-specific ulcer	Lateral tongue
Non-specific ulcer	Lateral tongue
Non-specific ulcer	Ventral tongue
Non-specific ulcer	Lateral tongue

Tissue Inflammation Model Demographics are displayed below:

Table 4.30: Inflammatory Tissue demographics

Age original biopsy	Sex	Tobacco	Alcohol
63	F	Unknown	Unknown
78	F	Unknown	Unknown
77	F	Unknown	Unknown
68	F	Unknown	Unknown
63	F	Unknown	Unknown
92	F	Unknown	Unknown
60	M	Unknown	Unknown
74	M	Negative	Unknown
68	F	Unknown	Unknown
64	F	Negative	Unknown

4.6 S100A7 IHC

4.6.1 Normal Tissue S100A7

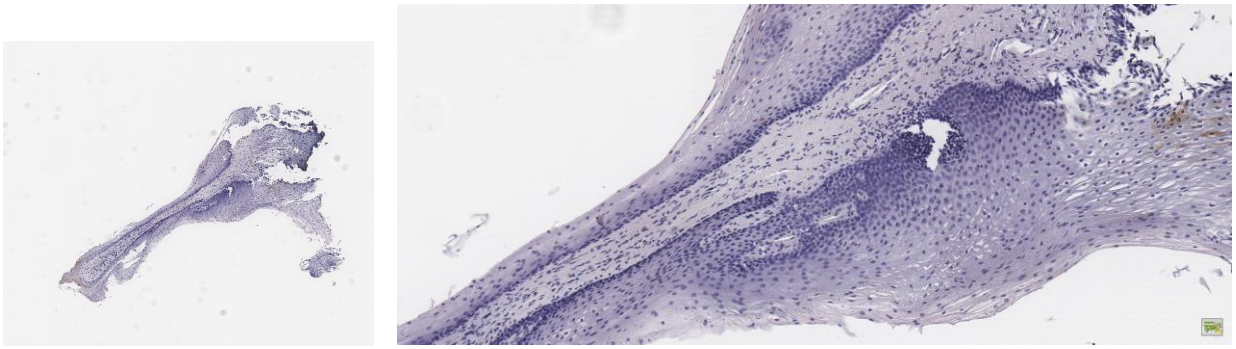

Figure 4.1 Illustrative S100A7 staining for biopsy of normal tissue (example 1)
Diagnosis- Tissue tag; manual score = (cell score =0; intensity score =0); Straticyte™ score =8%). Staining scant and demonstrating sparing of basal and Para basal layers. A = Low magnification; B = High magnification (15-7060).

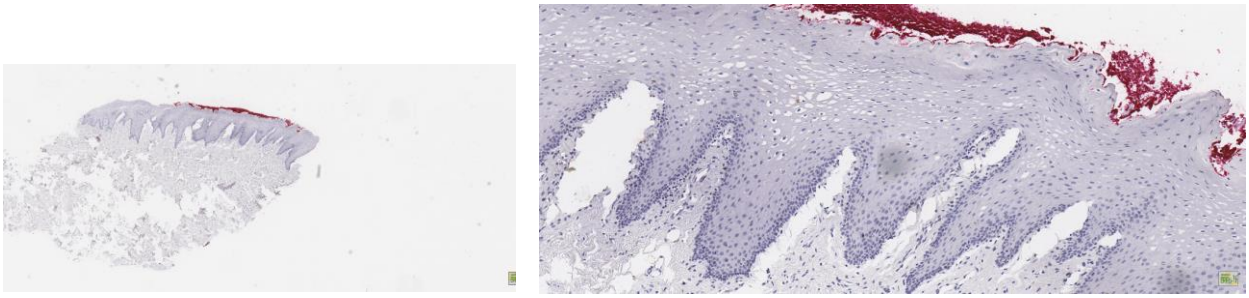

Figure 4.2 Illustrative S100A7 staining for biopsy of normal tissue (example 2)
Diagnosis- Tissue tag; manual score = (cell score=0; intensity score=0); Straticyte™ score=14%). Almost completely void of stain with sparing of parabasal and basal layers. A = Low magnification; B = High magnification (15-12700)

4.6.2 TUGSE/TU

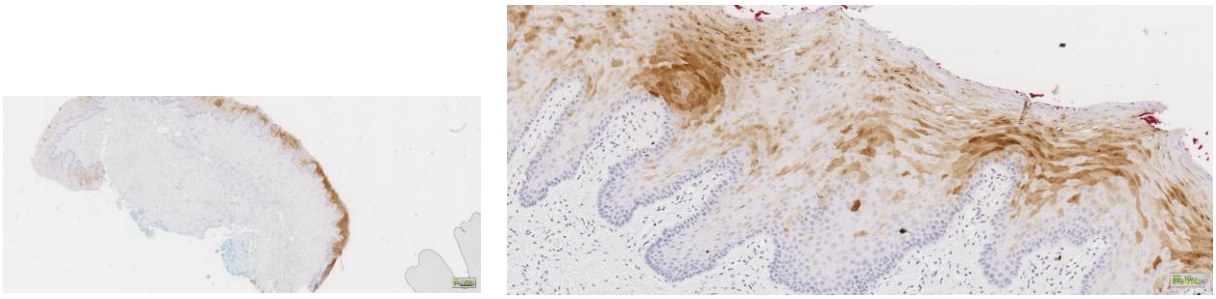

Figure 4.3 Illustrative S100A7 staining for biopsy of Inflammatory tissue (example 1)
Diagnosis- TUGSE; manual score = (cell score=5; intensity score=3); Straticyte™ score= 71%). A = Low magnification; B = High magnification. (19-7142)

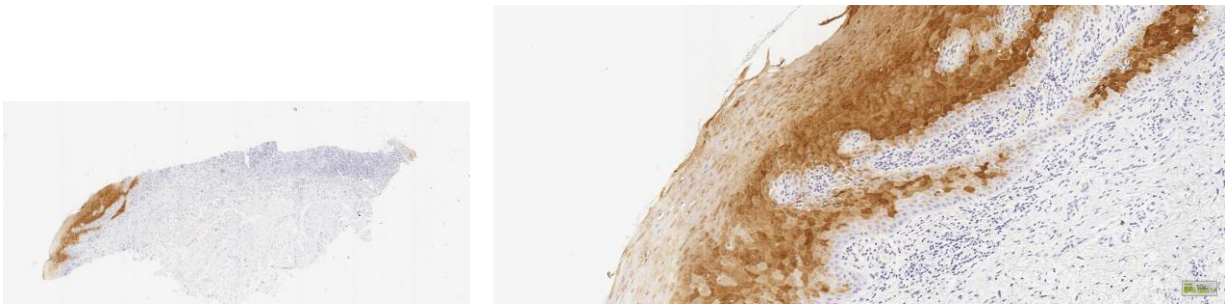

Figure 4.4 Illustrative S100A7 staining for biopsy of Inflammatory tissue (example 2)
Diagnosis- TUGSE; manual score = (cell score=4; intensity score=3); Straticyte™ score=63%). A = Low magnification; B = High magnification. (19-5851)

4.6.3 Lichen Planus IHC

LP Progressing to malignancy

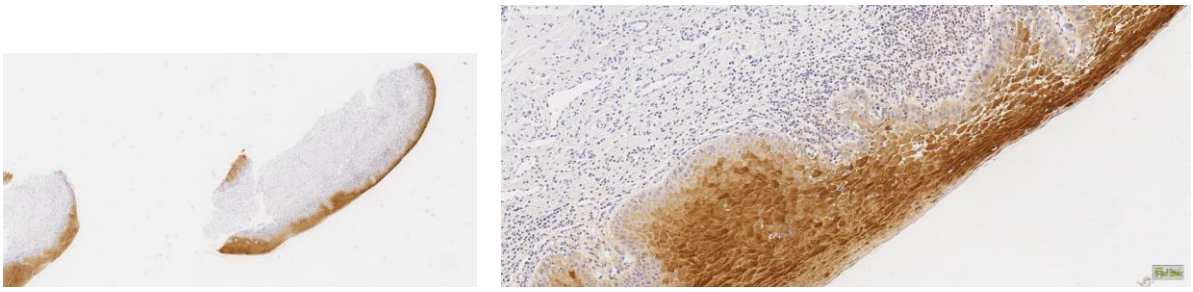

Figure 4.5 Illustrative S100A7 staining for biopsy of Lichen Planus progressing to malignancy (example 1)
Diagnosis- Lichen Planus; manual score = (cell score=5; intensity score=3); Straticyte™ score=62%). A = Low magnification; B = High magnification. (18-29600)

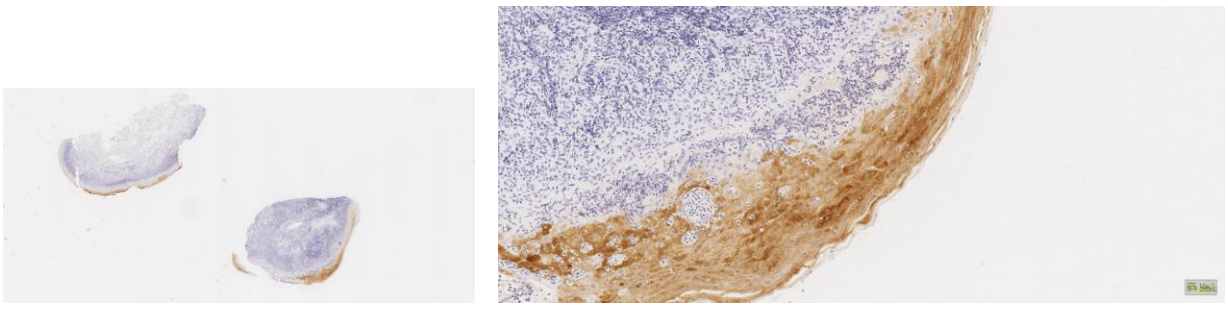

Figure 4.6 Illustrative S100A7 staining for biopsy of Lichen Planus progressing to malignancy (example 2)
Diagnosis- Lichen Planus; manual score = (cell score=1; intensity score=2); Straticyte™ score=52%). A = Low magnification; B = High magnification. (07-28982)

LP progressing to Dysplasia

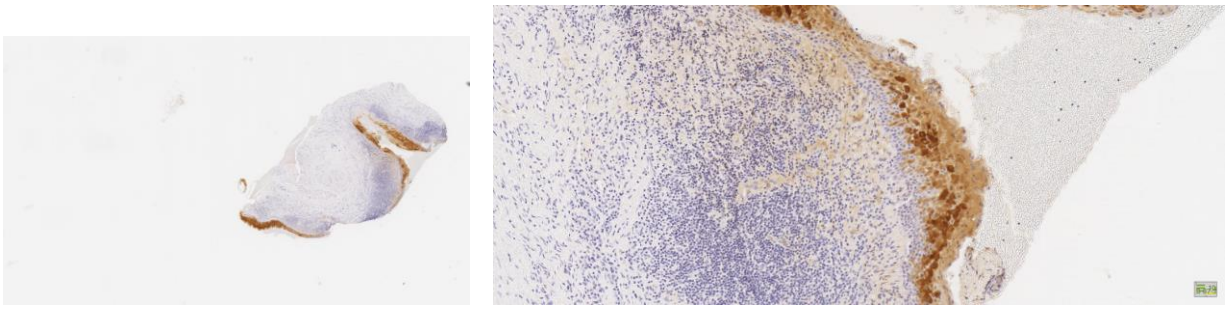

Figure 4.7 Illustrative S100A7 staining for biopsy of Lichen Planus progressing to dysplasia (example 1)
Diagnosis- Lichen Planus; manual score = (cell score=2; intensity score=2); Straticyte™ score=75%). A = Low magnification; B = High magnification. (07-34099)

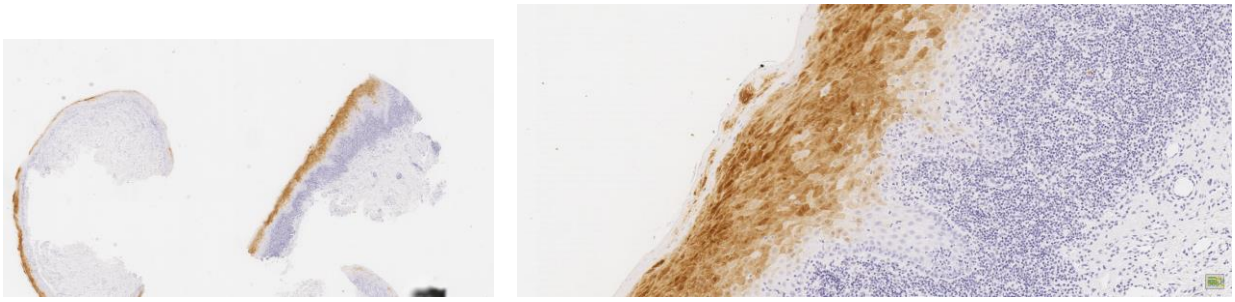

Figure 4.8 Illustrative S100A7 staining for biopsy of Lichen Planus progressing to dysplasia (example 2)
Diagnosis- Lichen Planus; manual score = (cell score=3; intensity score=2); Straticyte™ score=38%). A = Low magnification; B = High magnification. (06-33597)

LP Non-progressing

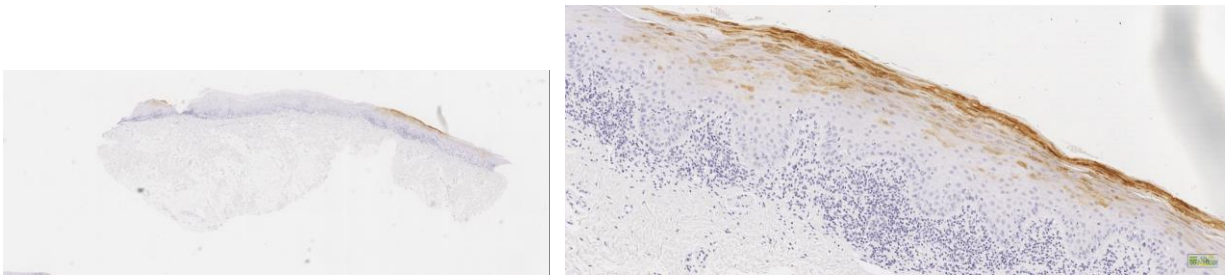

Figure 4.9 Illustrative S100A7 staining for biopsy of non-progressing Lichen Planus (example 1)
Diagnosis- Lichen Planus; manual score = (cell score=1; intensity score=1); Straticyte™ score= 15%). A = Low magnification; B = High magnification. (07-16028)

Figure 4.10 Illustrative S100A7 staining for biopsy of non-progressing Lichen Planus (example 2)
Diagnosis- Lichen Planus; manual score = (cell score=2; intensity score=1); Straticyte™ score= 20%). A = Low magnification; B = High magnification.

4.6.4 Lichenoid Mucositis IHC

LM Progressing

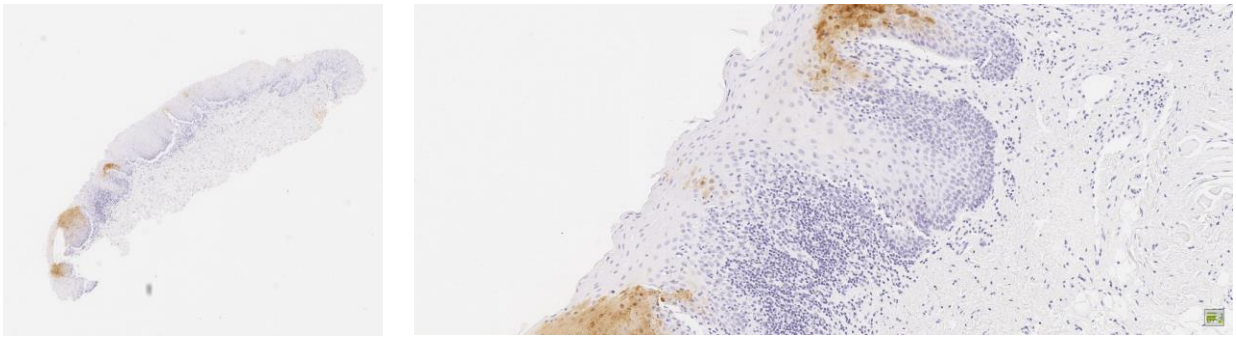

Figure 4.11 Illustrative S100A7 staining for biopsy of Lichenoid Mucositis progressing to cancer (example 1)
Diagnosis- Lichenoid Mucositis; manual score = (cell score= 1; intensity score= 1); Straticyte™ score= 23%). A = Low magnification; B = High magnification. (07-24656)

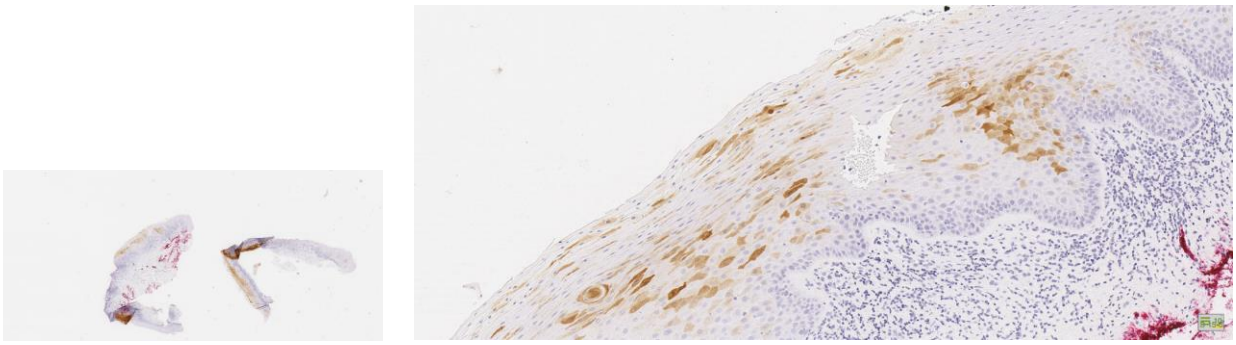

Figure 4.12 Illustrative S100A7 staining for biopsy of Lichenoid Mucositis progressing to cancer (example 2)
Diagnosis- Lichenoid Mucositis; manual score = (cell score=1; intensity score=1); Straticyte™ score=21%). A = Low magnification; B = High magnification. (15-52655)

4.6.5 S100A7 IHC Analyses

Immunoreactive Score Analysis

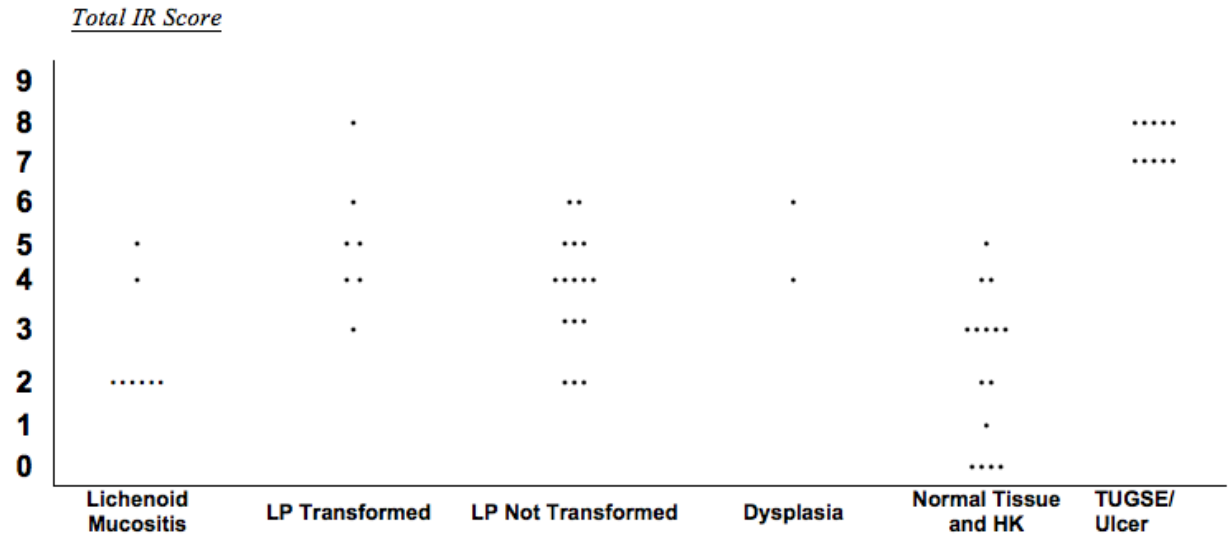

Figure 4.13 Descriptive Total Immunoreactive Score.
Dot plot showing the Total Immunoreactive Scores (Percentage cells stained + Intensity of cell stain) for tissue groups. Lichenoid mucositis, Lichen Planus transformed, Lichen Planus that did not transform, Dysplasia, Hyperkeratosis, Normal tissue, and Traumatic Ulcerative Granuloma with Stromal Eosinophilia/ Traumatic ulcer.

Qupath Analysis

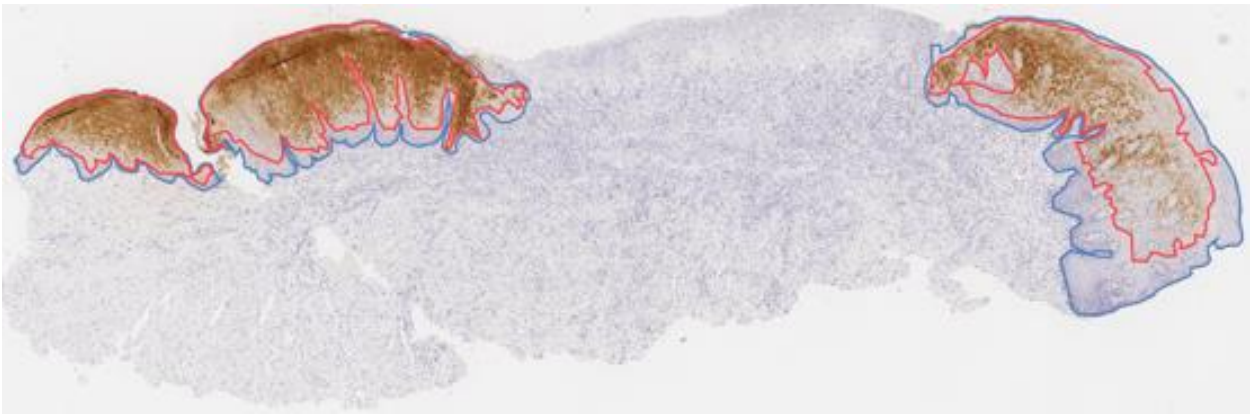

Figure 4.14 Qupath Analysis: An Example of Qupath analysis.
The Red line outlines the cells that have stained for S100A7. The blue line represents the total epithelial area. The proportion of stained cells relative to the total epithelial area is calculated from these measurements.

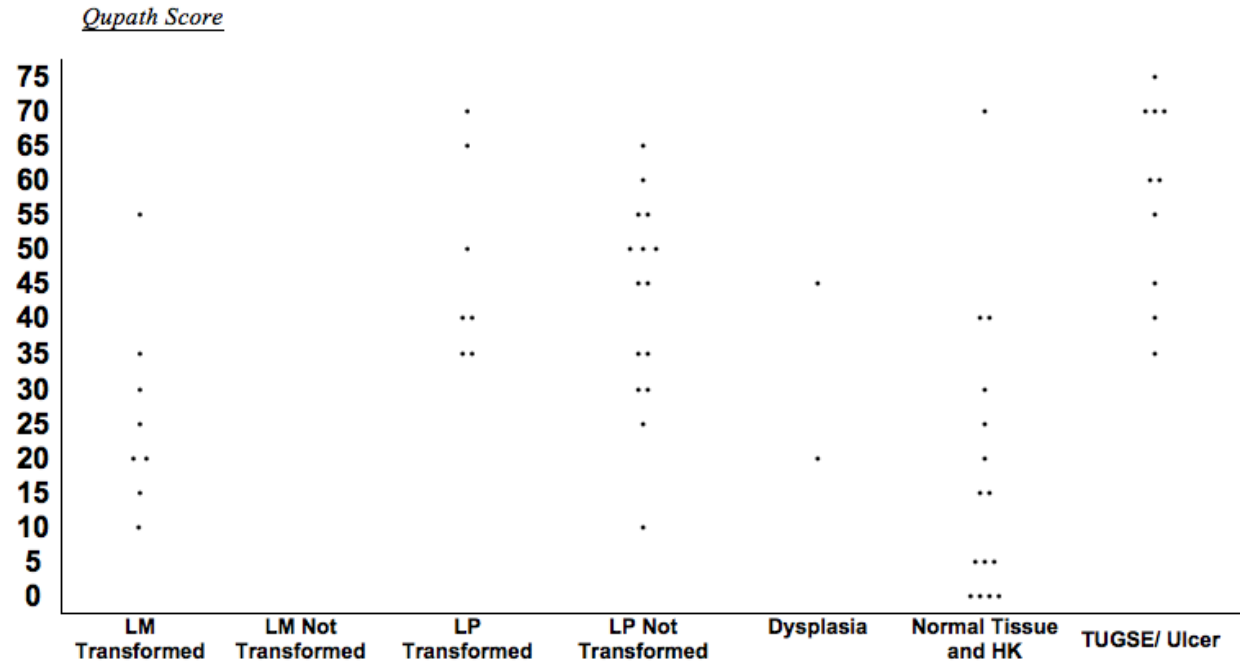

Figure 4.15 Descriptive Qupath Score: Dot plot showing the Qupath Scores for tissue groups
Lichenoid mucositis, Lichen Planus transformed, Lichen Planus that did not transform, Dysplasia, Hyperkeratosis, Normal tissue, and Traumatic Ulcerative Granuloma with Stromal Eosinophilia/ Traumatic ulcer.

Straticyte Analysis

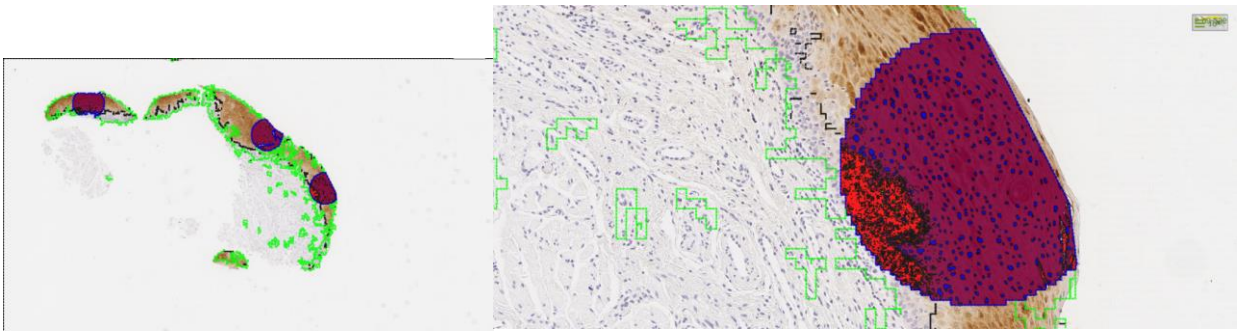

Figure 4.16 Straticyte™ Analysis Image
Regions of interest (ROIs) are outlined in dashed blue and two overlapping ROIs can be seen. Within the ROIs: red = S100A7- negative cytoplasm; green = S100A7-negative nuclei; maroon = S100A7-positive cytoplasm and blue = S100A7-positive nuclei. Image provided by Dr. J. Hwang, Proteocyte AI, Toronto, ON, Canada.

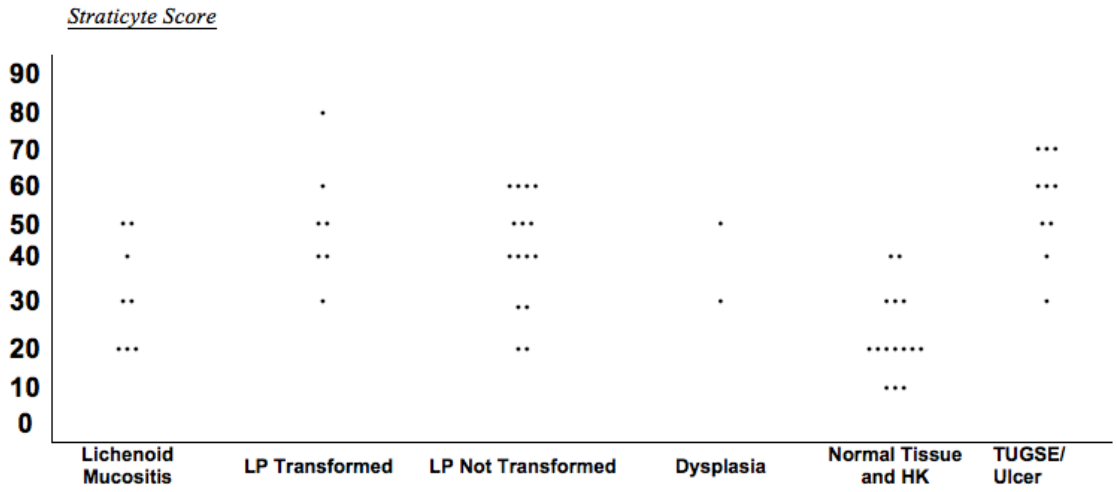

Figure 4.17 Descriptive Straticyte™ Score: Dot plot showing the Straticyte™ Scores for tissue groups
Lichenoid mucositis, Lichen Planus transformed, Lichen Planus that did not transform, Dysplasia, Hyperkeratosis, Normal tissue, and Traumatic Ulcerative Granuloma with Stromal Eosinophilia/ Traumatic ulcer.

4.7 MAPK IHC

4.7.1 Phospho-ERK1/2 IHC

A positive control was stained with Phospho-ERK1/2. The control tissue was Oral Squamous Cell Carcinoma. A Negative and positive is included below:

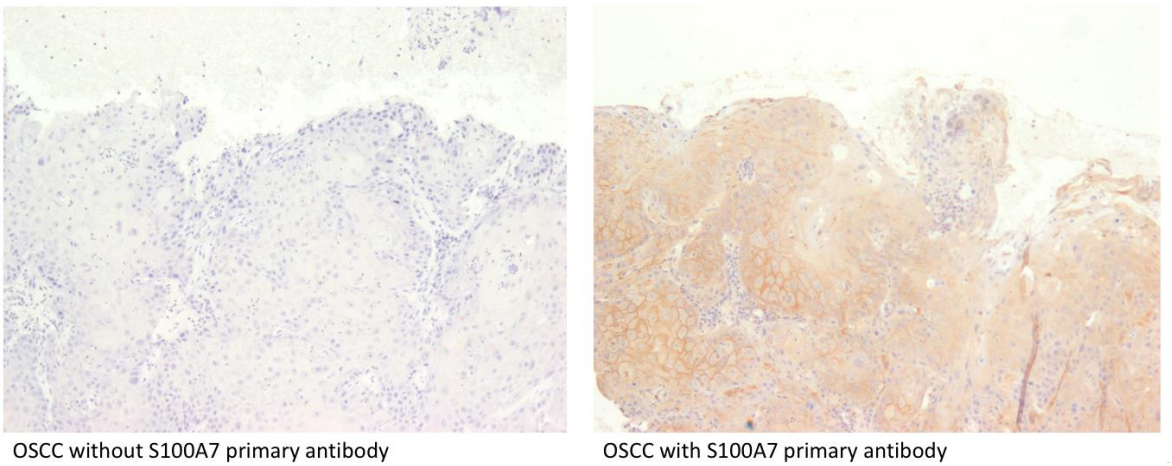

Figure 4.18 Phospho-ERK1/2 IHC positive control
A Squamous Cell Carcinoma was chosen as a positive control. A and B are the same tissue. A was not stained with the primary antibody. B was stained with the antibody.

An example of the Phospho-ERK1/2 stained Lichen Planus tissue that transformed to malignancy is provided in Figure 4.19.

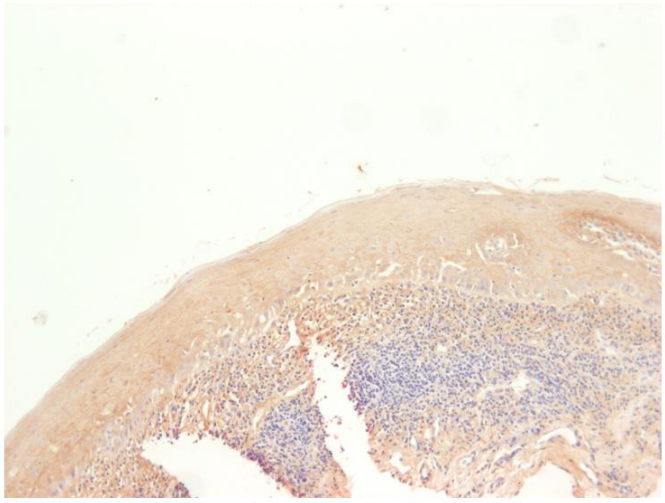

ERK1/2 stained Lichen Planus that eventually transformed to Malignancy

Figure 4.19 Phospho-ERK1/2 IHC Progressing Lichen Planus
An example of Phospho-ERK1/2 stained Lichen Planus that eventually progressed to malignancy.

An example of the Phospho-ERK1/2 stained Lichen planus that did not transform is provided below:

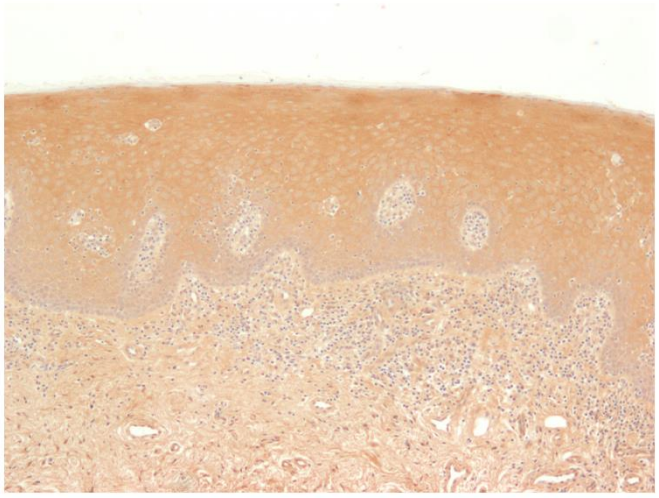

ERK1/2 stained Lichen Planus that did not transform on serial biopsy

Figure 4.20 Phospho-ERK1/2 IHC Non-Progressing Lichen Planus
An example of Phospho-ERK1/2 stained Lichen Planus that did not progress to malignancy on repeat biopsy.

4.7.2 Phospho-P38 IHC

A positive control consisting of Phospho-P38 stained OSCC is provided below:

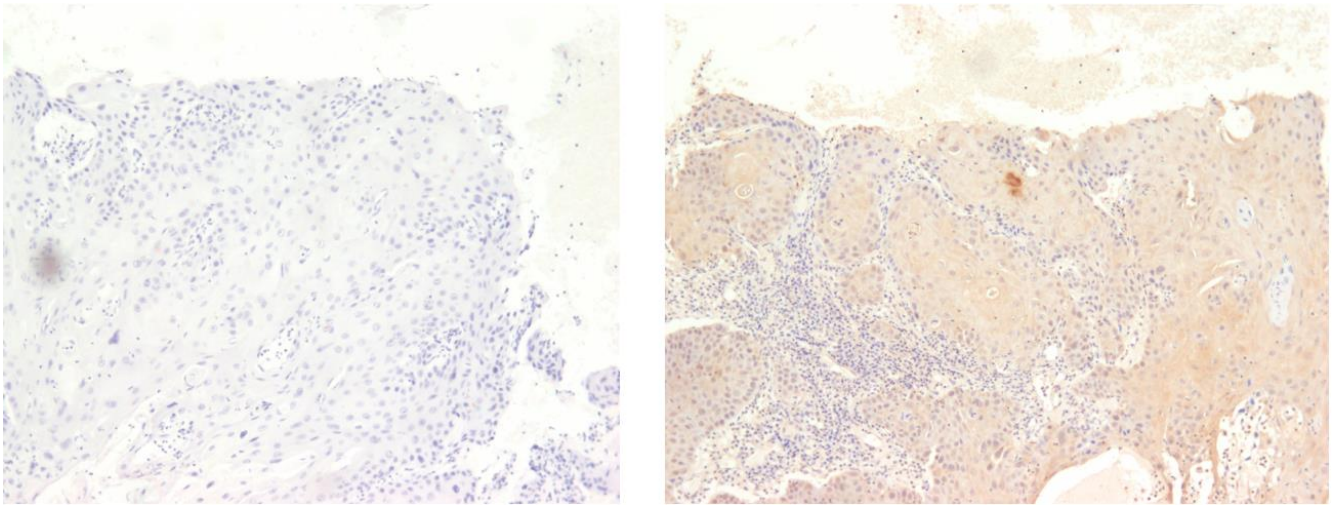

Figure 4.21 Phospho-P38 IHC positive control
A Squamous Cell Carcinoma was chosen as a positive control. A and B are the same tissue. A was not stained with the primary antibody. B was stained with the antibody.

An example of the Phospho-P38 stained Lichen Planus tissue that transformed to malignancy is provided below:

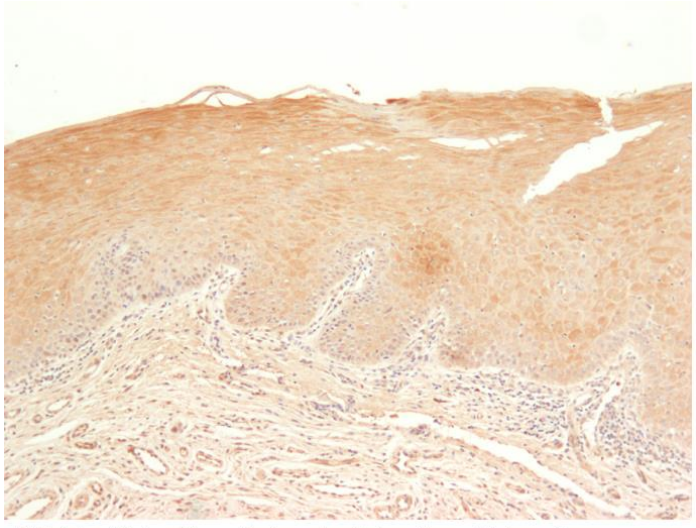

Figure 4.21 Phospho-P38 IHC Progressing Lichen Planus
An example of Phospho-P38 stained Lichen Planus that eventually progressed to malignancy.

An example of the Phospho-P38 stained Lichen planus that did not transform is provided below:

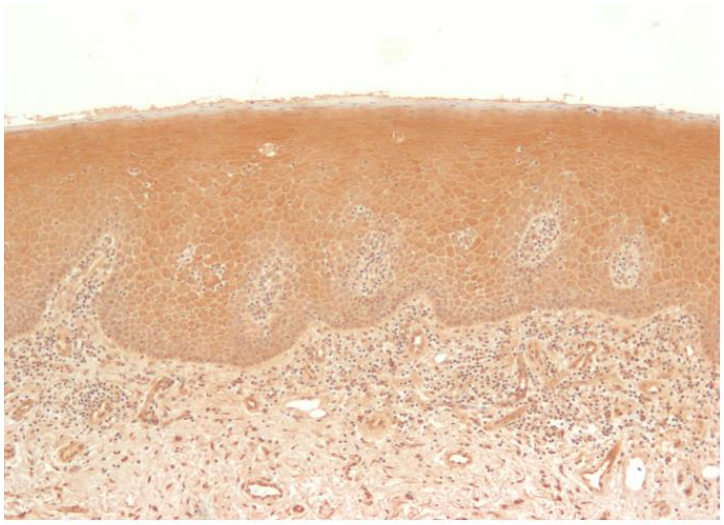

P38 stained Lichen Planus that did not transform on serial biopsy

Figure 4.22 Phospho-P38 IHC Non-Progressing Lichen Planus
An example of Phospho-P38 stained Lichen Planus that did not progress to malignancy on repeat biopsy.

4.7.3 Phospho-JNK IHC

An OSCC was used as a positive control as displayed below:

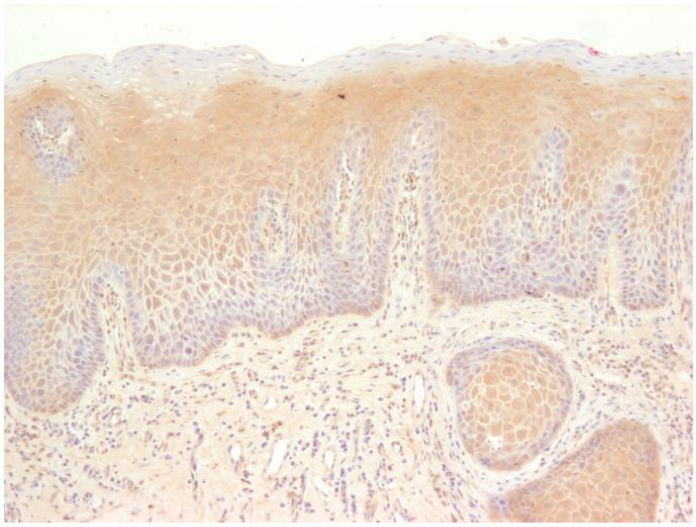

OSCC stained with primary antibody JNK1/2

Figure 4.23 Phospho-JNK1/2 IHC positive control
A Squamous Cell Carcinoma was chosen as a positive control.

An example of the Phospho-JNK1/2 stained Lichen Planus tissue that transformed to malignancy is provided below:

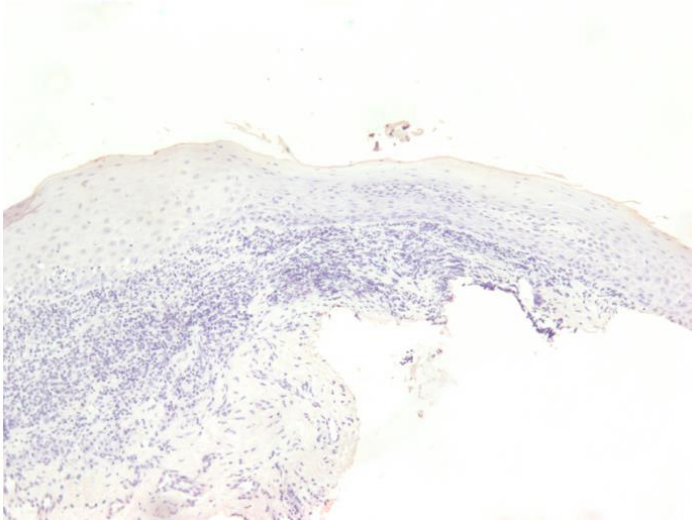

Figure 4.24 Phospho-JNK1/2 IHC Progressing Lichen Planus
An example of Phospho-JNK1/2 stained Lichen Planus that eventually progressed to malignancy.

An example of the Phospho-JNK1/2 stained Lichen planus that did not transform is provided below:

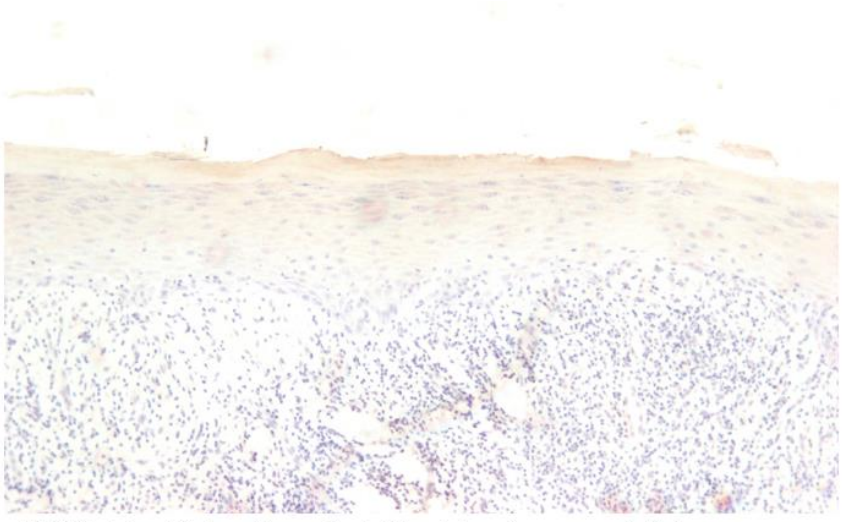

Figure 4.25 Phospho-JNK1/2 IHC Non-Progressing Lichen Planus
An example of Phospho-JNK1/2 stained Lichen Planus that did not progress to malignancy on repeat biopsy.

The MAPK stained tissues were qualitatively evaluated. Unfortunately, we are considering these failed assays due to staining concerns. Phospho-P38MAPK and Phospho-ERK1/2 positivity is quite diffuse and even outside of the epithelium causing a significant amount of background staining. Phospho-JNK1/2 was essentially negative and definitely did not show any nuclear positivity which does not seem to be in keeping with the inflammatory nature of LP.

4.8 Beta-Catenin and Cyclin D1 IHC

A qualitative analysis of Staining location and examination of a reciprocal nature with S100A7 was used. An example of Beta-Catenin and Cylcin D1 stained Lichen Planus that transformed is provided below:

A B

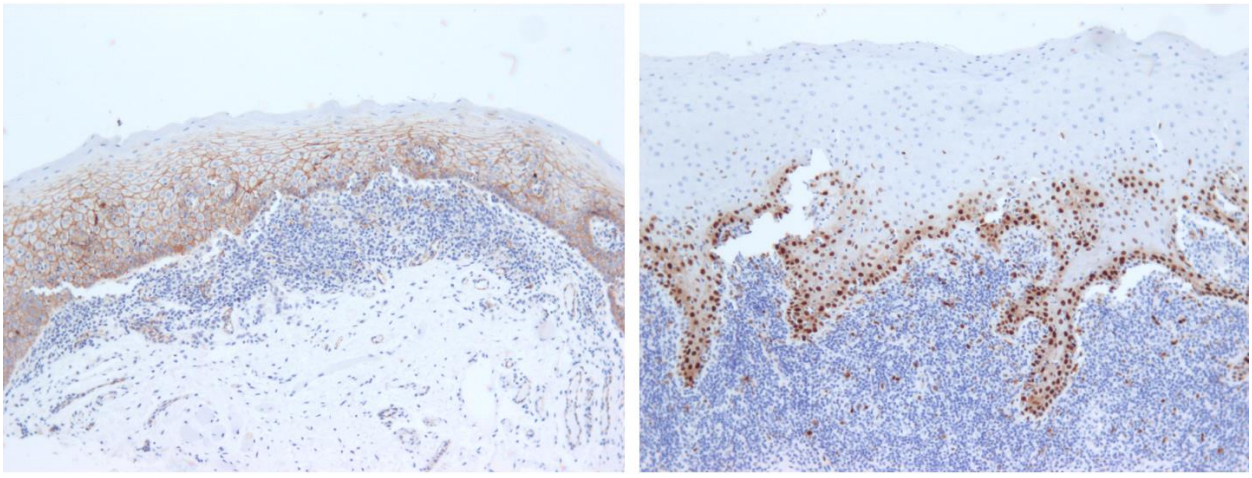

Figure 4.26 Beta-Catenin and Cyclin D1 IHC
A is an example of Lichen Planus tissue that did progress on serial biopsy stained with Beta-Catenin IHC. B is an example of Lichen Planus tissue that did progress on serial biopsy stained with Cyclin D1 IHC.

An example of Lichen Planus that did not progress is provided below:

A B

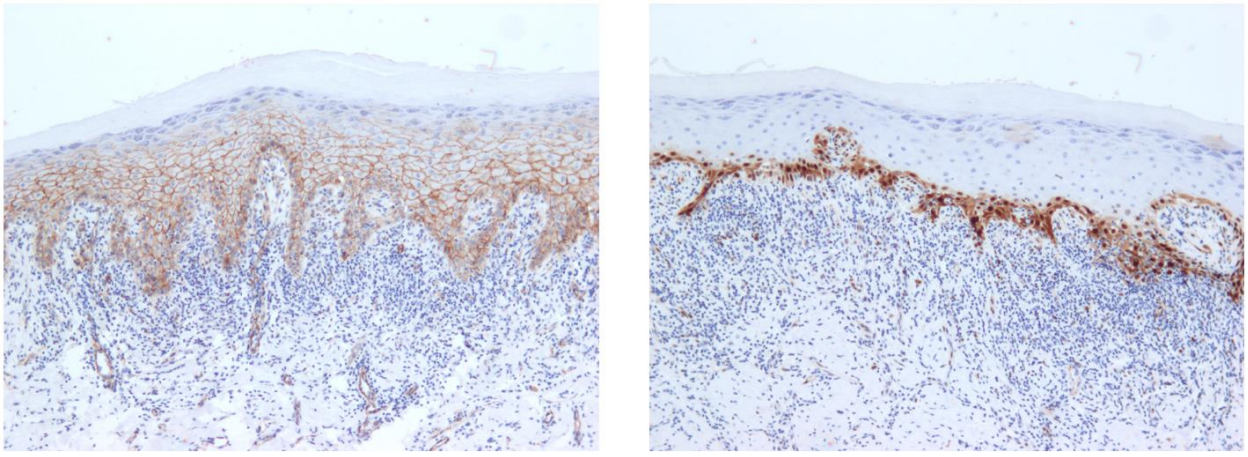

Figure 4.27 Beta-Catenin and Cyclin D1 IHC
A is an example of Lichen Planus tissue that did not progress on serial biopsy stained with Beta-Catenin IHC. B is an example of Lichen Planus tissue that did not progress on serial biopsy stained with Cyclin D1 IHC.

Qualitative analysis of the Beta-Catenin stain revealed that this protein was Present in the basal/suprabasal layers up to the granulosum in close proximity to the membrane in progressing and non-progressing Lichen Planus. Beta-Catenin seemed to also be present in the cytoplasm and nucleus of the proliferating basal layer of both groups as would be expected. In some of the progressing tissues, there appeared to be more cytoplasmic and nuclear staining in the suprabasal layers of the epithelium.

Qualitative analysis was completed on the Cyclin D1 stained tissues. Positive stain was appreciated in the basal layer (cytoplasm and nucleus) of progressing and Non-progressing LP. In some of the progressing tissues, there appears to be nuclear and cytoplasmic staining extending up into the spinous layer.

4.9 Tissue injury model

4.9.1 Rat tissue Experiment Positive Control Stained with S100A7

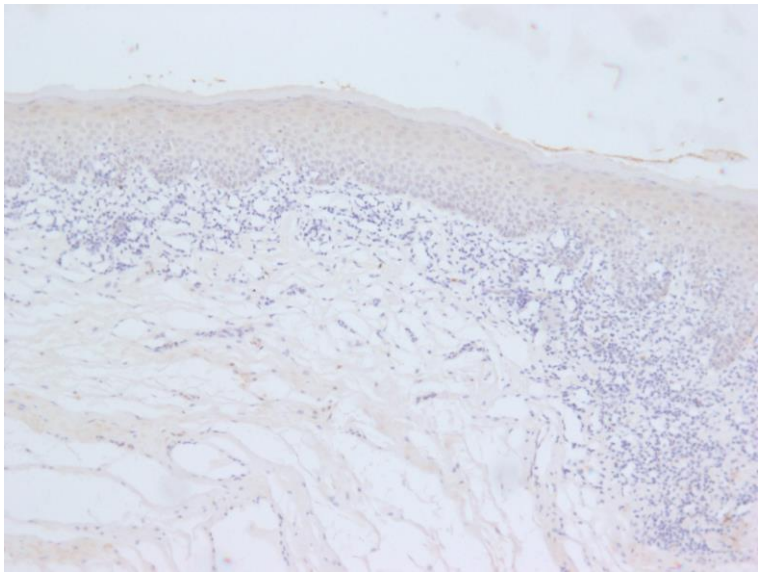

Figure 4.28: Positive Control

4.9.2 S100A7 pattern and location of staining 0, 3, and 7 days' post injury

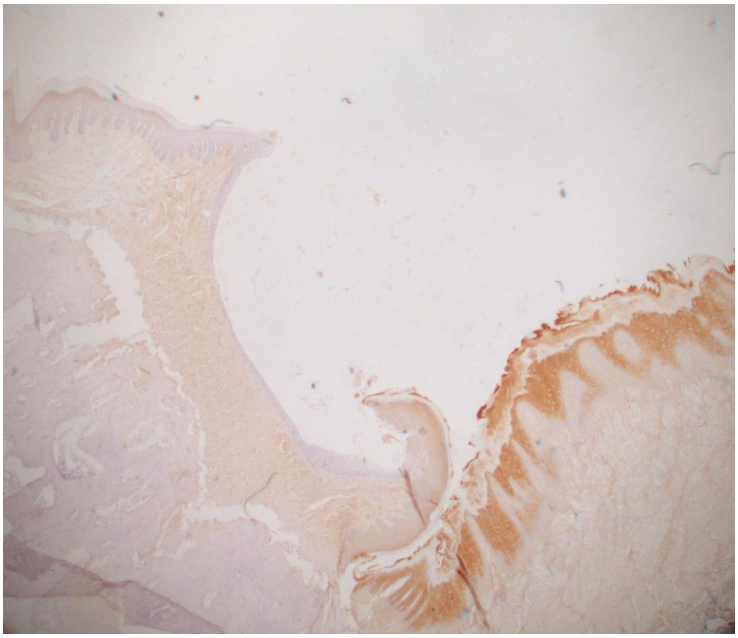

Figure 4.29: 8-week-old rat gingival tissue prior to injury stained with S100A7

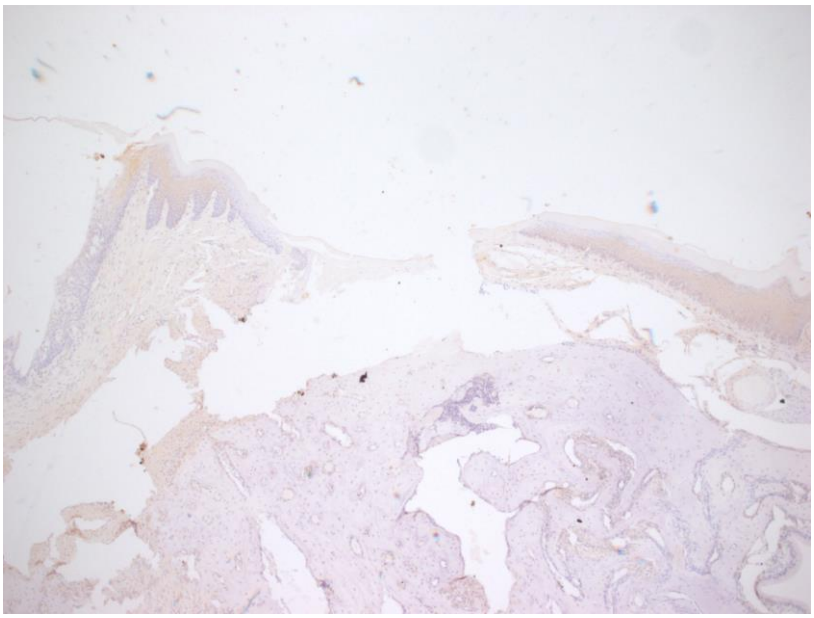

Figure 4.30: Rat gingival tissue day 0 following injury

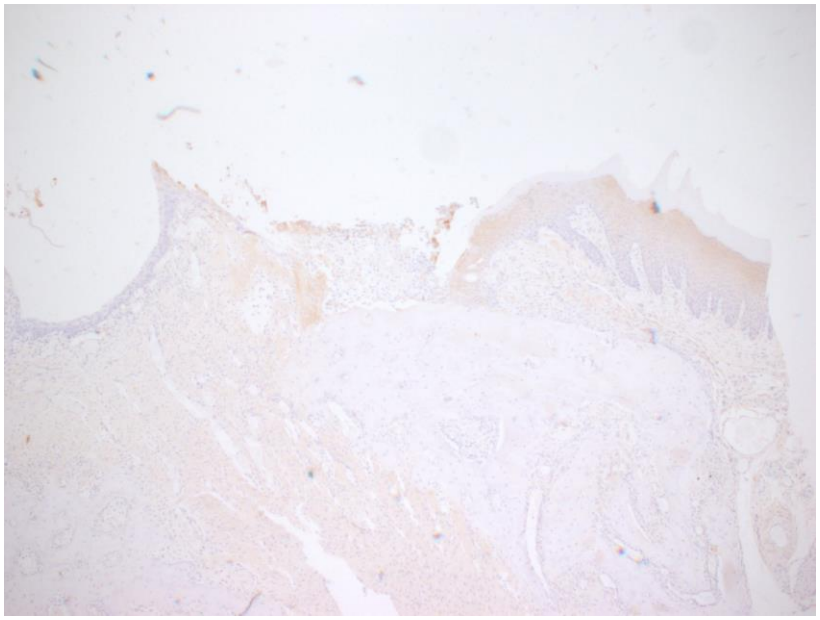

Figure 4.31: Rat gingival tissue day 3 following injury

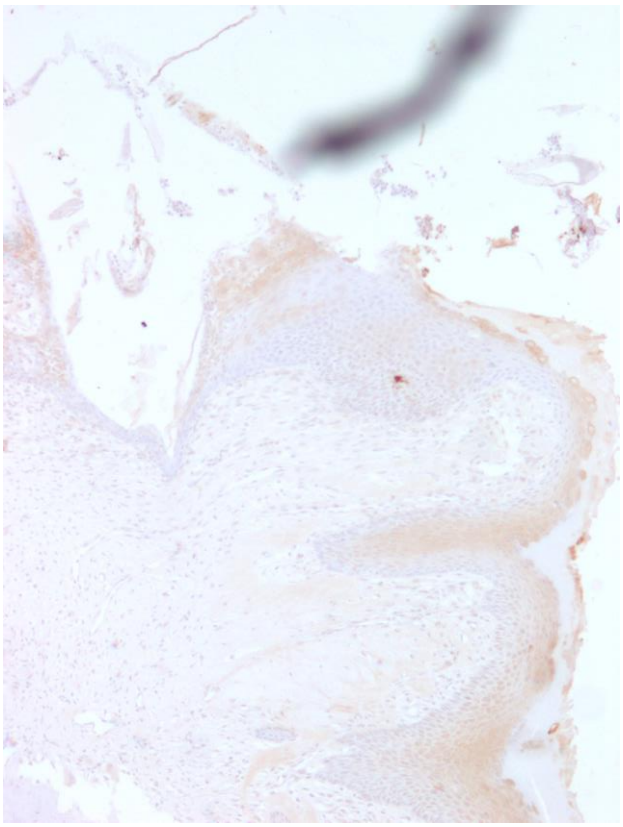

Figure 4.32: Rat gingival tissue day 7 following injury

At day 7 there appears to be downregulation of S100A7 in the epithelium immediately adjacent to the wound. There also appears to be no expression of biomarker S100A7 in the new epithelium traversing the wound.

4.10 Statistical Analysis

4.10.1 Correlative value between three predictors: IRS, Qupath, and Straticyte

Pearson's Correlation results for imputation of a missing value:

With 0.5 set as a threshold for significant correlation, when comparing the Manual Score to the Straticyte score, the Pearson coefficient was equal to .7106. When comparing Manual score to Qupath score, the Pearson Coefficient was equal to .6701. When the Qupath score was

compared to Straticyte, the Pearson Coefficient was equal to .6497. A plot of correlation matrix is displayed below:

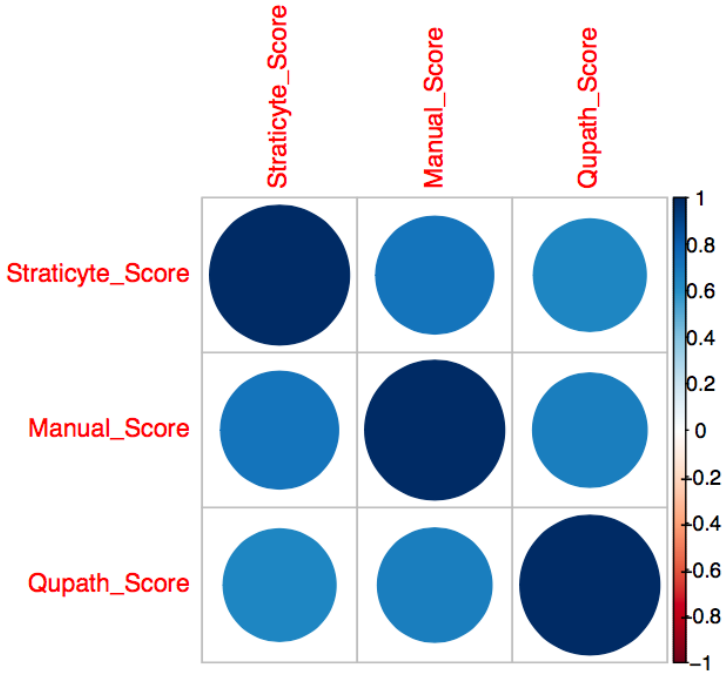

Figure 4.33 Correlative Value of S100A7 Scoring Indices
A Correlation matrix showing good correlation between Immunoreactive Score, Qupath analysis, and Straticyte

The three scores were found to be highly correlated so the missing value was imputed using Multivariate Imputation by Chained Equation (MICE).

Random Forest analysis to differentiate between Lichen Planus and Normal Tissue is displayed below:

Table 4.31: Confusion Matrix for Classification of Lichen Planus and Normal tissue

	ACTUAL	*Lichen Planus*	*Normal Tissue*	*Classification Error*
PREDICTED	Lichen Planus	20	3	.1304348
	Normal Tissue	5	6	.4545455

Out of 23 specimens predicted as Lichen Planus, 20 are actually Lichen Planus and 3 are normal tissue. The Out Of Bag (OOB) estimate of error is essentially the overall rate of incorrect classification as a percentage value. The result was (8/34) 23.53% suggesting the 3 predictors incorrectly classified Lichen Planus and Normal tissue approximately 23% of the time. Less than 25-30% OOB error was considered acceptable in this study. This suggests a potentially good fit.

Gradient Boosting Machine (GBM) method was then used as it is better with an unbalanced data set than Logistic Regression. The GBM results are depicted below:

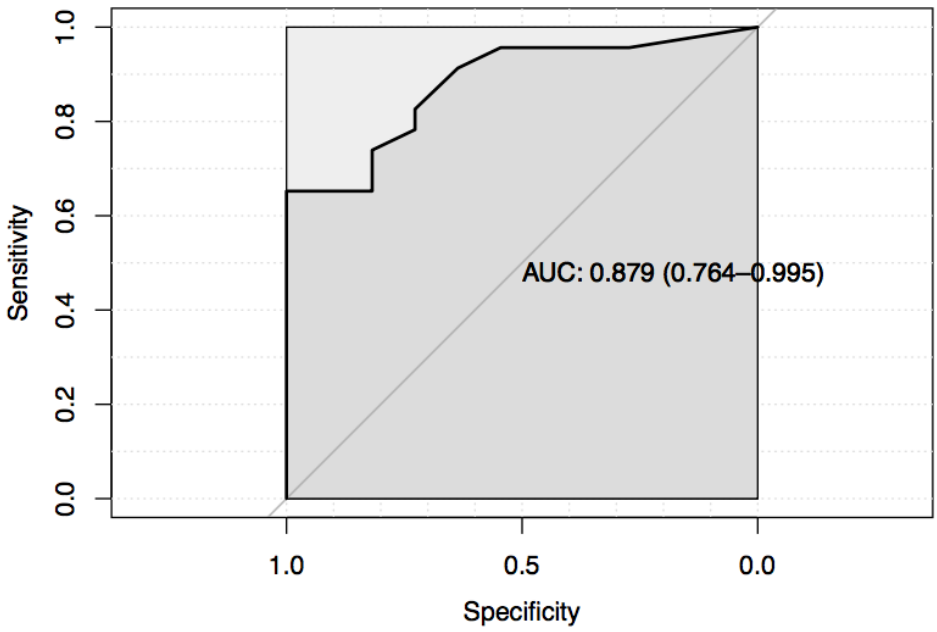

Figure 4.34 Illustrative results of GBM: Normal Tissue vs. Lichen Planus
Y axis is sensitivity, and X axis is specificity. When Specificity is high, sensitivity is also good showing a good fit when using S100A7 quantification to differentiate between the normal tissue and Lichen Planus groups.

A large Area Under Receiver Operating Characteristic Curve of .879 (88%) with a 95% CI of .764-.995) suggests a potentially good fit. A Perfect fit being 1 and 0.5 being random chance. Eighty percent was used as an acceptable threshold.

The Confusion Matrix for the Random Forest Analysis on whether the 3 predictors are able to classify whether Lichen Planus will progress or not is displayed below:

Table 4.32: Confusion Matrix for Classification of Progressing vs. Non- progressing Lichen Planus

	ACTUAL	*Lichen Planus Non-Progressing*	*Lichen Planus Progressing*	*Classification Error*
PREDICTED	Lichen Planus Progressing	14	1	.066666667
	Lichen Planus Non- Progressing	8	0	1.00000000

The Out of Bag estimate of error rate was (9/23) 39.13 suggesting a bad fit. As above, less than 25-30% OOB error was considered acceptable. As a result, this method will wrongly predict all 3 classes into the Non-Progressing category.

Gradient Boosting Machine Method was completed with the results below:

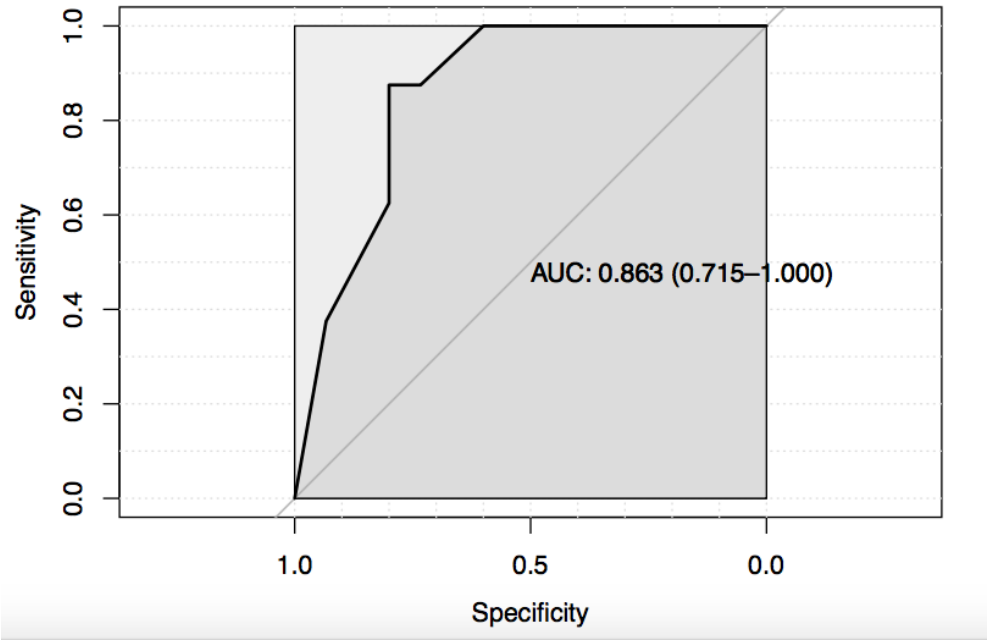

Figure 4.35 Illustrative results of GBM: Progressing Lichen Planus vs. Non- Progressing Lichen Planus
Y axis is sensitivity, and X axis is specificity. When specificity is high, sensitivity is low showing a poor fit when using S100A7 to predict progression in Lichen Planus lesions.

Area Under Receiver Operating Characteristic curve was .863 (86%) with a 95% CI being .715-1.0. This value is high, however, because data is unbalanced, can only be used as a reference.

Both Random Forest and GBM suggest that the 3 predictive scores can distinguish Lichen Planus from Normal tissue. However, since the data is quite unbalanced (4 normal and 23 LP), this result is not very reliable. Both Random Forest and GBM suggest that the 3 scores cannot predict which Lichen Planus lesion will progress. Below are three plots displaying the poor predictive value in determining whether Lichen planus will progress.

A

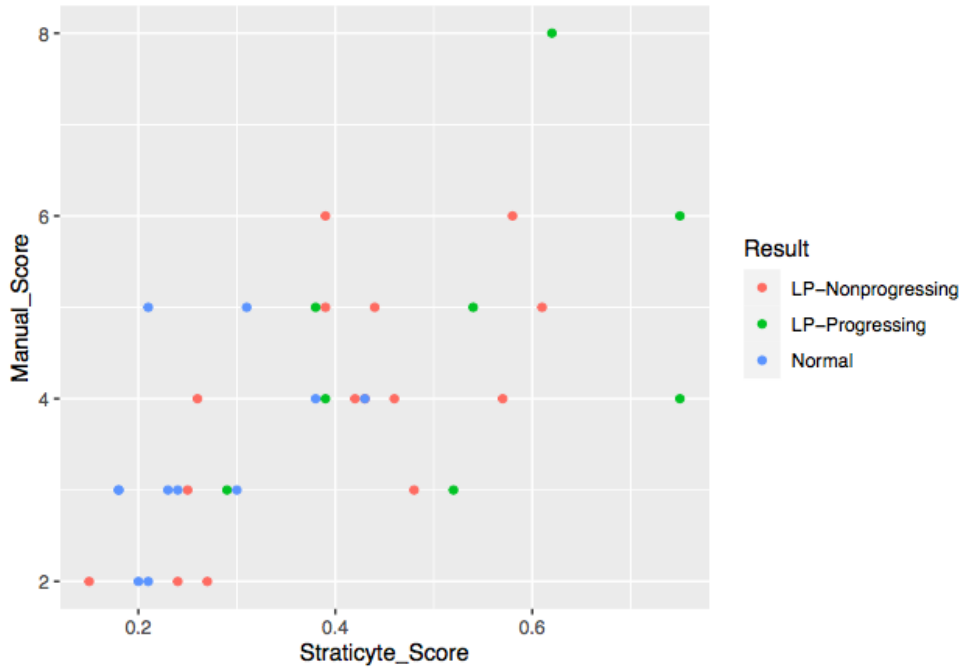

B

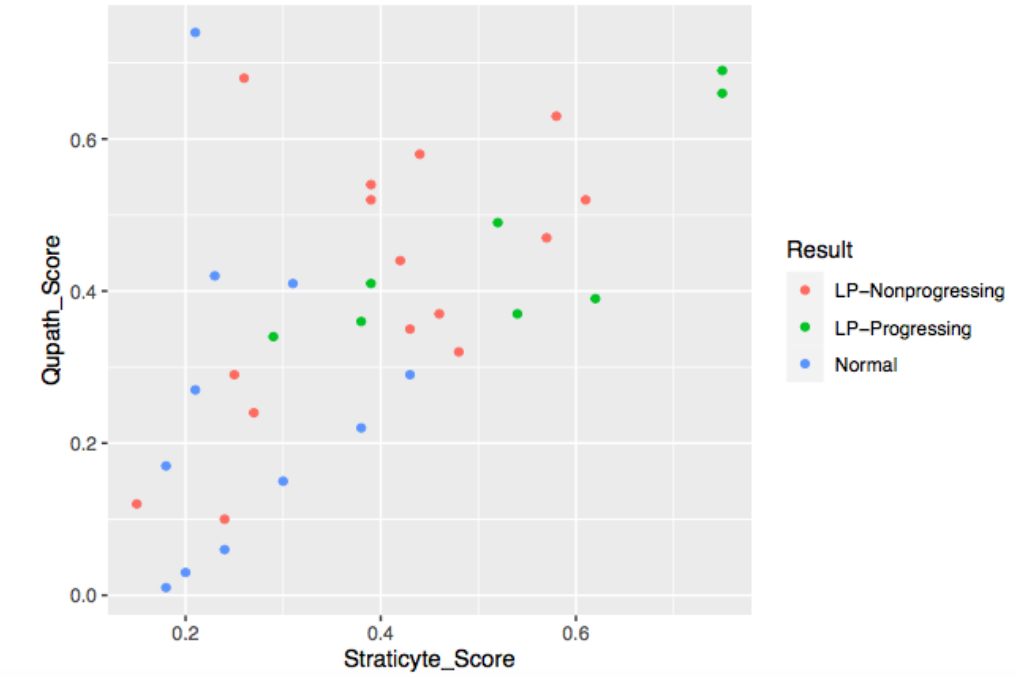

C

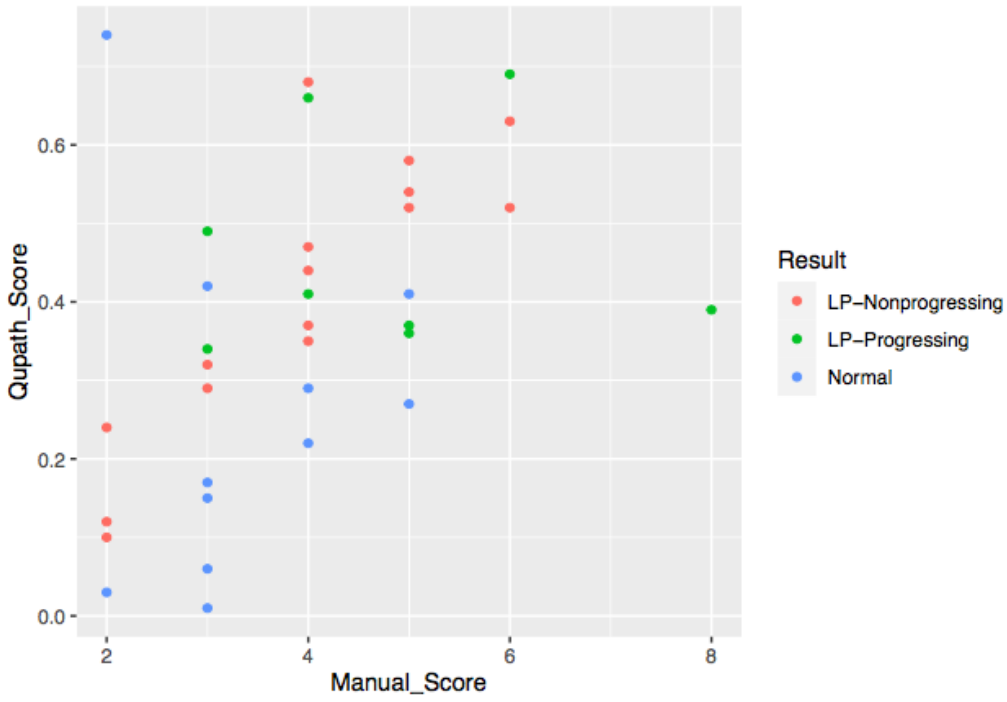

Figure 4.36 Predictive value of S100A7
A is a comparison between Manual Score and Straticyte score. B is a comparison between Qupath and Straticyte. C is a comparison between Manual score and Qupath.

If the predictive value was better, the coloured data points would be grouped together and separate from one another in graphic form. This tells us that the different scoring systems are not great at differentiating between the three groups.

Random Forest analysis to differentiate between Lichen Planus and Hyperkeratosis is displayed below:

Table 4.33: Confusion Matrix for Classification of Lichen planus vs. Hyperkeratosis

	ACTUAL	*Hyperkeratosis*	*Lichen Planus*	*Classification Error*
PREDICTED	Hyperkeratosis	6	5	.4545455
	Lichen Planus	3	20	.1304348

The OOB estimate of error rate was (8/34) 23.53% suggesting a potentially good fit.

The results of the GBM are below:

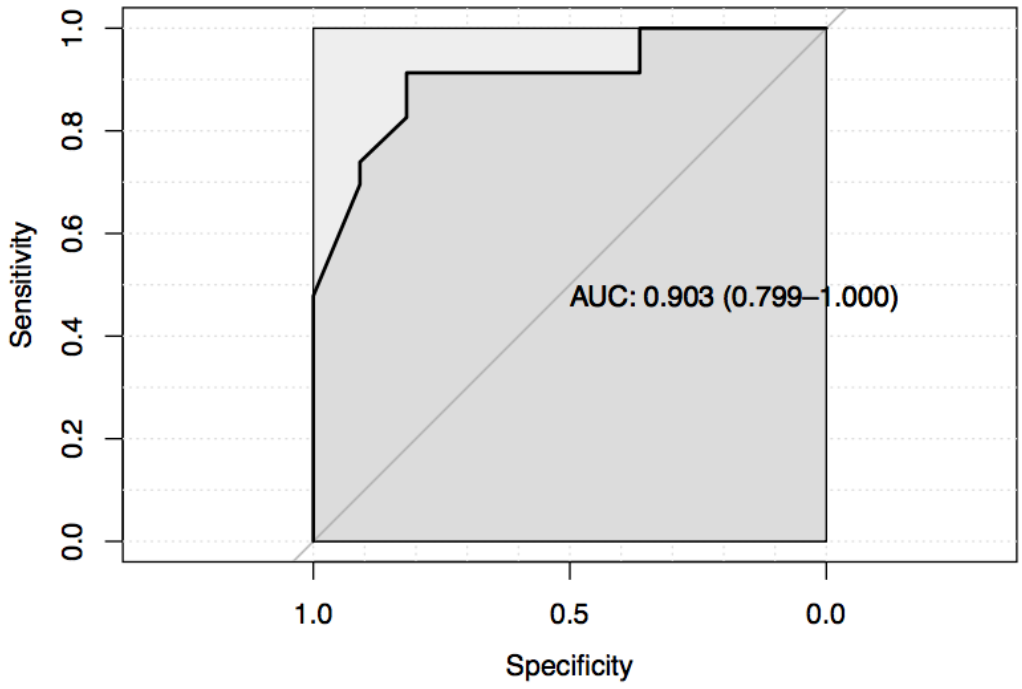

Figure 4.37 Illustrative results of GBM: Lichen Planus vs. Hyperkeratosis
Y axis is sensitivity, and X axis is specificity. When specificity is high, sensitivity is also good showing a good fit when using S100A7 to predict Lichen Planus vs. Hyperkeratosis.

Both results suggest that the 3 scores can help classify between “LP” and “HK”. But OOB error rate is high, so this is only for reference but not quite statistically significant.

To determine if the 3 scores could classify Lichen planus vs TUGSE Random Forest Analysis and Group Base Machine was completed with the results below:

Table 4.34: Confusion Matrix for Classification of Lichen Planus vs. TUGSE/TU

	ACTUAL	*Lichen Planus*	*TUGSE/TU*	*Classification Error*
PREDICTED	Lichen Planus	21	2	.08695652
	TUGSE/TU	1	9	.10000000

OOB estimate of error being 9.09%.

GBM results show:

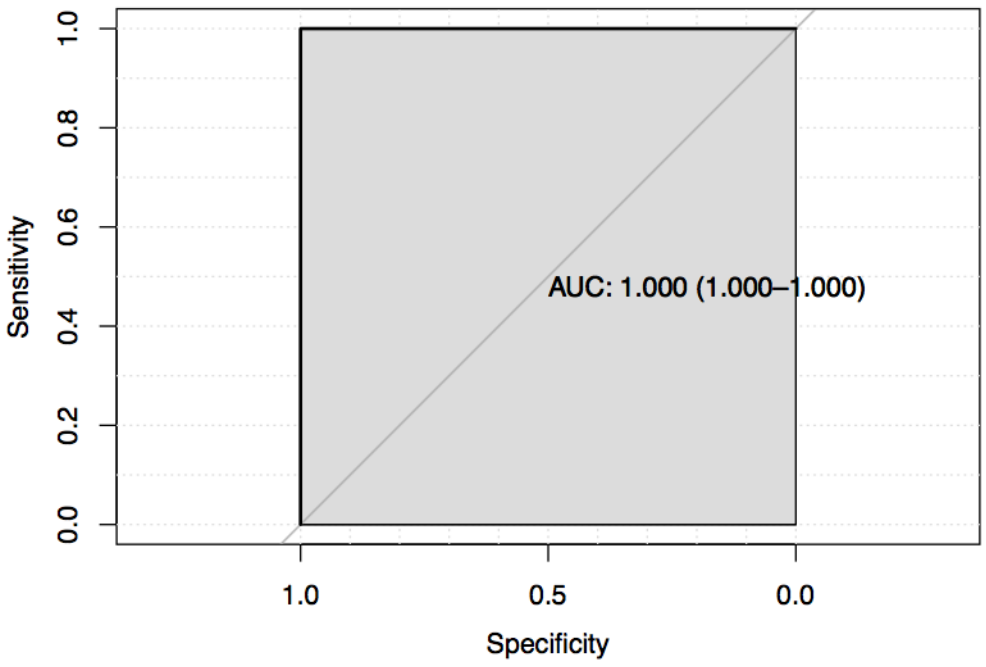

Figure 4.38 Illustrative results of GBM: Lichen Planus vs. TUGSE
Y axis is sensitivity, and X axis is specificity. When specificity is high, sensitivity is also high showing a good fit when using S100A7 to predict Lichen Planus vs. TUGSE.

Both results suggest that the 3 scores can help classify between “LP” and “TUGSE”. The OOB error rate is small, so this result is statistically significant.

Chapter 5

5.0 Discussion

5.1 OLP

5.1.1 Subtype of Lichen Planus

Within the oral cavity, the buccal mucosa, lateral tongue, and gingiva are commonly affected by OLP. The clinical subtypes of the lesions include reticular/hypertrophic, plaque-like, erosive, atrophic and bullous[24]. In the literature, the subtypes have been separated into white (hypertrophic, reticular, plaque-like), red (atrophic and erosive) and mixed[27]. Fitzpatrick et al. completed a relatively extensive review of the literature and found white variants to be most common followed by red and then mixed[27]. In terms of the subtypes that progressed to OSCC, the same author found 52% were red, 24% were white, and the remaining 24% were mixed[27].

In this study, the most common subtype in the progressing subgroup was hypertrophic /reticular (5/8) with erosive accounting for the remaining 3/8 cases of progression. The most common subtype in the non-progressing group was erosive (8/15) with hypertrophic accounting for 6/15, and 1/15 was the atrophic subtype. This seems to be in contrast to the available body of literature. However, a significant degree of uncertainty and error could be introduced by the clinician performing the biopsy. The diagnosis of clinical subtype relies heavily on what was written on the histopathology requisition. At times, the clinical description is less than optimal.

5.1.2 Age

A systematic review comprised of 16 studies and over 7000 cases of OLP was completed by Fitzpatrick *et al*[27]. They found an overall transformation rate of 1.09% for Oral Lichen

Planus. The average age at progression to OSCC was found to be 60.8 years. The average time from diagnosis of OLP or OLL to transformation was 51.4 months.

In this study, the median age at diagnosis of Oral Lichen Planus was 56.5 in the progressing subgroup and 59 in the non-progressing. The age demographic in this study is in keeping with the literature and the age demographic for development of OLP itself. Based on the results of this study, advanced age alone does not appear to be a good predictive factor for progression vs. non-progression.

The median time to progression was found to be 7.5 years/90 months. The average time to progression was found to be 6.75 years/81 months. In the Lichenoid Mucositis subgroup, the median age at original biopsy was 57. The median time to development of malignancy or dysplasia was found to be 6.5 years/78 months. The average time to progression was 6.75 years/81 months. This is slightly longer than what is quoted in the literature. This may be accounted for by a smaller sample size in this study.

5.1.3 *Sex*

Studies have found a slight female predominance in malignant transformation of OLP[27]. In this study, the vast majority of the progressing and no progressing subgroups were female (17/23). Within the progressing subgroup, the slight majority were also female at 5/8. This seems to be in keeping with the literature. The female predilection to develop Lichen Planus may account for the higher rate of transformation as well.

5.1.4 Location

In the literature, the most common site of transformation appears to be the tongue (51%) followed by the buccal mucosa at 32%[27]. According to Fitzpatrick et al, the gingiva, lips, and

floor of mouth accounted for 11%, 2%, and 1% of transformations respectively.

In this study, the most common sites of OLP malignant progression were the tongue (2/5) and buccal mucosa (2/5). The gingiva accounted for 1/5. The most common sites of OLP sampled in the non-progressing subtype was the gingival and buccal mucosa.

The relatively high rate of OSCC development on the buccal mucosa in individuals living with Lichen Planus is in contrast to the relatively low rate of development of OSCC in the same location outside of this group. This has also been demonstrated in previous studies[27]. Similarly, in contrast to the relatively low rate of development of OSCC on the dorsal tongue in the general population, its occurrence in the OLP population has been calculated to be twice as great[27]. In this study, of the two tongue Squamous Cell Carcinoma lesions, one was lateral and the other was not specified. The fact that there were no cases of transformation specifically localized to the dorsal tongue is likely reflective of the smaller sample size.

Development of OSCC in the floor of mouth and gingiva has been found to be under-represented in the literature in comparison to the development of OSCC in these regions in the absence of OLP. The gingiva is commonly affected by Lichen Planus, but does not appear to be a site that commonly transforms, having lower overall rate of OLP related gingival SCC than would be expected in the OSCC population. This is reflective of the gingiva accounting for 9/23 (39%) of the initial biopsies in the progressing and non-progressing groups.

Complicating matters, OSCC does not necessarily develop within the OLP lesion itself, but may occur in any part of the oral cavity[114]. Only 2/5 OLP cases in our study that progressed to cancer were site specific. These sites were the tongue and gingiva. Of the 3 OLP cases that progressed to dysplasia, all of them were site specific.

5.1.5 Immunosuppression, alcohol, tobacco use

Immunosuppressive factors such as diabetes and chronic steroid use are known to be independent risk factors in developing malignancy[27]. Likewise, tobacco and alcohol use are known independent factors that contribute to the development of oral cancer[27]. Unfortunately, due to privacy limitations, these risk factors were poorly accounted for. Of the 23 individuals with progressing and non-progressing Lichen Planus, tobacco use history was known in only 5. Of these 5, one individual was a lifelong non-smoker. One individual was a remote smoker having quit 30 years prior to histopathologic diagnosis of OLP. The remaining 3 individuals had an unknown duration and quantity of tobacco use. Of the 8 progressing cases, 2 had a history of tobacco use. One of the individuals had a remote history and the other was actively using. Of the non-progressing cases, 2 had a positive smoking history of unknown duration. One individual had known negative history for tobacco use. In the large review completed by Fitzpatrick et al, more than half of the patients with OLP that transformed to SCC did not report a history of alcohol or tobacco use[27].

5.2 OLL/OLM

Oral Lichenoid Lesions/ OLM are clinically and histopathologically similar to OLP. Differentiation between the OLP and OLL is usually through identification of a specific etiology such as a dental restorative material or medication. Subsequently, elimination of this inciting factor results in regression of the lesion[115]. A second clue to differentiate OLL from OLP is its likely unilateral nature and close proximity to a dental restorative material. In the current study, 8 cases of OLM/OLL were selected. Three of these cases progressed to cancer and 5 progressed to dysplasia.

5.2.1 Subtype

OLL can have all of the subtypes that are present with Lichen Planus. In this study, of the 8 progressing cases of OLL, 1 fit the clinical description of a mixed lesion and the second a white/reticular lesion. The remaining 6 cases were unspecified making any possible clinical correlation with subtype and progression difficult.

5.2.2 Age

The median age at histopathologic diagnosis of OLL/OLM in this study was 57. The median age at diagnosis of OLL seems to be similar to the median age of diagnosis of OLP within this study.

5.2.3 Sex

The sex distribution is in contrast to the female predominance above with 6 of the cases being male and 2 being female. This could be due to the fact that OLP may have an autoimmune etiology which generally favors the female sex. In contrast, The OLL/OLM population usually has a known etiologic agent vs. immune predisposition.

5.2.4 Location

The Location of OLM/OLL in this study is 5 on the tongue, 1 on the buccal mucosa, 1 on the FOM, and 1 on the gingiva. Of the tongue lesions, the ventral and lateral tongue are highly favored which is in keeping with higher incidence of cancer development in general and these eight lesions all transformed. This may be in contrast with OLP which has a higher predominance of dorsal tongue and buccal Mucosa.

5.2.5 Time to Progression vs. OLP

In a study completed by Fitzpatrick *et al*, 125 Oral lichenoid lesions were separated from Oral Lichen Planus based on Van der Meij and Van der Wal's modification of the 2003 WHO

criteria[27,116]. Four out of the one hundred and twenty-five Oral Lichenoid lesions transformed into Squamous Cell Carcinoma. The rate of transformation of OLL to SCC was 3.2%, however there was only one study in this review who differentiated between OLL and OLP. Fitzpatrick *et al* concluded that there was inadequate level of evidence to comment on differences in rate of transformation between OLP and OLL[27]. A study by Van der Meij consisting of 192 patients with OLL and OLP found a malignant transformation rate of 2.1% for OLL vs .5% for OLP[117]. The transformation rate was the same in male and female participants. The length of follow-up before malignant transformation was noted to be 11-70 months with a mean of 40 months. The median time to development of dysplasia/malignancy in our study was 78 months. The 78 months is at the higher range. This is likely due to the small sample size. The median time to progression is 78 months for OLL vs. 90 moths for OLP. This may suggest that OLL may progress more quickly than OLP and therefore should be monitored more frequently. However, it is difficult to draw this conclusion based on the small sample of OLL cases in this study.

5.2.6 Immune suppression, Alcohol, Tobacco use

The tobacco use status was more complete in this group as opposed to the OLP group. 50% of this the OLM group had a known history of tobacco use. One individual had a known negative history and the rest were unknown. This could be in keeping with tobacco being a major confounder and independent risk factor for the development of dysplasia and oral cancer. In terms of alcohol, there was 1 individual with relatively heavy alcohol use. The remainder were unknown. This is potentially a large confounding variable, as alcohol is also known to be associated with the development of oral cancer.

5.3 Hyperkeratosis

As per the 2017 WHO guidelines, Oral Leukoplakia is the most common oral potentially malignant disorder. Oral Leukoplakias are further defined as “white plaques of questionable risk, once other specific conditions and other OPMDs have been ruled out”[118]. Hyperkeratosis is considered one of these other conditions that are reactive and have a distinct etiology other than OPMDs. Most of the reactive lesions inclusive of hyperkeratosis are caused by parafunctional habits, mechanical friction, contact reactions, chemical reactions, and tobacco related changes[118]. Histologically, the epithelium exhibits a prominent granular cell layer, epithelial hyperplasia, and intracellular edema in the spinous layer. There is generally a lack of inflammatory infiltrate in the superficial connective tissue unless an ulcer is superimposed. Mitotic figures are present in the basal and parabasal layers and features of dysplasia are otherwise absent[118]. The prevalence of hyperkeratosis is quoted to be in the 26-5.3% range and is most common in the fifth to sixth decade of life[118]. According to Muller, a clinical diagnosis of hyperkeratosis is generally adequate and tissue sampling is not needed. There are times when the source/etiology is not obvious and the lesion is in a high-risk area for OPMDs. Therefore, it is generally considered prudent to sample any questionable lesion to rule out OPMD such as PVL, CHC, OHL or even frank dysplasia/SCC.

5.3.1 Subtype

The clinical subtype was not explicitly stated for any of the hyperkeratosis lesions.

5.3.2 Age

The median age at diagnosis was 53 years, which is in keeping with Muller’s data[118].

5.3.3 Sex

The sample consisted of nearly an equivalent number of males vs. females.

5.3.4 Location

Of the lesions, 6 were located on the ventral or lateral tongue, 3 were located on the retro molar trigone, and 2 were on the gingiva. All three of these sites are higher risk sites for OPMDs, dysplasia, and cancer. This shows that the clinicians taking the biopsy likely had some level of concern for OPMD/dysplasia/cancer due to a combination of clinical appearance and location of the lesions.

5.3.5 Tobacco, Alcohol, Immunosuppression

Five of 11 individuals had a known history of tobacco use. Six of 11 had a known negative history of tobacco use. Alcohol and immune suppression were unknown for all 11 cases.

5.4 Normal Tissue and TUGSE/TU

Mucosal tags are the oral equivalent of a skin tag. They are commonly found inside of the upper lip and on the frenulum. Clinically, they appear as small, soft, pink bump. Histopathologically, they are usually void of inflammation unless recently traumatized. They are also void of dysplasia. These lesions are not known as Potentially Malignant and are generally void of significant inflammatory infiltrate. This makes the tag a good surrogate for normal tissue. Of the 4 mucosal tags selected, the patient age.

Traumatic ulcerative granulomas with stromal eosinophilia are relatively common reactive benign lesions of the oral mucosa. They usually affect the tongue. This lesion has been associated with trauma, but the etiology is uncertain[119]. The clinical appearance can be similar to malignancy, being an ulcer with an underlying/adjacent indurated submucosal mass. However, they have no malignancy within and tend to resolve spontaneously[119]. Histopathologically, they

have a diffuse polymorphic cell infiltrate consisting of eosinophils, lymphocytes, macrophages and plasma cells[119].

The traumatic ulcer is another benign and reactive lesion of the oral mucosa that also resolves with removal of the etiologic factor[119]. The histopathology of a traumatic ulcer is similar to the TUGSE in that there is ulceration with a dense inflammatory infiltrate. Both of the TUGSE and traumatic ulcer can mimic oral cancer clinically. For this inflammatory subgroup, no specific age or sex were excluded and the smoking and alcohol use was largely unknown. There were two patients that were known non-smokers.

5.5 Biomarker S100A7

5.5.1 Expression in Normal Tissues

Zhou and others found no expression in the dividing basal layer of normal tongue tissue[97]. The same author found low level scattered expression of S100A7 in the suprabasal layers of normal tongue epithelium. Other studies have produced similar results and have found low levels of expression of S100A7 in normal keratinocytes and fetal skin[98]. These findings are consistent with the results of this study. The level of expression of S100A7 was low relative to the lichenoid lesions, hyperkeratosis, and the inflammatory lesion as measured by Immunoreactive score, Qupath, and Straticyte. As a result, the three predictors could differentiate between normal tissue with an incorrect classification rate of only 23%. Although interesting, this does not have great clinical relevance as a clinician would be unlikely to mistake a lichenoid lesion or malignancy with the clinical appearance of normal tissue. The proposed reason for minimal expression of S100A7 in normal tissue is consistent with the lack of cellular stressors on these tissues such as inflammation, wounding, hyperplasia, and neoplasia.

5.5.2 Expression in inflammatory lesions

S100A7 has been shown to be upregulated and present in the cytoplasm and nucleus of keratinocytes in benign hyperplastic epithelium, wounded epithelium, inflammatory epidermal conditions (psoriasis, atopic dermatitis, mycosis fungoides, Darier's disease, and lichen sclerosis et atrophicus)[97]. In this study, TUGSE and traumatic ulcers were used as an inflammatory surrogate. In the present study, the inflammatory surrogate tissues stained relatively high in S100A7 via all three measurement indices in comparison to the other tissue types. S100A7 expression in Lichen Planus and TUGSE/TU was compared statistically. Random Forest Analysis was used in combination with Gradient Boosting Machine Method and had a very low rate of incorrect classification and an OOB error of 9.09%. Clinically, this is not of significant value as histopathologically and sometimes clinically these two lesions can be differentiated. What may be of more value is redemonstration that S100A7 seems to be upregulated in inflammatory lesions and may be a confounder in the prediction of OLP to malignancy. In contrast, it could demonstrate the lichenoid lesions with a higher level of inflammation are more likely to transform. Inflammation has been shown to increase the risk of malignant transformation in other tissues. Lichen Planus may be the same[97].

5.5.3 Expression in healing tissue

S100A7 is thought to be associated with keratinocyte growth, proliferation, differentiation, adhesion, and migration - processes which are fundamental in wound healing. S100A7 has been shown to be upregulated in the suprabasal layers of acutely wounded epidermis as compared to chronic wounds and unwounded tissue[98]. The same study found that S100A7 was upregulated in accordance with cellular mitotic rate. In vitro experiments have shown downregulation of

S100A7 at wound edges leading to increased rate of cell migration across a wound. It is thought that S100A7, when present, may block an alternative pathway that leads to cell migration. Multiple studies have confirmed an increase rate of keratinocyte migration in S100A7 deficient cells. Interestingly, a study by Lee and Eckert (2006) proposed that S100A7 is upregulated in wounded tissue, secreted into wound exudate and serves an antibacterial function as well. In this study, a rat injury model was used to demonstrate S100A7 expression qualitatively at different points in time post-acute trauma. From day 0 to day 7 post injury there appears to be progressive downregulation of S100A7 adjacent to the wound itself. There is minimal to no expression in the epithelial cells traversing the wound. Both of these findings seem to be in keeping with studies suggesting that the protein may have a reciprocal relationship with Beta-Catenin and may actually be downregulated in proliferation and invasion. The decreased expression of S100A7 in the epithelium adjacent to the wound and in the new proliferating epithelium traversing the wound may be in keeping with its protective/anti proliferative role in inflammation, neoplasia, and injury.

5.5.4 Qupath, IRS, and Straticyte use to predict progression of Lichen Planus

Cancer Development (tumorigenesis) is a multistep process. This process consists of an accumulation of genetic defects and molecular changes, followed by clonal selection and expansion of altered cells. This can lead to the development of carcinoma[98]. The molecular changes precede cellular or clinical changes and detection of these molecular changes would allow for earlier diagnosis of high-risk states and improved prognosis[98]. Specific to Lichen Planus, a more recent study by Carenzo *et al* purports that clinical examination has limited value in detecting malignant potential of OPLs since their macroscopic appearance often does not reflect their histopathologic and molecular features[120]. Secondly, histopathology is highly

subjective and is not capable of providing a reliable measure of risk in a specific lesion. Hence the utility of biomarkers in predicting transformation in OLP and other potentially malignant lesions. Clinically, the most important question in the current study is: are we able to determine which Lichen Planus Lesions are at higher risk to transform to malignancy? If one could predict which lesion(s) are at highest risk of transformation, it could change the way a clinician would monitor/treat said individual living with Lichen Planus. There have been studies investigating the utility of S100A7 as a prognostic indicator in head and neck cancer[120]. Mclean *et al* investigated the utility of S100A7 and Straticyte for predicting progression in oral dysplasia[110]. There has not been another study investigating the utility of S100A7 for predicting transformation in OLP which by definition lacks dysplasia.

Mclean et al determined that S100A7 was not a useful predictor of dysplasia progression[110]. We hypothesized that S100A7 would be upregulated in progressing OLP lesions vs non-progressing. Although S100A7 is upregulated in OLP vs normal tissue, increasing quantity does not appear to accurately predict progression in this study. This may be in keeping with using a single biomarker to predict transformation in a process with significant heterogeneity: tumorigenesis. Focusing on a single biomarker to predict malignant transformation in Oral Potentially Malignant Lesions may be problematic as tumorigenesis is not a uniform/universal process. Cancer as a disease may not be accounted for by building a prediction model based on one molecular biomarker. It is well known that several factors may affect the susceptibility of an individual affected by OPMD to develop a malignant tumor. Likewise, the molecular signature of a tumor may differ according to the clinical and sociodemographic profile of the individual[121]. Weber Mello *et al* states that it is well established that a single genetic pathogenic variant may neither be sufficient nor necessary for the

development of head and neck cancers and that finding a single marker to predict malignant transformation would be challenging, if not impossible[121]. This is mainly due to the high heterogeneity of disease molecular profiles and evolution across different populations and individuals. The utility of a combination of clinical characteristics and multiple biomarkers could be investigated for their combined prognostic value.

5.5.4 MAPK Cascade as a potential pathway influenced by S100A7 expression

In context, the MAPK signaling pathway assays were considered to be unsuccessful for the purposes of this study. Further investigation of the MAPK proteins as biomarkers could be investigated. In terms of the phosphorylated P38 and JNK proteins, these are activated by many stress stimuli and appear to have both pro-tumorigenic and anti- tumorigenic properties. These proteins may not be useful as biomarkers for predicting malignant transformation in OLP. Phospho-ERK1/2 upregulation is already known to be associated with HNSCC and is a target for chemotherapeutic agent Cetuximab. Investigating Phospho-ERK1/2 only in OLP may be more fruitful.

5.5.5 Potential effects of S100A7 on Beta-Catenin and Cyclin D1

Malignant transformation in many carcinomas is associated with epithelial to mesenchymal transition (EMT)[122]. EMT features may be found early in the development of OSCC and dysplasia. Chaw et al state that “identification of these genes and products that play a role in the transition process may be potential biomarkers for malignant transformation”. The hallmark of EMT is downregulation of E-Cadherin and upregulation of Vimentin.

Some of these genes/products of EMT are components of the WNT signaling pathway. WNT proteins bind to their membrane components followed by Beta-Catenin translocating to the nucleus where it associates with T-cell factor (TCF) to form a transcription factor. This

functional transcription factor transcribes target genes involved in tumor progression, invasion, and metastasis[122].

Beta Catenin is a central molecule in the canonical Wnt-Beta-Catenin pathway and its expression is altered in head and neck SCC. To date, no activating mutations have been identified in this molecule[122]. E- cadherin/Beta-Catenin complex functions in cell adhesion. It is thought loss of E-cadherin could affect the WNT pathway signaling by binding Beta-Catenin and preventing accumulation of it in the cytoplasm and translocation to the nucleus to activate TCF. This would ultimately activate certain oncogenes such as C-Myc and Vimentin. It is thought that this pathway could be involved with not only promoting tumor invasion and metastasis but also an earlier role by supporting malignant transformation. Chaw et al examined Beta-Catenin and E-Cadherin expression through IHC in normal oral mucosa, various grades of dysplasia, and OSCC. They found moderate staining in the membranous region in the lower two thirds of normal oral epithelium and mild epithelial dysplasia. The mild ED did have less membranous staining than normal tissue and some cytoplasmic staining was noted in the basal layer. Interestingly, membranous Beta-Catenin was significantly reduced in moderate to severe dysplasia and localization of Beta-Catenin to the cytoplasm and nucleus[122].

The results of our study were similar to the findings in the research by Chaw *et al*[122]. There was Beta-Catenin IHC membrane positivity in the basal/suprabasal layers up to the granulosum in progressing and non-progressing OLP. Beta-Catenin was present in the cytoplasm and nucleus of the basal layer of both groups as would be expected. However, qualitatively, there seemed to be increased cytoplasmic and nuclear staining in the suprabasal layers of the progressing cases of LP. We also stained for oncogene Cyclin D1, which is a transcription end product of the WNT pathway. Both of the progressing and non-progressing Lichen Planus

specimens were stained for Cyclin D1. There was nuclear and cytoplasmic positivity in the basal layer of both groups. In the progressing specimen, there appears to be nuclear and cytoplasmic staining extending up into the spinous layer.

According to Zhou *et al* a proposed mechanism may be through reciprocal negative regulation between S100A7 and Beta-Catenin, such that downregulation of S100A7 upregulates Beta-Catenin and transcription of the Cyclin D1[97]. Moving forward quantitative analysis via RT-PCR of WNT pathway associated molecules: Beta-Catenin, Cyclin D1, Vimentin, and E-Cadherin may be helpful. A dual stain of Beta-Catenin and S100A7 may better show any relationship.

5.6 Limitations and Future Directions

This study had a relatively small sample size with unequal distribution of participants into the progressing, non-progressing, and normal tissue subgroups. An attempt to account for the unequal distribution of samples was made with Random Forest Analysis and GBM as opposed to Logistic Regression. Nonetheless, a larger multicenter study may provide for a larger sample size and would be useful to draw from as the transformation of OLP is a relatively uncommon occurrence.

Another potential source of error relates to the diagnosis of OLP itself as defined by the WHO Criteria. Reliance on clinical description by the individual clinician to make a definitive diagnosis of OLP could be fraught with error. The WHO definition is quite specific. We had to rely on the biopsy requisition/subjective account of the individual clinician to determine whether a tissue sample satisfies the clinical criteria. An attempt was made to contact the individual clinicians for clinical notes/photos, however, due to privacy and confidentiality issues coupled

with the time lapse since biopsy, this was not possible. A prospective study including clinical photos and complete documentation would be helpful in the future to avoid this predicament.

Likewise, confounding variables such as smoking, alcohol, and immunosuppression were generally poorly accounted for. Again, improved documentation/prospective study design could help to better account for these individual risk factors for cancer development.

Focusing on a single biomarker to predict malignant transformation in Oral Potentially Malignant Lesions may be problematic. Tumorigenesis is not a uniform/universal process and the heterogeneity of cancer as a disease may not be accounted for by building a prediction model based on one molecular biomarker. It is well known that several factors may affect the susceptibility of an individual affected by OPMD to develop a malignant tumor. Likewise, the molecular signature of a tumor may differ according to the clinical and sociodemographic profile of the individual (Weber Mello et al 2020). Weber Mello et al states that it is well established that a single genetic pathogenic variant may neither be sufficient nor necessary for the development of head and neck cancers and that finding a single marker to predict malignant transformation would be challenging, if not impossible. This is mainly due to the high heterogeneity of disease molecular profiles and evolution across different populations and individuals. The utility of a combination of clinical characteristics and multiple biomarkers could be investigated for their combined prognostic value.

Another viable alternative could be further investigation into the WNT pathway. More specifically, Beta-Catenin and its biphasic and reciprocal relationship with S100A7. Lastly, Carenzo *et al* described another potential method to predict transformation in premalignant lesions[120]. This author states that in contrast to head and neck squamous cell carcinoma (HNSCC), few studies have been performed to comprehensively profile the molecular and

cellular alterations in premalignant lesions, loss of heterozygosity (LOH) being the most effective in predicting progression to oral cancer. The same study states that patients with an oral potentially malignant lesion in combination with LOH at 3p14 and/or 9p21 plus LOH at another locus have an expected 3-year risk of developing oral cancer of 35%[120].

Chapter 6

6.0 Conclusion

The biomarker S100A7 is upregulated in Lichen planus vs. normal tissue; however, it could not be used to predict progression to dysplasia or malignancy. The pathway/ mechanisms involved in progression of this inflammatory lesion remain uncertain. The MAPK cascade may have a role; however, this study was unable to provide clarity. EMT through the canonical WNT pathway may show promising results and should be examined further. Beta-Catenin, Cyclin D1 and Vimentin are potential biomarkers. The results of the Straticyte test correlated well with the two other scoring methods but also failed to predict which lesions are at high risk of transformation. Biomarker S100A7 does not appear to aid in accurate prediction of transformation in potentially malignant lesion Lichen Planus and hence should not be used to guide clinical management.

References

1. Warnakulasuriya, S. *et al.* Oral potentially malignant disorders: nomenclature and classification. *Oral Dis.* 0–3 (2020).
2. Rotaru, D. I., Sofineti, D., Bolboacă, S. D. & Bulboacă, A. E. Diagnostic Criteria of oral lichen planus: A narrative review. *Acta Clin. Croat.* **59**, 513–522 (2020).
3. Edwards, P. & Kelsch, R. Oral Lichen Planus: Clinical Presentation and Management. *J. Can. Dent. Assoc. (Tor).* **68**, 494–499 (2002).
4. Elenbaas, A., Enciso, R. & Al-Eryani, K. Oral Lichen Planus: A review of clinical features, etiologies, and treatments. *Dent. Rev.* **2**, 100007 (2022).
5. Dudhia, B., Dudhia, S., Patel, P. & Jani, Y. Oral lichen planus to oral lichenoid lesions: Evolution or revolution. *J. Oral Maxillofac. Pathol.* **19**, 364–370 (2015).
6. Parashar, P. Oral lichen planus. *Otolaryngol. Clin. North Am.* **44**, 89–107 (2011).
7. Aghbari, S. M. H. *et al.* Malignant transformation of oral lichen planus and oral lichenoid lesions: A meta-analysis of 20095 patient data. *Oral Oncol.* **68**, 92–102 (2017).
8. Speight, P. M. & Eng, F. Oral potentially malignant disorders : risk of progression to. *Oral Surg. Oral Med. Oral Pathol. Oral Radiol.* (2018). doi:10.1016/j.oooo.2017.12.011
9. Sperandio, M. *et al.* Image-based DNA ploidy analysis AIDS prediction of malignant transformation in oral lichen planus. *Oral Surg. Oral Med. Oral Pathol. Oral Radiol.* **121**, 643–650 (2016).
10. Tadakamadla, J., Kumar, S., Lalloo, R., Gandhi Babu, D. B. & Johnson, N. W. Impact of oral potentially malignant disorders on quality of life. *J. Oral Pathol. Med.* **47**, 60–65 (2018).
11. Nagai, H. & Kim, Y. H. Cancer prevention from the perspective of global cancer burden

patterns. *J. Thorac. Dis.* **9**, 448–451 (2017).

12. Ford, P. J. & Farah, C. S. Early detection and diagnosis of oral cancer: Strategies for improvement. *J. Cancer Policy* **1**, e2–e7 (2013).
13. Farooq, I. & Bugshan, A. Oral squamous cell carcinoma: Metastasis, potentially associated malignant disorders, etiology and recent advancements in diagnosis. *F1000Research* **9**, (2020).
14. Tampa, M. *et al.* Markers of oral lichen planus malignant transformation. *Dis. Markers* **2018**, 7–10 (2018).
15. Mortazavi, H., Baharvand, M. & Mehdipour, M. Oral Potentially Malignant Disorders: An Overview of More than 20 Entities. *J. Dent. Res. Dent. Clin. Dent. Prospects* **8**, 6–14 (2014).
16. Abbas, S. A. *et al.* Assessment of Factors Affecting Quality of Life in Oral Squamous Cell Carcinoma Patients Using University of Washington Quality of Life Questionnaire. *Cureus* (2019). doi:10.7759/cureus.3904
17. Gondivkar, S. M. *et al.* Oral and general health-related quality of life in oral squamous cell carcinoma patients- comparative analysis of different treatment regims. *J. Oral Biol. Craniofacial Res.* **11**, 125–131 (2021).
18. Richards, D. Prevalence of oral potentially malignant disorders. *Evid. Based. Dent.* **19**, 120–121 (2018).
19. Steele, A. T., Editor, C. & Meyers, A. D. Premalignant Conditions of the Oral Cavity. *World Health* 6–13 (2011).
20. Martone, C. H., Wolf, S. M. & Wesley, R. K. of the Oral Cavity. 1340–1342 (1992).
21. Carnelio, S., Rodrigues, G. S., Shenoy, R. & Fernandes, D. A Brief Review of Common

Oral Premalignant Lesions with Emphasis on Their Management and Cancer Prevention. *Indian J. Surg.* **73**, 256–261 (2011).

22. Goodson, M. L., Sloan, P., Robinson, C. M., Cocks, K. & Thomson, P. J. Oral precursor lesions and malignant transformation - Who, where, what, and when? *Br. J. Oral Maxillofac. Surg.* **53**, 831–835 (2015).
23. Satelur, K. P., Bopaiah, S., Bavle, R. M. & Ramachandra, P. Role of cathepsin B as a marker of malignant transformation in oral lichen planus: An immunohistochemical study. *J. Clin. Diagnostic Res.* **11**, ZC81–ZC84 (2017).
24. Mehdipour, M. *et al.* Diagnostic and prognostic relevance of salivary microRNA-21, -125a, -31 and -200a levels in patients with oral lichen planus - a short report. *Cell. Oncol.* **41**, 329–334 (2018).
25. Giuliani, M. *et al.* Rate of malignant transformation of oral lichen planus : A systematic review. 693–709 (2019). doi:10.1111/odi.12885
26. Krupaa, R. J., Sankari, S. L., Masthan, K. M. K. & Rajesh, E. Oral lichen planus: An overview. *J. Pharm. Bioallied Sci.* **7**, S158–S161 (2015).
27. Fitzpatrick, S. G., Hirsch, S. A. & Gordon, S. C. The malignant transformation of oral lichen planus and oral lichenoid lesions A systematic review. *J. Am. Dent. Assoc.* **145**, 45–56 (2014).
28. Tampa, M. *et al.* Markers of oral lichen planus malignant transformation. *Dis. Markers* **2018**, 7–10 (2018).
29. Al-Jamaei, A. A. H. *et al.* Significance of immunohistochemistry biomarkers in prediction of malignant transformation of oral lichen planus: A systematic review. *Med. Oral Patol. Oral y Cir. Bucal* **27**, e480–e488 (2022).

30. Humberto, J. S. M., Pavanin, J. V., da Rocha, M. J. A. & Motta, A. C. F. Cytokines, cortisol, and nitric oxide as salivary biomarkers in oral lichen planus: a systematic review. *Braz. Oral Res.* **32**, 1–11 (2018).

31. Maher, S. *et al.* Evaluating the accuracy of microRNA27b and microRNA137 as biomarkers of activity and potential malignant transformation in oral lichen planus patients. *Arch. Dermatol. Res.* **310**, 209–220 (2018).

32. Almangush, A. *et al.* Prognostic biomarkers for oral tongue squamous cell carcinoma: A systematic review and meta-analysis. *Br. J. Cancer* **117**, 856–866 (2017).

33. Rivera, C., Oliveira, A. K., Costa, R. A. P., De Rossi, T. & Paes Leme, A. F. Prognostic biomarkers in oral squamous cell carcinoma: A systematic review. *Oral Oncol.* **72**, 38–47 (2017).

34. Aghbari, S. M. H., Gaafar, S. M., Shaker, O. G., Ashiry, S. El & Zayed, S. O. Evaluating the accuracy of microRNA27b and microRNA137 as biomarkers of activity and potential malignant transformation in oral lichen planus patients. *Arch. Dermatol. Res.* **310**, 209–220 (2018).

35. Melguizo-Rodríguez, L., Costela-Ruiz, V. J., Manzano-Moreno, F. J., Ruiz, C. & Illescas-Montes, R. Salivary biomarkers and their application in the diagnosis and monitoring of the most common oral pathologies. *Int. J. Mol. Sci.* **21**, 1–17 (2020).

36. González-Moles, M. Á., Keim-del Pino, C. & Ramos-García, P. Hallmarks of Cancer Expression in Oral Lichen Planus: A Scoping Review of Systematic Reviews and Meta-Analyses. *Int. J. Mol. Sci.* **23**, 13099 (2022).

37. Roopashree, M. R. *et al.* Pathogenesis of oral lichen planus - a review. *J. Oral Pathol. Med.* **39**, 729–734 (2010).

38. Kastenhuber, E. R. & Lowe, S. W. Putting p53 in Context. *Cell* **170**, 1062–1078 (2017).

39. Valente, G. *et al.* Sequential immunohistochemical p53 expression in biopsies of oral lichen planus undergoing malignant evolution. *J. Oral Pathol. Med.* **30**, 135–140 (2001).

40. Tanda, N., Mori, S., Saito, K., Ikawa, K. & Sakamoto, S. Expression of apoptotic signaling proteins in leukoplakia and oral lichen planus: Quantitative and topographical studies. *J. Oral Pathol. Med.* **29**, 385–393 (2000).

41. Cruz, I. B. *et al.* P53 Expression Above the Basal Cell Layer in Oral Mucosa Is an Early Event of Malignant Transformation and Has Predictive Value for Developing Oral Squamous Cell Carcinoma. *J. Pathol.* **184**, 360–368 (1998).

42. Stindt, M. H., Carter, S., Vigneron, A. M., Ryan, K. M. & Vousden, K. H. MDM2 promotes SUMO-2/3 modification of p53 to modulate transcriptional activity. *Cell Cycle* **10**, 3176–3188 (2011).

43. Buschmann, T., Fuchs, S. Y., Lee, C. G., Pan, Z. Q. & Ronai, Z. SUMO-1 modification of Mdm2 prevents its self-ubiquitination and increases Mdm2 ability to ubiquitinate p53. *Cell* **101**, 753–762 (2000).

44. Oliveira Alves, M. G. *et al.* Evaluation of the expression of p53, MDM2, and SUMO-1 in oral lichen planus. *Oral Dis.* **19**, 775–780 (2013).

45. Westphal, D., Kluck, R. M. & Dewson, G. Building blocks of the apoptotic pore: How Bax and Bak are activated and oligomerize during apoptosis. *Cell Death Differ.* **21**, 196–205 (2014).

46. Pigatti, F. M., Taveira, L. A. de A. & Soares, C. T. Immunohistochemical expression of Bcl-2 and Ki-67 in oral lichen planus and leukoplakia with different degrees of dysplasia. *Int. J. Dermatol.* **54**, 150–155 (2015).

47. Sancho, M., Leiva, D., Lucendo, E. & Orzáez, M. Understanding MCL1: from cellular function and regulation to pharmacological inhibition. *FEBS J.* **289**, 6209–6234 (2022).

48. Shin, J. A., Seo, J. M., Oh, S., Cho, S. D. & Lee, K. E. Myeloid cell leukemia-1 is a molecular indicator for malignant transformation of oral lichen planus. *Oncol. Lett.* **11**, 1603–1607 (2016).

49. Shin, J. A., Jung, J. Y., Ryu, M. H., Safe, S. & Cho, S. D. Mithramycin A inhibits myeloid cell leukemia-1 to induce apoptosis in oral squamous cell carcinomas and tumor xenograft through activation of bax and oligomerization. *Mol. Pharmacol.* **83**, 33–41 (2013).

50. Li, D., Hu, C. & Li, H. Survivin as a novel target protein for reducing the proliferation of cancer cells (review). *Biomed. Reports* **8**, 399–406 (2018).

51. Suganya, G. *et al.* Survivin expression in oral lichen planus: Role in malignant transformation. *J. Oral Maxillofac. Pathol.* **20**, 234–238 (2016).

52. Lo Muzio, L. *et al.* Survivin expression in oral squamous cell carcinoma. *Br. J. Cancer* **89**, 2244–2248 (2003).

53. Hirota, M. *et al.* Cell proliferation activity and the expression of cell cycle regulatory proteins in oral lichen planus. *J. Oral Pathol. Med.* **31**, 204–212 (2002).

54. González-Moles, M. A. *et al.* Cell cycle regulating mechanisms in oral lichen planus: Molecular bases in epithelium predisposed to malignant transformation. *Arch. Oral Biol.* **51**, 1093–1103 (2006).

55. Malumbres, M. Characterization of in vitro and in vivo metabolism of AG-024322, a novel cyclin-dependent kinase (CDK) inhibitor. 1–10 (2014).

56. Sherr, C. J. & Roberts, J. M. CDK inhibitors: Positive and negative regulators of G1-phase progression. *Genes Dev.* **13**, 1501–1512 (1999).

57. Montebugnoli, L. *et al.* Immunohistochemical expression of p16 INK4A protein in oral lichen planus. *Oral Surgery, Oral Med. Oral Pathol. Oral Radiol. Endodontology* **112**, 222–227 (2011).

58. Goel, S., Khurana, N., Marvah, A. & Gupta, S. Expression of cdk4 and p16 in Oral Lichen Planus. *J. Oral Maxillofac. Res.* **6**, 2–8 (2015).

59. Siddique 2012.pdf.

60. Ma, L. *et al.* Bmi1 expression in oral lichen planus and the risk of progression to oral squamous cell carcinoma. *Ann. Diagn. Pathol.* **17**, 327–330 (2013).

61. Sun, X. & Kaufman, P. D. Ki-67: more than a proliferation marker. *Chromosoma* **127**, 175–186 (2018).

62. Zargaran, M., Jamshidi, S., Eshghyar, N. & Moghimbeigi, A. Suitability/unsuitability of cell proliferation as an indicator of malignant potential in oral lichen planus: An immunohistochemical study. *Asian Pacific J. Cancer Prev.* **14**, 6979–6983 (2013).

63. Venugopal, A. & Uma Maheswari, T. Expression of matrix metalloproteinase-9 in oral potentially malignant disorders: A systematic review. *J. Oral Maxillofac. Pathol.* **20**, 474–479 (2016).

64. Quintero-Fabián, S. *et al.* Role of Matrix Metalloproteinases in Angiogenesis and Cancer. *Front. Oncol.* **9**, 1–21 (2019).

65. Bourboulia, D. & Stetler-Stevenson, W. G. Matrix metalloproteinases (MMPs) and tissue inhibitors of metalloproteinases (TIMPs): Positive and negative regulators in tumor cell adhesion. *Semin. Cancer Biol.* **20**, 161–168 (2010).

66. Chen, L. & Chen, J. MDM2-ARF complex regulates p53 sumoylation. *Oncogene* **22**, 5348–5357 (2003).

67. Zhou, X. J., Sugerman, P. B., Savage, N. W. & Walsh, L. J. MMP and TIMP expression in OLP. 72–82 (2001).

68. Sivadasan, P. *et al. Salivary proteins from dysplastic leukoplakia and oral squamous cell carcinoma and their potential for early detection*. *Journal of Proteomics* **212**, (Elsevier B.V, 2020).

69. Fitzpatrick, F. Cyclooxygenase Enzymes: Regulation and Function. *Curr. Pharm. Des.* **10**, 577–588 (2005).

70. Hashemi Goradel, N., Najafi, M., Salehi, E., Farhood, B. & Mortezaee, K. Cyclooxygenase-2 in cancer: A review. *J. Cell. Physiol.* **234**, 5683–5699 (2019).

71. Chankong, T. *et al.* Increased cyclooxygenase 2 expression in association with oral lichen planus severity. *J. Dent. Sci.* **11**, 238–244 (2016).

72. Neppelberg, E. & Johannessen, A. C. DNA content, Cyclooxygenase-2 expression and loss of E-cadherin expression do not predict risk of malignant transformation in oral lichen planus. *Eur. Arch. Oto-Rhino-Laryngology* **264**, 1223–1230 (2007).

73. Muniz, J. M. *et al.* Galectin-9 as an important marker in the differential diagnosis between oral squamous cell carcinoma, oral leukoplakia and oral lichen planus. *Immunobiology* **220**, 1006–1011 (2015).

74. Zhang, X., Kim, K., Zheng, Z., Bazarsad, S. & Kim, J. Nomogram for risk prediction of malignant transformation in oral leukoplakia patients using combined biomarkers. *Oral Oncol.* **72**, 132–139 (2017).

75. Cousin, J. & Cloninger, M. The Role of Galectin-1 in Cancer Progression,and Synthetic Multivalent Systems for theStudy of Galectin-1. *Int. J. Mol. Sci.* **17**, 1–22 (2016).

76. Pećina-Šlaus, N. Tumor suppressor gene E-cadherin and its role in normal and malignant

cells. *Cancer Cell Int.* **3**, 1–7 (2003).

77. Sridevi, U., Jain, A., Nagalaxmi, V., Kumar, U. V. & Goyal, S. Expression of E-cadherin in normal oral mucosa, in oral precancerous lesions and in oral carcinomas. *Eur. J. Dent.* **9**, 364–372 (2015).

78. Hämäläinen, L., Soini, Y., Pasonen-Seppänen, S. & Siponen, M. Alterations in the expression of EMT-related proteins claudin-1, claudin-4 and claudin-7, E-cadherin, TWIST1 and ZEB1 in oral lichen planus. *J. Oral Pathol. Med.* **48**, 735–744 (2019).

79. C., S. & J., L. Expression of MiRNA-137 in oral squamous cell carcinoma and its clinical significance. *J. B.U.ON.* **23**, 167–172 (2018).

80. Fridolfsson, H. N., Roth, D. M., Insel, P. A. & Patel, H. H. Regulation of intracellular signaling and function by caveolin. *FASEB J.* **28**, 3823–3831 (2014).

81. Díaz, M. I. *et al.* Caveolin-1 suppresses tumor formation through the inhibition of the unfolded protein response. *Cell Death Dis.* **11**, (2020).

82. Xue, J., Chen, H., Diao, L., Chen, X. & Xia, D. Expression of caveolin-1 in tongue squamous cell carcinoma by quantum dots. *Eur. J. Histochem.* **54**, 99–103 (2010).

83. Jaafari-Ashkavandi, Z. & Aslani, E. Caveolin-1 expression in oral lichen planus, dysplastic lesions and squamous cell carcinoma. *Pathol. Res. Pract.* **213**, 809–814 (2017).

84. Gu, Y. *et al.* TUSC3 promotes colorectal cancer progression and epithelial-mesenchymal transition (EMT) through WNT/β-catenin and MAPK signalling. *J. Pathol.* **239**, 60–71 (2016).

85. Braicu, C. *et al.* A Comprehensive Review on MAPK: A Promising Therapeutic Target in Cancer. 1–25 (2019).

86. Lavoie, H., Gagnon, J. & Therrien, M. ERK signalling: a master regulator of cell

behaviour, life and fate. *Nat. Rev. Mol. Cell Biol.* **21**, 607–632 (2020).

87. Leicht, D. T. *et al.* Raf kinases: Function, regulation and role in human cancer. *Biochim. Biophys. Acta - Mol. Cell Res.* **1773**, 1196–1212 (2007).

88. Stokoe, D., P, K. E., Campbell, D. G., Cohen, P. & Oaestep, M. small :: mammahan heat : Sh0ck : p 0t ins. *FEBS Lett.* **313**, 307–313 (1992).

89. Albanell, J. *et al.* Activated extracellular signal-regulated kinases: Association with epidermal growth factor receptor/transforming growth factor α expression in head and neck squamous carcinoma and inhibition by anti-epidermal growth factor receptor treatments. *Cancer Res.* **61**, 6500–6510 (2001).

90. Cuenda, A. & Rousseau, S. p38 MAP-Kinases pathway regulation, function and role in human diseases. *Biochim. Biophys. Acta - Mol. Cell Res.* **1773**, 1358–1375 (2007).

91. Wagner, E. F. & Nebreda, Á. R. Signal integration by JNK and p38 MAPK pathways in cancer development. *Nat. Rev. Cancer* **9**, 537–549 (2009).

92. Gkouveris, I. & Nikitakis, N. G. Role of JNK signaling in oral cancer : A mini review. (2017). doi:10.1177/1010428317711659

93. Kurtzeborn, K. & Kwon, H. N. MAPK / ERK Signaling in Regulation of Renal Di ff erentiation. *Mol. Sci.* (2019).

94. Gonzalez, L. L., Garrie, K. & Turner, M. D. Role of S100 proteins in health and disease. *Biochim. Biophys. Acta - Mol. Cell Res.* **1867**, 118677 (2020).

95. Heizmann, C. W. [Frontiers in Bioscience 7, d1356-1368, May 1, 2002] S100 PROTEINS: STRUCTURE, FUNCTIONS AND PATHOLOGY Claus W. Heizmann, Günter Fritz and Beat W. Schäfer. *Front. Biosci.* **7**, 1356–1368 (2002).

96. Martinsson, H., Yhr, M. & Enerbäck, C. Expression patterns of S100A7 (psoriasin) and

S100A9 (calgranulin-B) in keratinocyte differentiation. *Exp. Dermatol.* **14**, 161–168 (2005).

97. Zhou, G. *et al.* Reciprocal negative regulation between S100A7 / psoriasin and b -catenin signaling plays an important role in tumor progression of squamous cell carcinoma of oral cavity. 3527–3538 (2008). doi:10.1038/sj.onc.1211015

98. Rangaraj, A. *et al.* Molecular and cellular impact of Psoriasin (S100A7) on the healing of human wounds. 2151–2160 (2017). doi:10.3892/etm.2017.4275

99. Eckert, R. L. & Lee, K. C. S100A7 (Psoriasin): A story of mice and men. *J. Invest. Dermatol.* **126**, 1442–1444 (2006).

100. Tian, T. *et al.* S100A7 promotes the migration, invasion and metastasis of human cervical cancer cells through epithelial-mesenchymal transition. *Oncotarget* **8**, 24964–24977 (2017).

101. Alowami, S., Qing, G., Emberley, E., Snell, L. & Watson, P. H. Psoriasin (S100A7) expression is altered during skin tumorigenesis. **7**, 1–7 (2003).

102. Østergaard, M. *et al.* Proteome profiling of bladder squamous cell carcinomas: Identification of markers that define their degree of differentiation. *Cancer Res.* **57**, 4111–4117 (1997).

103. Deol, Y. S., Nasser, M. W., Yu, L., Zou, X. & Ganju, R. K. Tumor-suppressive effects of psoriasin (S100A7) are mediated through the β-catenin/T cell factor 4 protein pathway in estrogen receptor-positive breast cancer cells. *J. Biol. Chem.* **286**, 44845–44854 (2011).

104. Van de Wetering, M. *et al.* The β-catenin/TCF-4 complex imposes a crypt progenitor phenotype on colorectal cancer cells. *Cell* **111**, 241–250 (2002).

105. Reischl, J. *et al.* Increased expression of Wnt5a in psoriatic plaques. *J. Invest. Dermatol.*

127, 163–169 (2007).

106. Muoio, M. G. *et al.* Activation of the s100a7/rage pathway by igf-1 contributes to angiogenesis in breast cancer. *Cancers (Basel).* **13**, 1–19 (2021).

107. Nasser, M. W. *et al.* RAGE mediates S100A7-induced breast cancer growth and metastasis by modulating the tumor microenvironment. *Cancer Res.* **75**, 974–985 (2015).

108. Dey, K. K. *et al.* S100A7 has an oncogenic role in oral squamous cell carcinoma by activating p38/MAPK and RAB2A signaling pathway. *Cancer Gene Ther.* **23**, 382–391 (2016).

109. Kaur, J. *et al.* S100A7 overexpression is a predictive marker for high risk of malignant transformation in oral dysplasia. *Int. J. Cancer* **134**, 1379–1388 (2014).

110. Scholarship, W., Dysplasia Lachlan McLean, D. & Joint Supervisor Armstrong, O. Evaluating the Utility of Protein Biomarker, S100A7, and Diagnostic Test, Straticyte, in Predicting the Progression of Oral Dysplasia. (2019).

111. Voldborg, B. R., Damstrup, L. & Poulsen, H. S. and Possible Role in Clinical Trials. *Ann. Oncol.* 1197–1206 (1997).

112. Hwang, J. T. K. *et al.* Individualized five-year risk assessment for oral premalignant lesion progression to cancer. *Oral Surg. Oral Med. Oral Pathol. Oral Radiol.* **123**, 374–381 (2017).

113. Sood, A. *et al.* Role of S100 A7 as a diagnostic biomarker in oral potentially malignant disorders and oral cancer. *J. oral Maxillofac. Pathol.* **26**, 166–172 (2022).

114. Gonzalez-Moles, M. A., Scully, C. & Gil-Montoya, J. A. Oral lichen planus: Controversies surrounding malignant transformation. *Oral Dis.* **14**, 229–243 (2008).

115. Kamath, V. Oral Lichenoid Lesions - A Review and Update E-IJD REVIEW ARTICLE

Oral Lichenoid Lesions - A Review and Update. (2016). doi:10.4103/0019-5154.147830

116. Schepman, K. P., van der Meij, E. H., Smeele, L. E. & van der Waal, I. Malignant transformation of oral leukoplakia: a follow-up study of a hospital-based population of 166 patients with oral leukoplakia from The Netherlands. *Oral Oncol.* **34**, 270–275 (1998).

117. van der Meij, E. H., Mast, H. & van der Waal, I. The possible premalignant character of oral lichen planus and oral lichenoid lesions: A prospective five-year follow-up study of 192 patients. *Oral Oncol.* **43**, 742–748 (2007).

118. Müller, S. Frictional Keratosis , Contact Keratosis and Smokeless Tobacco Keratosis : Features of Reactive White Lesions of the Oral Mucosa. *Head Neck Pathol.* **13**, 16–24 (2019).

119. Sharma, B., Koshy, G. & Kapoor, S. Traumatic Ulcerative Granuloma with Stromal Eosinophila : A Case Report and Review of Pathogenesis. **10**, 9–11 (2016).

120. Carenzo, A. *et al.* Gene Expression Clustering and Selected Head and Neck Cancer Gene Signatures Highlight Risk Probability Differences in Oral Premalignant Lesions. *Cells* **9**, 1–15 (2020).

121. Mello, F. W. *et al. Oral potentially malignant disorders: A scoping review of prognostic biomarkers*. *Critical Reviews in Oncology/Hematology* **153**, (Elsevier Ireland Ltd, 2020).

122. Chaw, S. Y. *et al.* Epithelial to mesenchymal transition (EMT) biomarkers - E-cadherin, beta-catenin, APC and Vimentin - In oral squamous cell carcinogenesis and transformation. *Oral Oncol.* **48**, 997–1006 (2012).

Ethics

Western Research

Date: 20 April 2022

To: Mark Darling

Project ID: 105954

Study Title: Mechanisms underlying the transformation of potentially malignant oral lesions to oral cancer.

Application Type: Continuing Ethics Review (CER) Form

Review Type: Delegated

Date Approval Issued: 20/Apr/2022

REB Approval Expiry Date: 23/Apr/2023

Dear Mark Darling,

The Western University Research Ethics Board has reviewed the application. This study, including all currently approved documents, has been re-approved until the expiry date noted above.

REB members involved in the research project do not participate in the review, discussion or decision.

Western University REB operates in compliance with, and is constituted in accordance with, the requirements of the Tri-Council Policy Statement: Ethical Conduct for Research Involving Humans (TCPS 2); the International Conference on Harmonisation Good Clinical Practice Consolidated Guideline (ICH GCP); Part C, Division 5 of the Food and Drug Regulations; Part 4 of the Natural Health Products Regulations; Part 3 of the Medical Devices Regulations and the provisions of the Ontario Personal Health Information Protection Act (PHIPA 2004) and its applicable regulations. The REB is registered with the U.S. Department of Health & Human Services under the IRB registration number IRB 00000940.

Please do not hesitate to contact us if you have any questions.

Sincerely,

The Office of Human Research Ethics

Note: This correspondence includes an electronic signature (validation and approval via an online system that is compliant with all regulations).

CV

Jeffrey Lovell BSc, DDS, MD
Oral and Maxillofacial Surgery Resident, London Health Sciences Centre

EDUCATION

2017-2023	Degree and institution:	**Oral and Maxillofacial surgery (Candidate)** Western University/ London Health Sciences Centre
2017-2022	Degree and institution:	**Masters of Pathology (Candidate)** Western University/ Pathology and Laboratory Medicine
2019-2022	Degree and institution:	**Doctor of Medicine** Western University/ Schulich School of Medicine & Dentistry
2014-2015	Degree and institution:	**Dental Clinical Fellowship** Western University/ London Health Sciences Centre
2010-2014	Degree and institution:	**Doctor of Dental Surgery** Western University/ Schulich School of Medicine & Dentistry
2003-2007	Degree and institution:	**Bachelor of Science (Honours in Kinesiology)** Western University

RESEARCH AND PUBLICATIONS

2022 Thesis: S100A7 as a biomarker for predicting transformation in a potentially malignant lesion: lichen planus. Supervisor: Dr. Mark Darling DDS (Oral Pathologist)

2023 **Lovell, J**., Laschuk, M. & Stapleford, R. Combined BMP and allograft for SABG. *Oral Health*. (pending publication)

EMPLOYMENT EXPERIENCE

July 2015–June 2017	**Arkona dental office** General practice dentistry
September 2015-June 2017	**Schulich school of Medicine and Dentistry, Western University** Instructor in Oral Surgery
August 2013-Sept 2013	**Schulich school of Medicine and Dentistry, Western University** Student dentist at Western University emergency clinic Worked in emergency clinic; dental diagnosis and emergency treatment

August 2007 to July 2008	**AMTEL Geological Services** Laboratory Technician Performed laboratory duties; panned samples to determine composition
May 2005-August 2005	**Natural History Project, M.S. Clinic, London Health Sciences Centre** Lab Assistant under Dr. Kremenchutzky (neurology) Conducted medical and statistical research; reinforced proper lab conduct and lab procedure
April 2005-August 2005 April 2004-August 2004 April 2003-August 2003	**Peter's Lawn Service** Landscape Worker Maintained lawn and properties for homeowners and businesses.
June 2004-August 2004 June 2003-August 2003	**Town of Gravenhurst** Beach Lifeguard/Swimming Instructor
December 2002-March 2003 December 2001-March 2002	**Devil's Glen Ski Club** Ski Coach

VOLUNTEER EXPERIENCE

September 2018- June 2019	**St Joseph's Hospital London Ontario** Volunteer in recreational therapy at Mount Hope LTCF
September 2012-2014	**Dental Outreach Community Service** Dispensary duties and volunteer dental services
September 2004-2017	**St. John's the Evangelist Church** Cook/Food Distributor at church dinners
December 2001-2017	**London Food Bank** Assignment Volunteer to sort and distribute food

PROFESSIONAL DEVELOPMENT

September 2019-Present	Member of AO North America (CMF division)
October-November 2016	Dr. Ken Hebel's implant prosthetic and surgical course
September 2014- 2018	Study club with other general practitioners/specialists
July 2014- July 2015	General practice residency program Western University

ACADEMIC HONORS AND AWARDS

2014	Alpha omega award	Western University
2014	Igor Bolta restorative dentistry award	Western University
2012-2013	Prosthodontics award	Western University

2010-2011	General Medicine Award	Western University
2010-2011	Royal College of Dental Surgeons of Ontario Scholarship	Western University
2004-2007	Dean's Honour List	Western University

PROFESSIONAL MEMBERSHIPS

Ontario Dental Association

Ontario Medical Association

Canadian Dental Association

Canadian Medical Association

Royal College of Dental Surgeons of Ontario

AO North America (AONA- CMF)